Quark PDFs and α_s from DIS and LHC

S.Alekhin (*Univ. of Hamburg & IHEP Protvino*)

- Theory reminder: factorization and scheme dependence

- Recent data: HERA, Tevatron and LHC

- Interplay of α_s and t-quark mass: vacuum stability

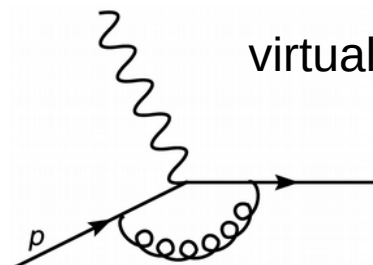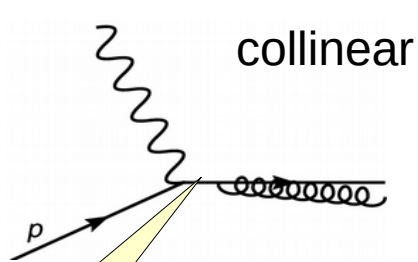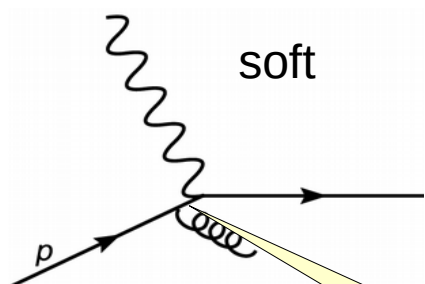- Strange sea: ATLAS determination and other data sets

- Intrinsic charm

PIC2017, Prag, 5 May 2017

Theory reminder: factorization

QPM: electro-production inclusive
structure function

$$F_2(x,Q^2)=\Sigma_q \, e^2_q \, p_q(x)$$

$p_q(x)$ – parton probability distributions
(PDFs)

QCD radiative corrections:

ep scattering

large distances

small distances

courtesy of S.Magill

soft

collinear

virtual

courtesy of M.H.Seymour

Mass singularity

Mass singularity appears for the massless partons,
however, t can be absorbed into PDFs ⇒ PDF evolution

Better theoretical accuracy / Scheme dependence of PDFs

State-of-art:

NNLO   **Moch, Vermaseren Vogt NPB 688, 101 (2004); NPB 691, 129 (2004)**

N3LO   **Moch et al. hep-ph/1707.08315; Velizhanin hep-ph/1411.1331; Baikov, Chetyrkin NPPS 160, 76 (2006)**
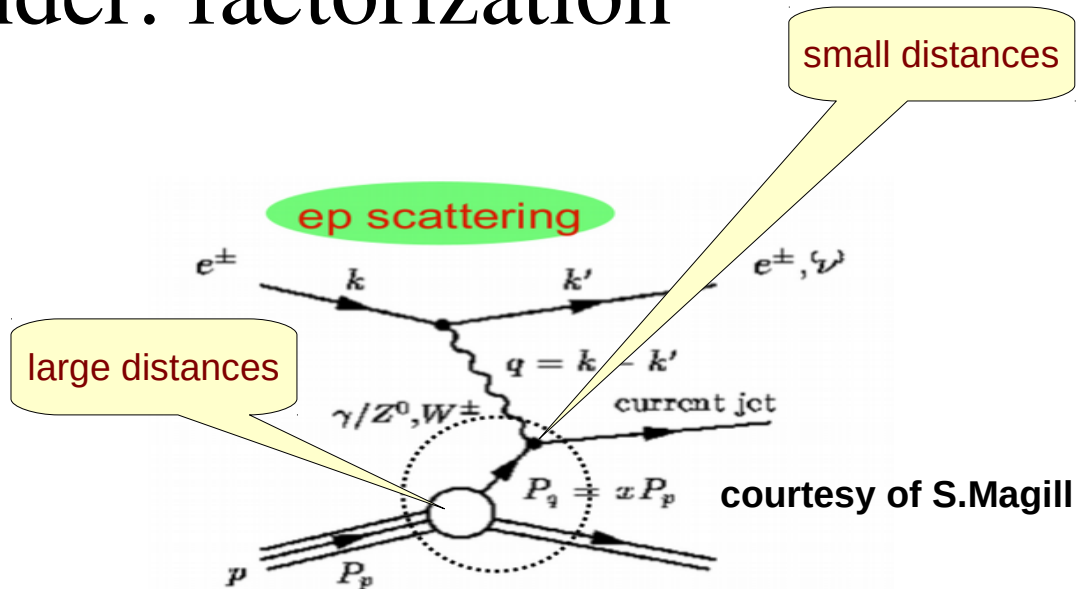
Heavy-quark electro-production with FFN and VFN

- Only 3 light flavors appear in the initial state

- The dominant mechanism is photon-gluon fusion

- The coefficient functions are known up to the NLO
  Witten NPB 104, 445 (1976)
  Laenen, Riemersma, Smith, van Neerven NPB 392, 162 (1993)

- Involved high-order calculations:

  – NNLO terms due to threshold resummation
  Laenen, Moch PRD 59, 034027 (1999)
  Lo Presti, Kawamura, Lo Presti, Moch, Vogt NPB 864, 399 (2012)
  sa, Moch, Blümlein PRD 96, 014011 (2017)

  – limited set of the NNLO Mellin moments
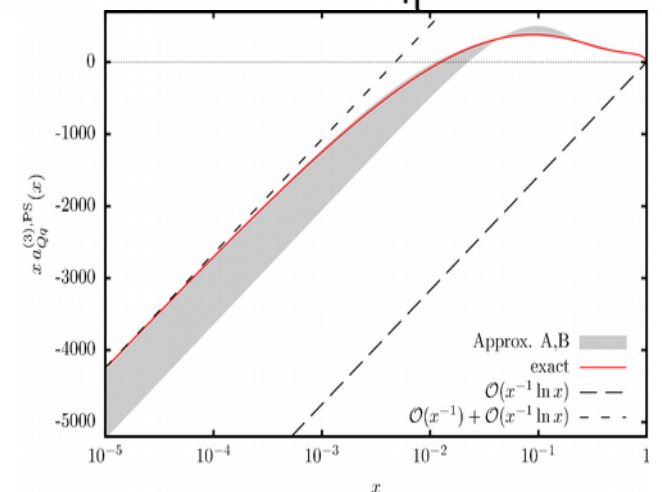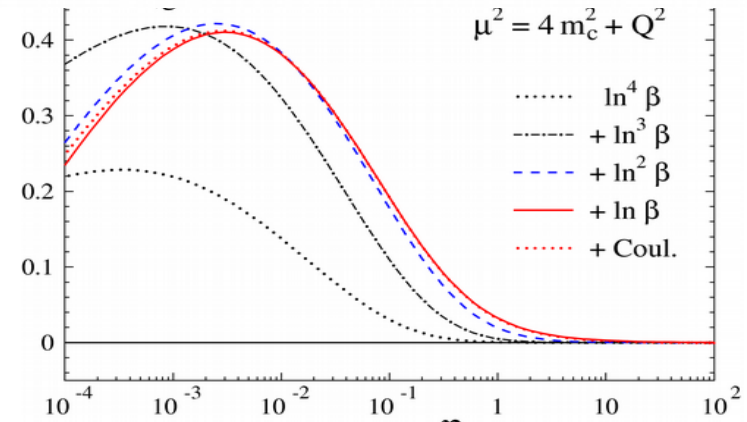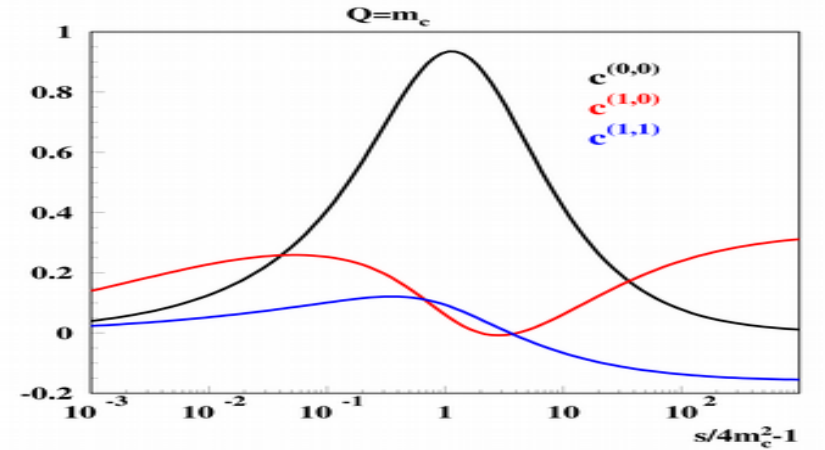 **Ablinger at al. NPB 844, 26 (2011)**
  Bierenbaum, Blümlein, Klein NPB 829, 417 (2009)
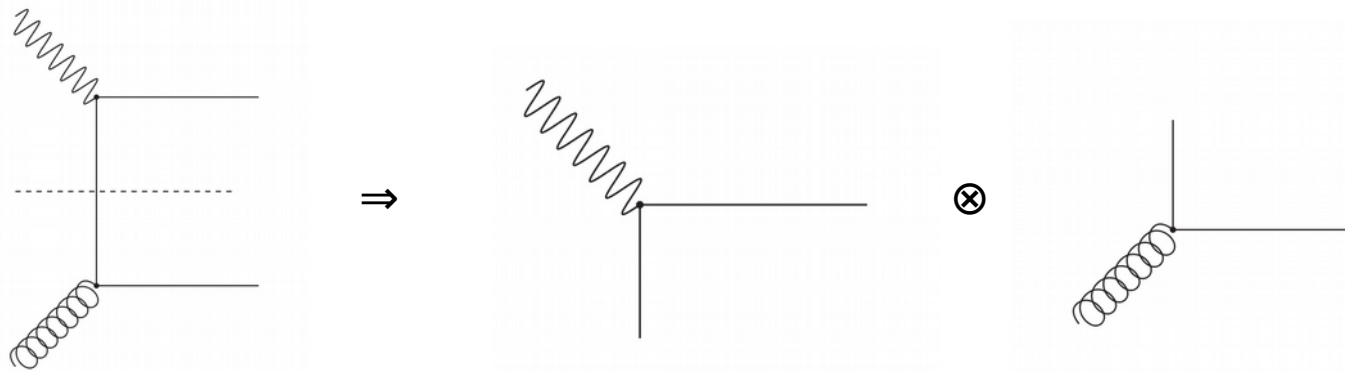 **Ablinger et al. NPB 890, 48 (2014)**

- At large Q the leading-order coefficient $\rightarrow ln(Q/m_h)$
and may be quite big despite the suppression by factor of α_s and should be resummed
  Shifman, Vainstein, Zakharov NPB 136, 157 (1978)

- $\rightarrow$ a motivation to derive the VFN scheme matched to the FFNS (ACOT...., RT..., FONLL....)

FFN and VFN schemes

Collins, Tung NPB 278, 934 (1986)

$$H_{g,2}^{\text{asymp}} = a_s(N_f) A_{hg}^{(1)}$$ Asymptotic 3-flavor coefficient function

LO $$A_{ij}^{(1)}\left(z, \frac{m_h^2}{\mu^2}\right) = a_{ij}^{(1,1)}(z) \ln\left(\frac{\mu^2}{m_h^2}\right)$$ Massive operator matrix elements (OMEs)

$$h^{(1)}(x,\mu^2) = a_s(N_f+1,\mu^2)\left[A_{hg}^{(1)}\left(\frac{m_h^2}{\mu^2}\right) \otimes G^{(2)}\left(N_f,\mu^2\right)\right](x)$$ Matching condition for the heavy-quark PDFs

$$F_{g,2}^{\text{asymp}} = e_h^2 x h^{(1)}(x,\mu^2)$$

Buza, Matiounine, Smith, van Neerven EPJC 1, 301 (1998)

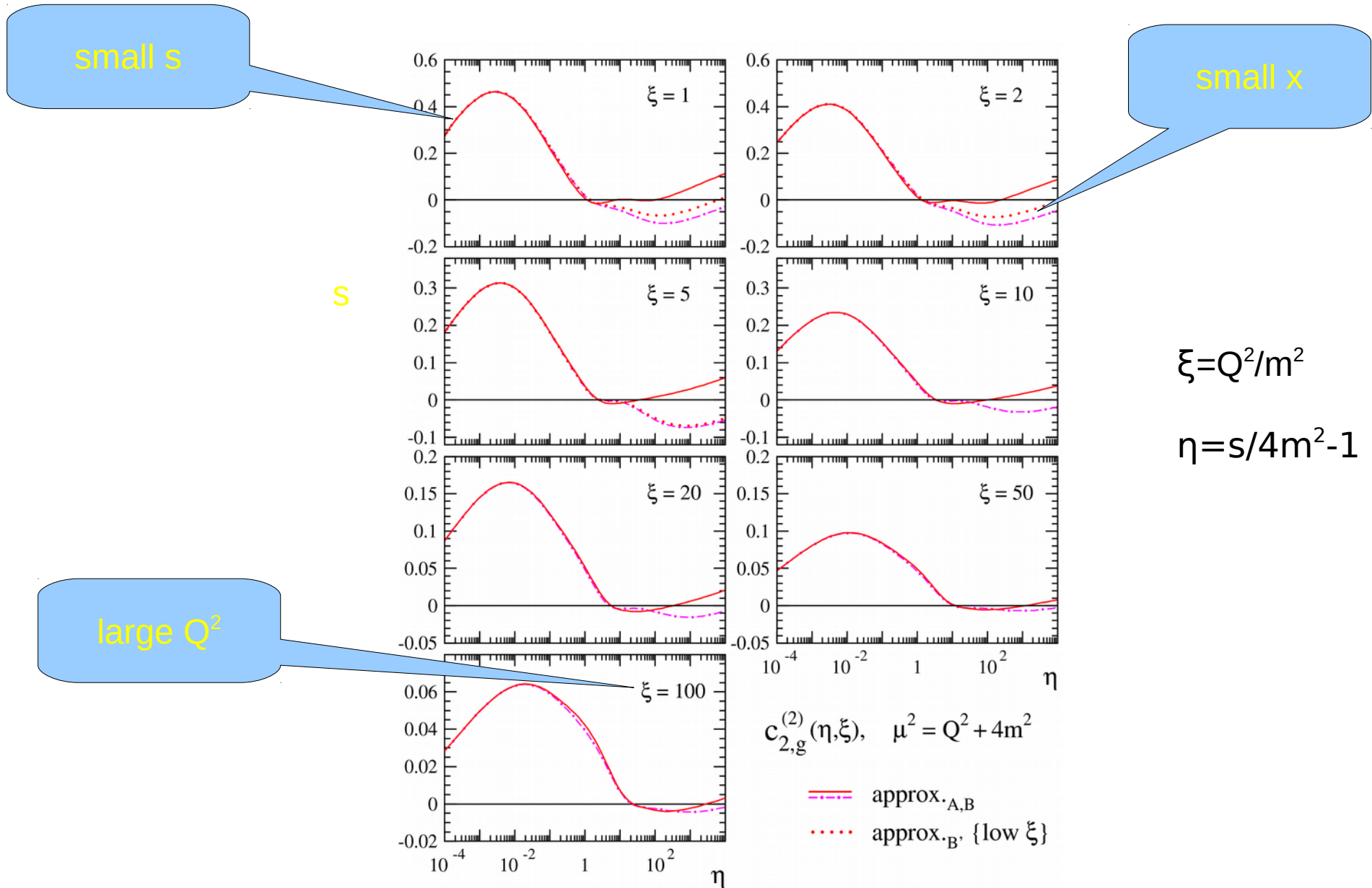NLO   . . .

$$A_{ij}^{(2)}\left(z, \frac{m_h^2}{\mu^2}\right) = a_{ij}^{(2,2)}(z) \ln^2\left(\frac{\mu^2}{m_h^2}\right) + a_{ij}^{(2,1)}(z) \ln\left(\frac{\mu^2}{m_h^2}\right) + a_{ij}^{(2,0)}(z)$$

NNLO   **Blümlein, et al., work in progress**

- The VFN scheme works well at $\mu \gg m_h$ (W,Z,t-quark production,....)
- Problematic for DIS $\Rightarrow$ additional modeling of power-like terms required (ACOT, BMSN, FONLL, RT....)

4

Modeling NNLO massive coefficients

small s

small x

s

large Q^2

$\xi = 1$

$\xi = 2$

$\xi = 5$

$\xi = 10$

$\xi = 20$

$\xi = 50$

$\xi = 100$

$\xi = Q^2/m^2$

$\eta = s/4m^2 - 1$

$c_{2,g}^{(2)}(\eta, \xi), \quad \mu^2 = Q^2 + 4m^2$

approx.$_{A,B}$

approx.$_B$, {low ξ}

Combination of the threshold corrections (small s), high-energy limit (small x), and the NNLO massive OMEs (large Q^2)

Kawamura, Lo Presti, Moch, Vogt NPB 864, 399 (2012)

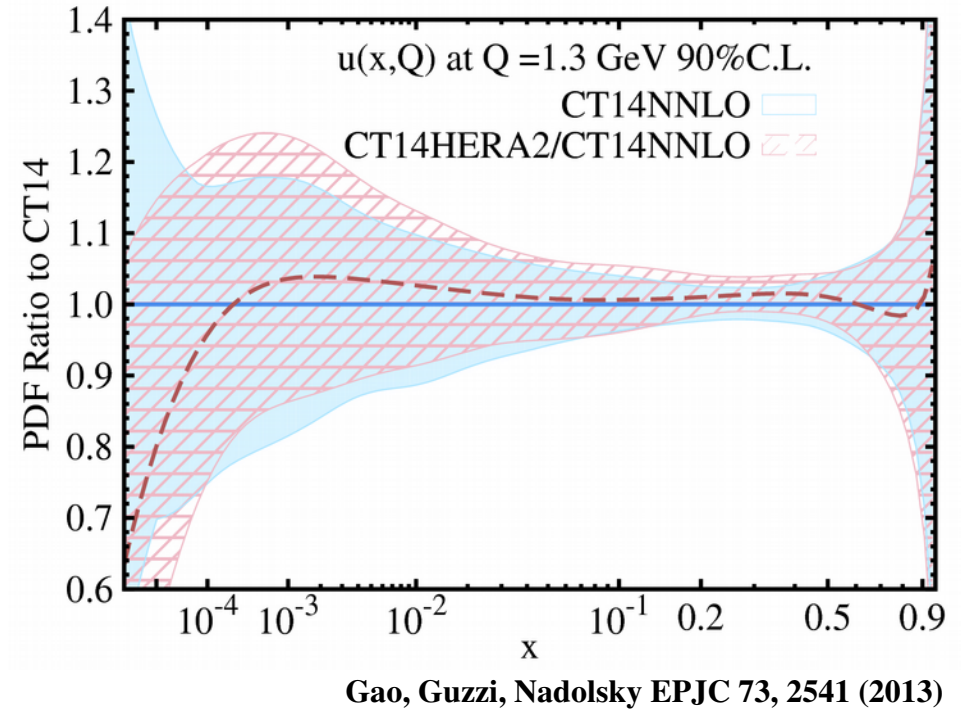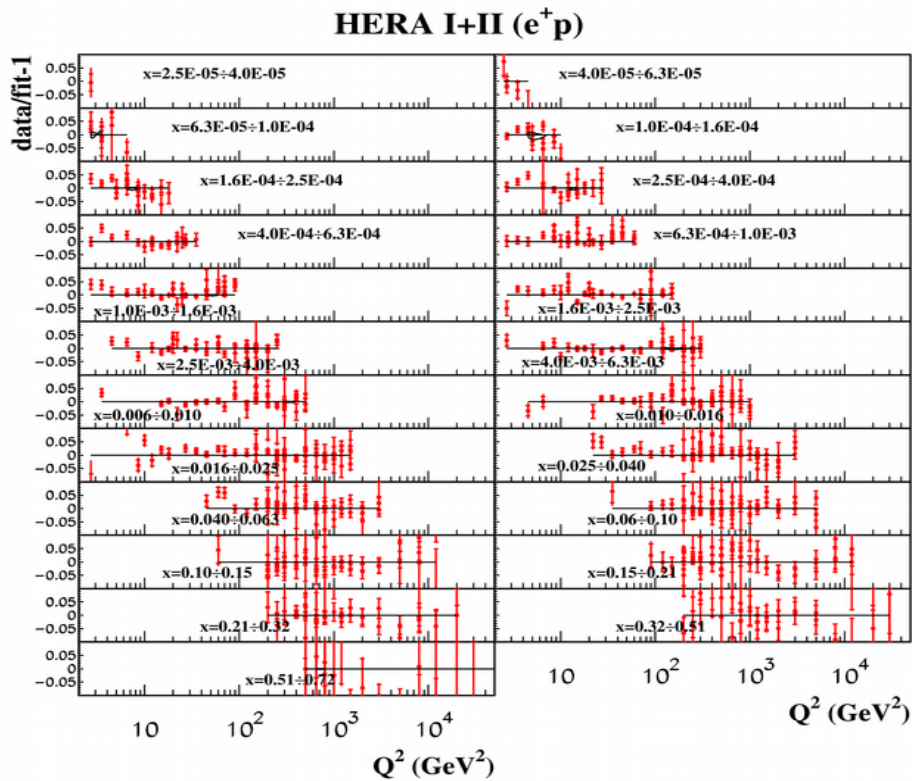# Recent progress in massive DIS coefficients
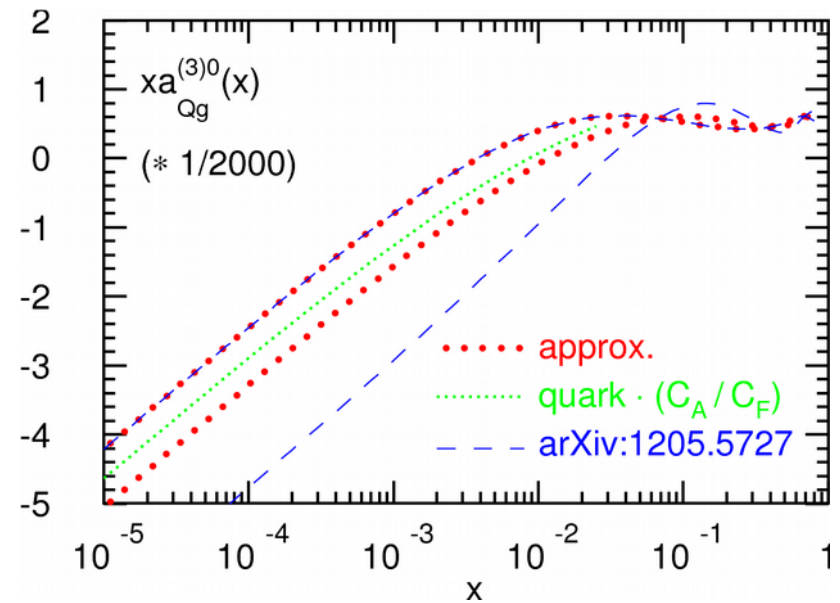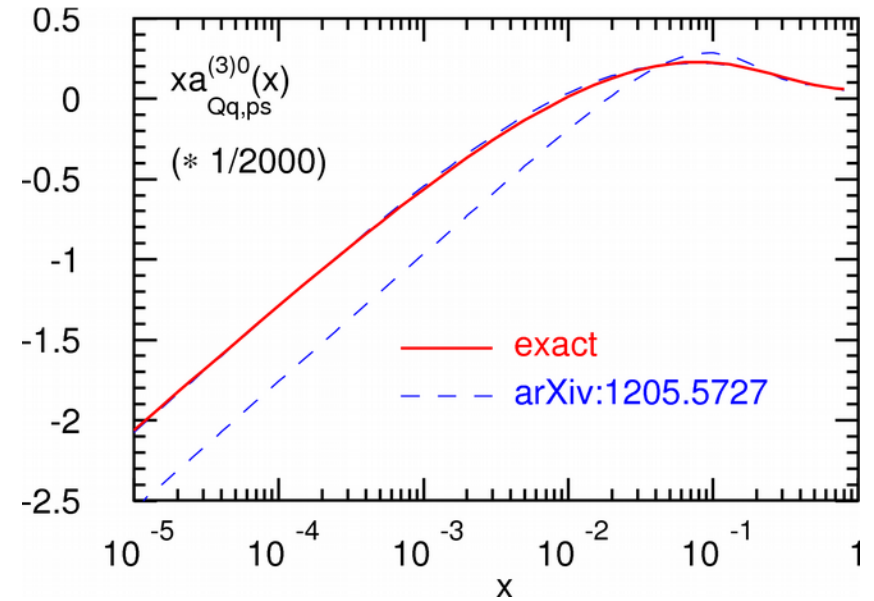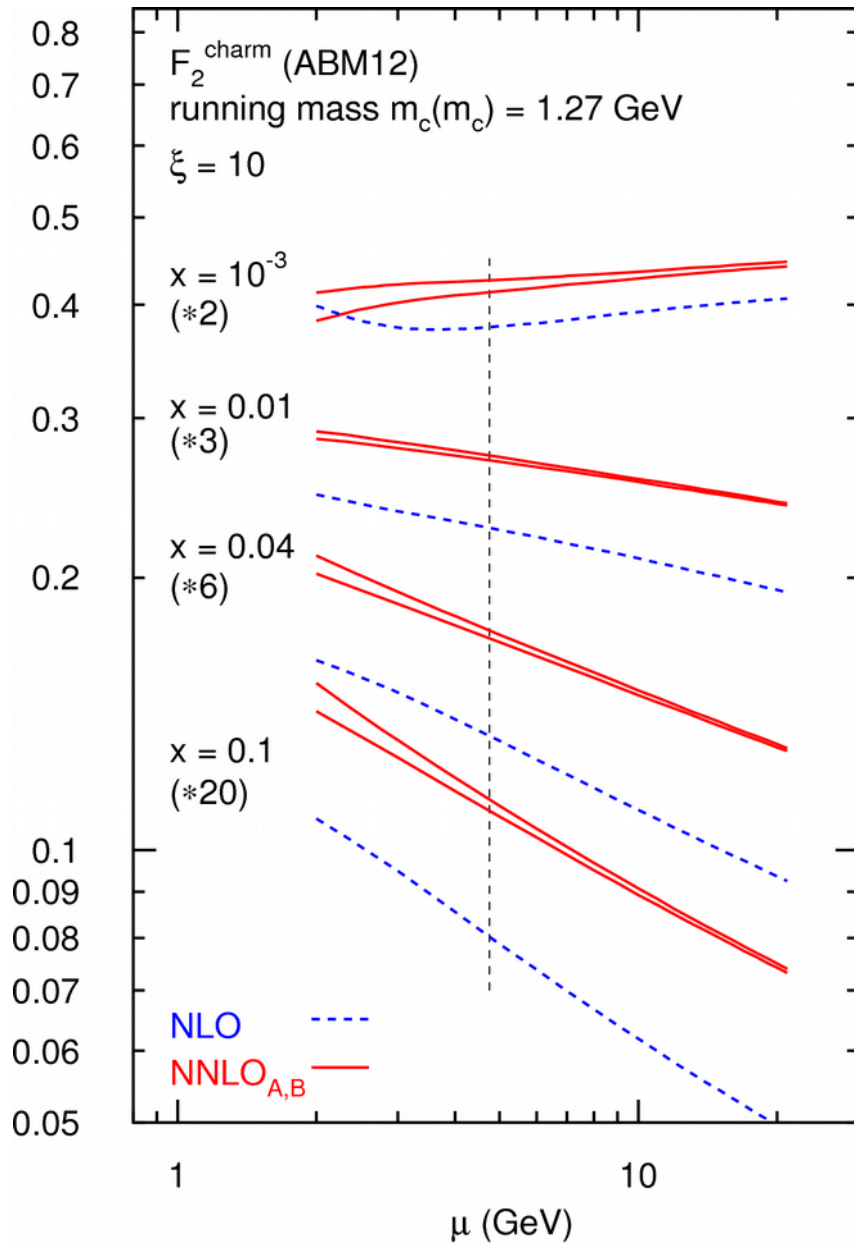
Update with the pure singlet massive OMEs → improved theoretical uncertainties

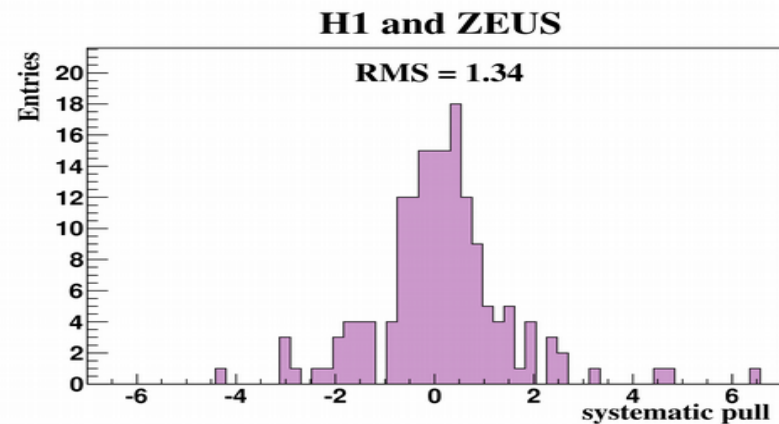**sa, Moch, Blümlein PRD 96, 014011 (2017)**

Inclusive HERA I+II data

HERA I+II (e^+p)

$u(x,Q)$ at $Q =1.3$ GeV 90%C.L.
CT14NNLO
CT14HERA2/CT14NNLO

Q^2(HERA)	χ^2/NDP(HERA)
>2.5 GeV^2	1509/1168=1.29
>5 GeV^2	1354/1092=1.24
>10 GeV^2	1228/1007=1.22

H1 and ZEUS
RMS = 1.34

The value of χ^2/NDP is bigger than 1, however still comparable to the pull distribution width

Factorization scheme benchmarking

H1 and ZEUS

ACOT NLO, F_L $O(\alpha_s)$
FONLL-B NLO, F_L $O(\alpha_s)$ RTOPT NLO, F_L $O(\alpha_s^2)$
FF3B NLO, F_L $O(\alpha_s)$ FF3A NLO, F_L $O(\alpha_s^2)$

H1 and ZEUS EPJC 75, 580 (2015)
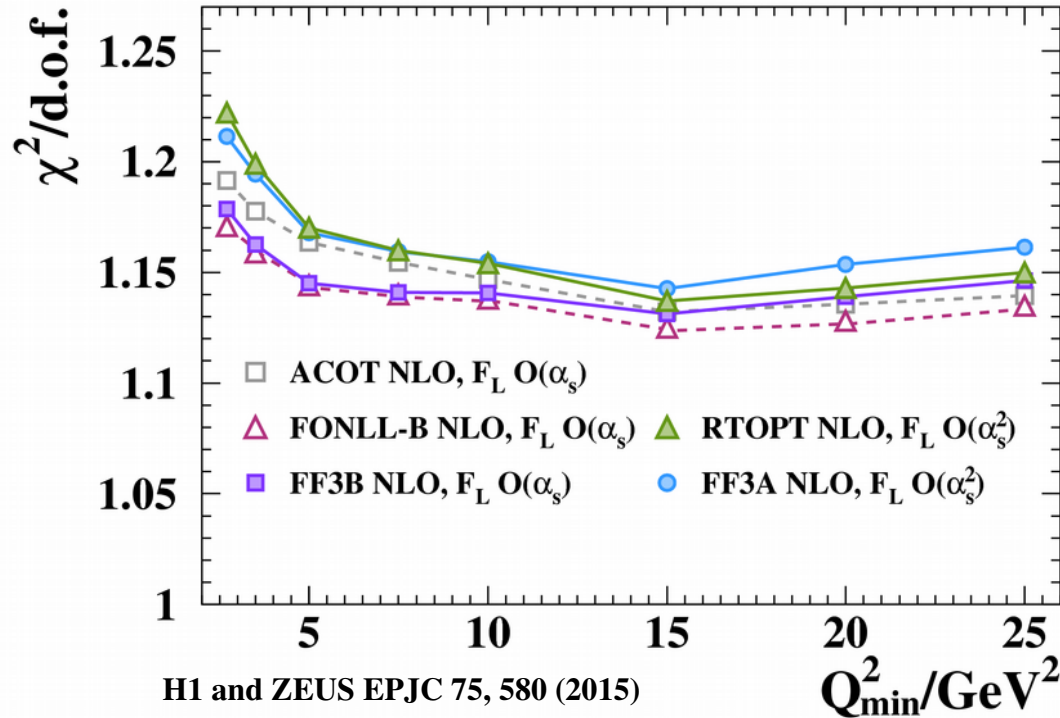
- Data allow to discriminate factorization schemes

- FFN scheme works very well in case of correct setting (running mass definition and correct value of m_c) → no traces of big logs due to resummation

x_{min}	x_{max}	Q^2_{min} (GeV)	Q^2_{max} (GeV)	$\Delta\chi^2$ (DIS)	N^{DIS}_{dat}	$\Delta\chi^2$ (HERA-I)	N^{hera-I}_{dat}
$4 \cdot 10^{-5}$	1	3	10^6	72.2	2936	77.1	592
$4 \cdot 10^{-5}$	0.1	3	10^6	87.1	1055	67.8	405
$4 \cdot 10^{-5}$	0.01	3	10^6	40.9	422	17.8	202
$4 \cdot 10^{-5}$	1	10	10^6	53.6	2109	76.4	537
$4 \cdot 10^{-5}$	1	100	10^6	91.4	620	97.7	412
$4 \cdot 10^{-5}$	0.1	10	10^6	84.9	583	67.4	350
$4 \cdot 10^{-5}$	0.1	100	10^6	87.7	321	87.1	227

"We conclude that the FFN fit is actually based on a less precise theory, in that it does not include full resummation of the contribution of heavy quarks to perturbative PDF evolution, and thus provides a less accurate description of the data" **NNPDF PLB 723, 330(2013)**
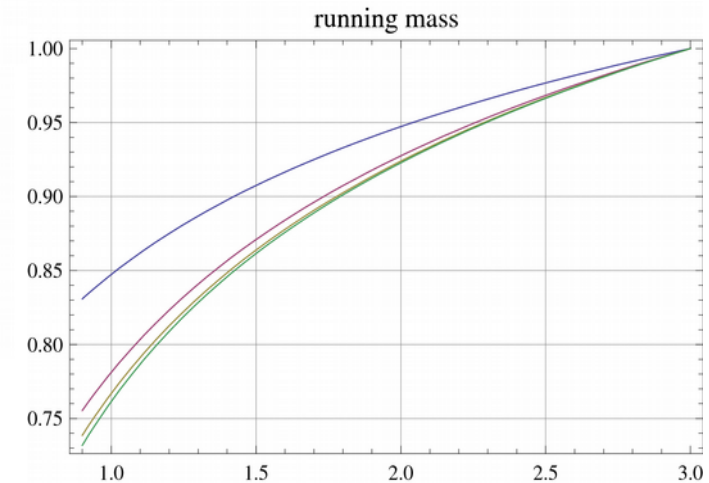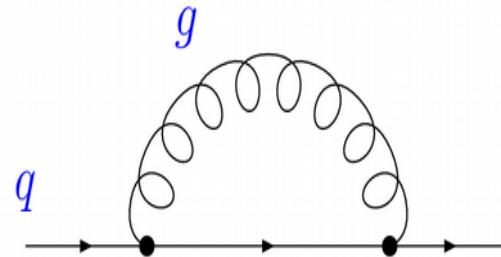
8

Running mass in DIS

The pole mass is defined for the free (*unobserved*) quarks as a the QCD Lagrangian parameter and is commonly used in the QCD calculations

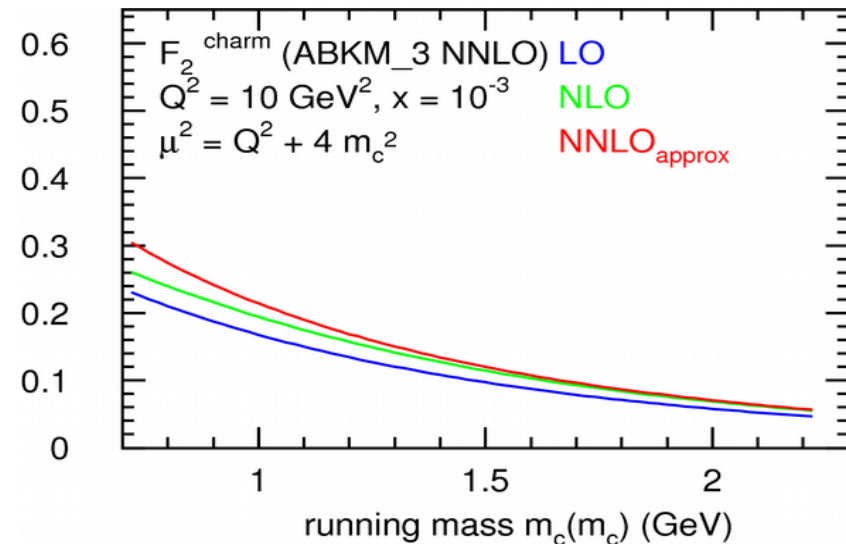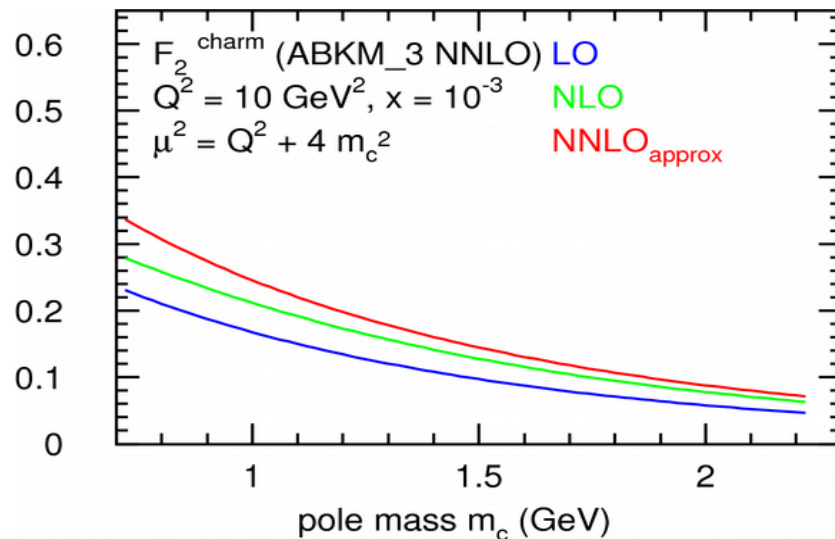$$\mathcal{L} = -\frac{1}{4} F_{\mu\nu} F^{\mu\nu} + \sum_{\text{flavors}} \bar{q}\,(i\slashed{D} - m_q)\,q$$

$$\slashed{p} - m_q - \Sigma(p, m_q)\Big|_{p^2 = m_q^2}$$

running mass

The quantum corrections due to the self-energy loop Integrals receive contribution down to scale of $O(\Lambda_{QCD})$

→ sensitivity to the high order corrections, particularly at the production threshold

$$\mu^2 \frac{d}{d\mu^2} m(\mu) = \gamma(\alpha_s)\,m(\mu)$$

F_2^{charm} (ABKM_3 NNLO) LO
$Q^2 = 10$ GeV^2, x = 10^{-3} NLO
$\mu^2 = Q^2 + 4\,m_c^2$ NNLO$_{\text{approx}}$

pole mass m_c (GeV)

F_2^{charm} (ABKM_3 NNLO) LO
$Q^2 = 10$ GeV^2, x = 10^{-3} NLO
$\mu^2 = Q^2 + 4\,m_c^2$ NNLO$_{\text{approx}}$

running mass $m_c(m_c)$ (GeV)

sa, Moch PLB 699, 345 (2011)

9

c-quark mass in the CMVFN schemes

The values of pole mass m_c used by different groups and preferred by the PDF fits are systematically lower than the PDG value

H1/ZEUS PLB 718, 550 (2012)
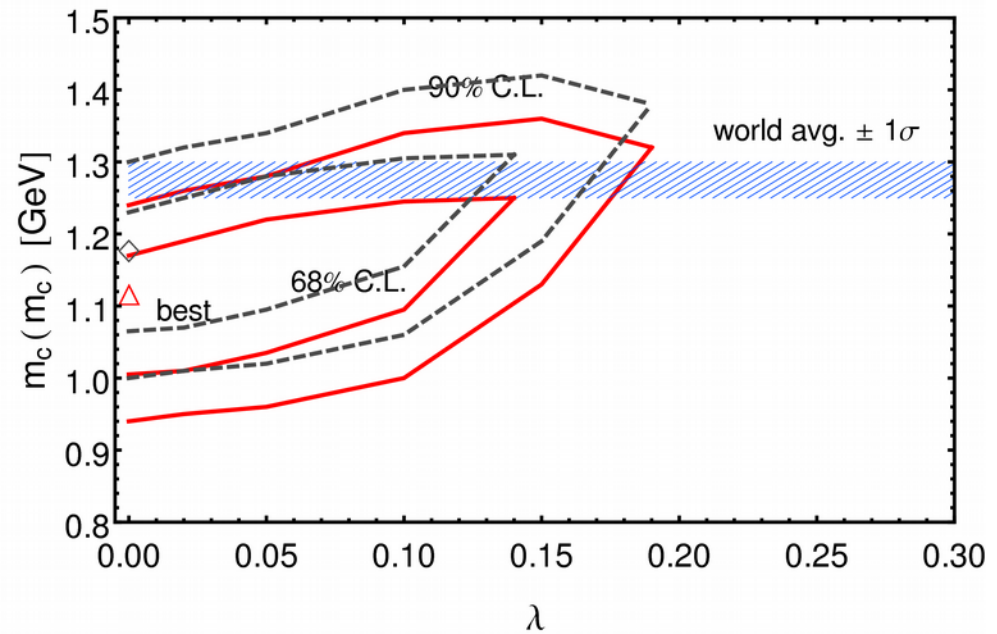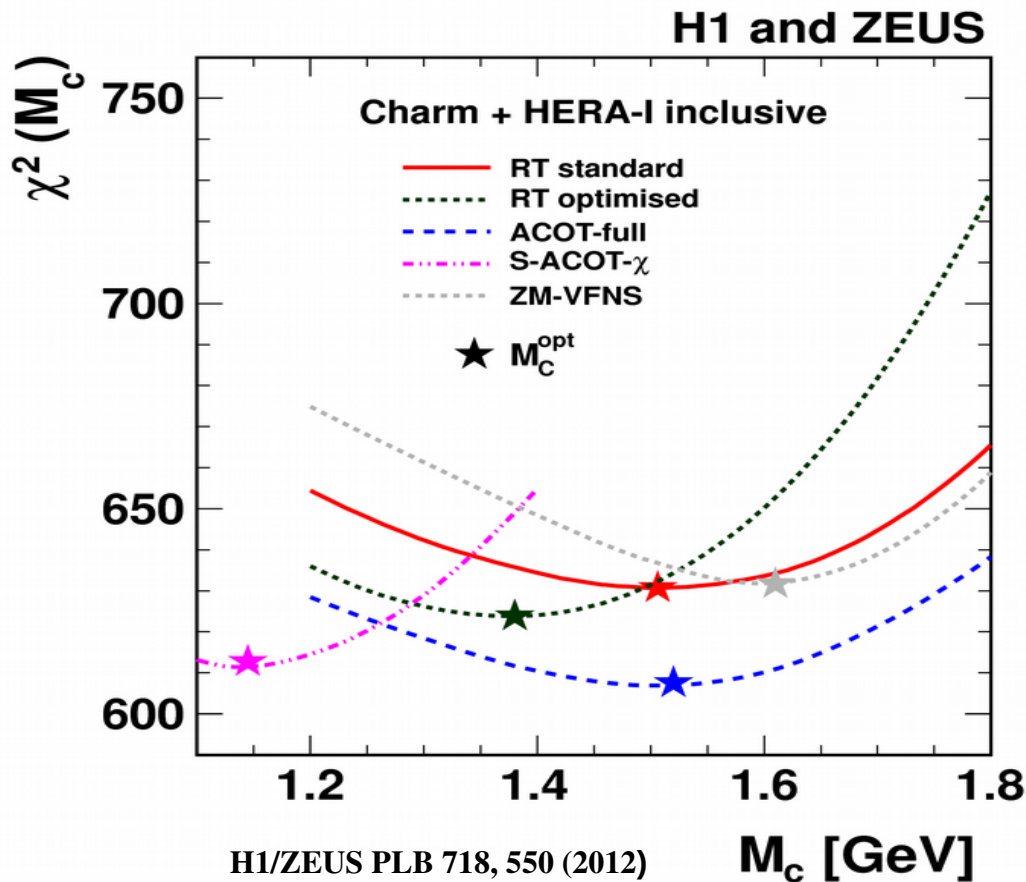
$m_c(m_c)$=1.19+0.08-0.15 GeV ACOT....
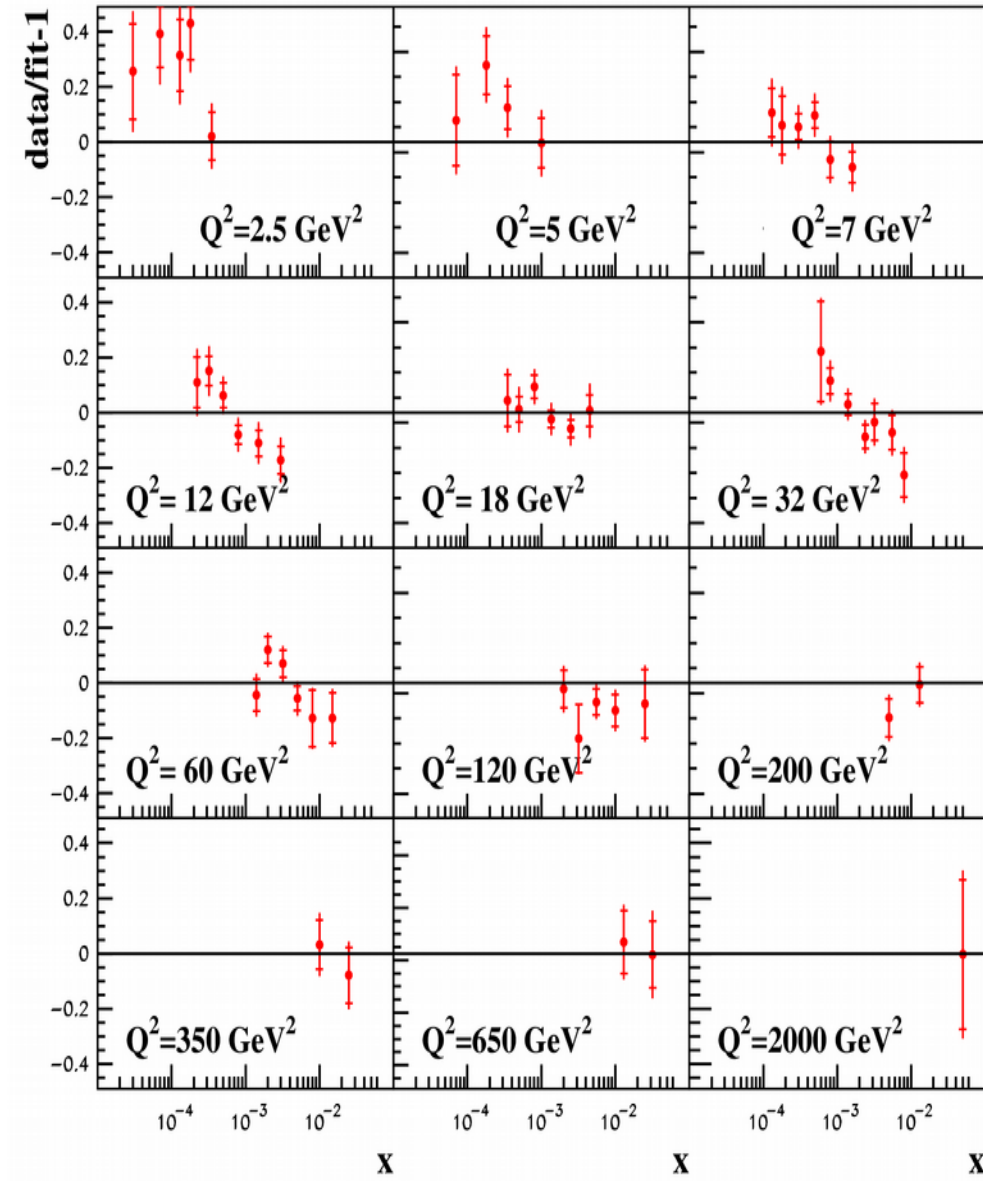
Gao, Guzzi, Nadolsky EPJC 73, 2541 (2013)

$m_c(m_c)$=1.34+0.04-0.01 GeV FONLL

Bertone et. al JHEP 1608, 050 (2016)

Wide spread of the m_c obtained in different version of the GMVFN schemes →
quantitative illustration of the GMVFNS uncertainties

HERA charm data and $m_c(m_c)$

HERA I+II (ep --> e charm X)

X^2/NDP=66/52
$m_c(m_c)$=1.252±0.018(exp.)-0.01(th.) GeV
ABMP16

$m_c(m_c)$=1.24±0.03(exp.) GeV   ABM12

m_c(pole)~1.9 GeV (NNLO)

- RT optimal
  X^2/NDP=82/52   NNLO
  m_c(pole)=1.25 GeV

- S-ACOT-χ
  X^2/NDP=59/47   NNLO
  m_c(pole)=1.3 GeV

- F0NLL
  X^2/NDP=60/47   NNLO
  m_c(pole)=1.275 GeV

- F0NLL
  X^2/NDP=54/37   NNLO
  m_c(pole)=1.51 GeV, intrinsic charm included

$m_c(m_c)$=1.246±0.023 (h.o.) GeV NNLO

Forward DY kinematics at Tevatron and the LHC

In the forward region $x_2 \gg x_1$

$\sigma(W^+) \sim u(x_2)\, dbar(x_1)$

$\sigma(W^-) \sim d(x_2)\, ubar(x_1)$
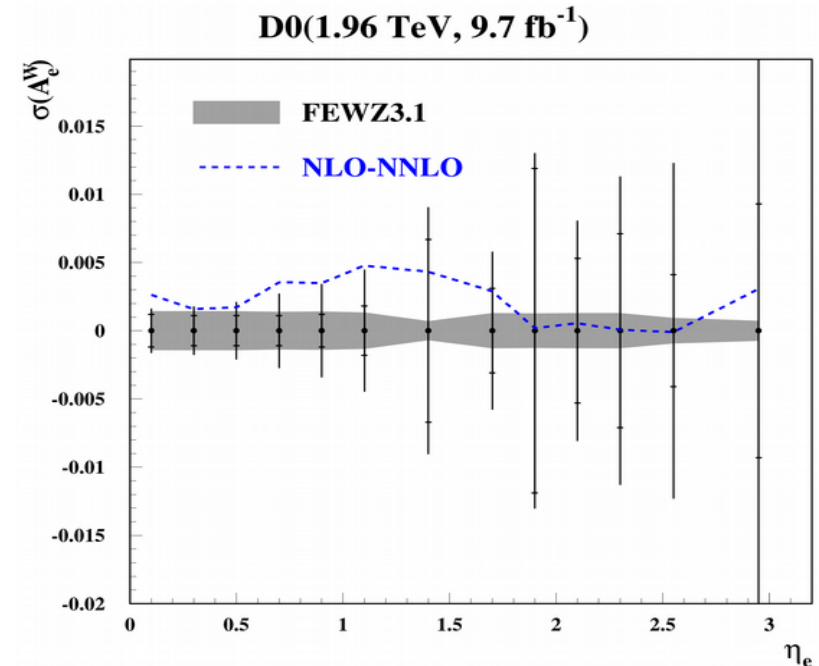
$\sigma(Z) \sim Q_U^2 u(x_2)\, ubar(x_1) + Q_D^2 d(x_2)\, dbar(x_1)$

$\sigma(DIS) \sim q_u^2 u(x_2) + q_d^2 d(x_2)$

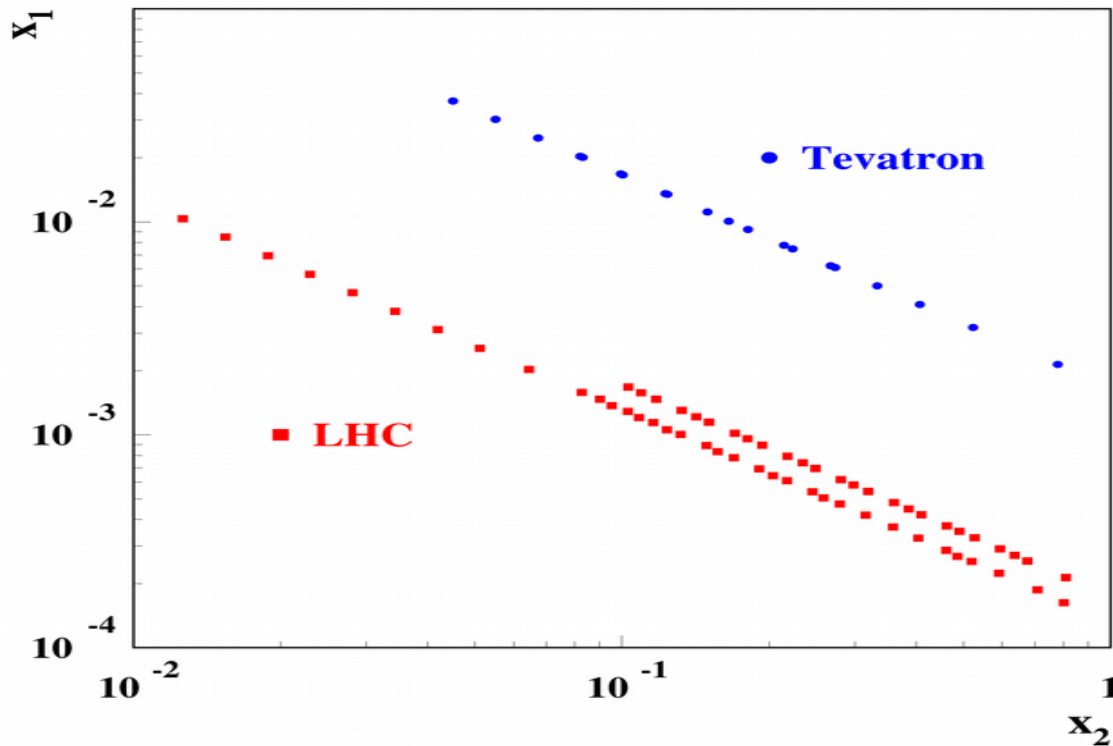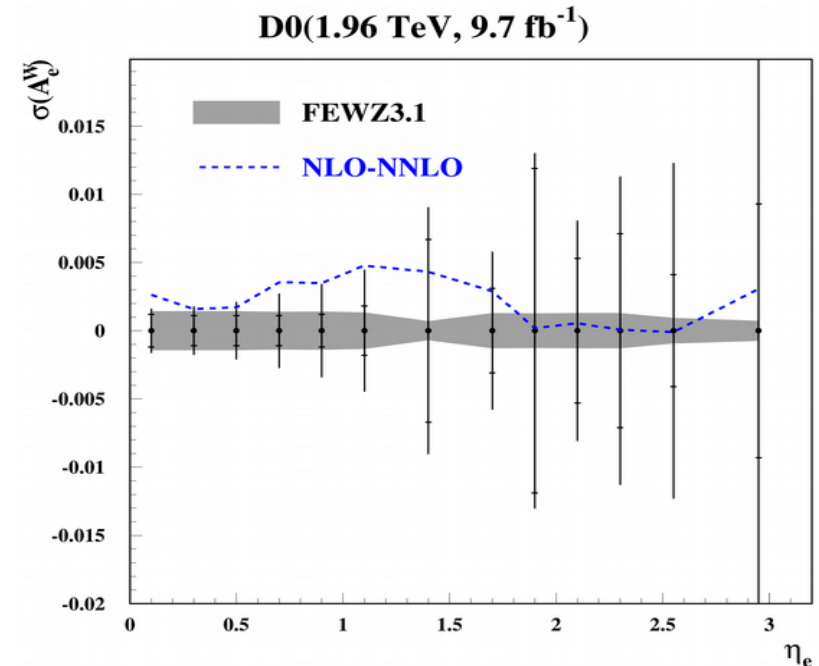*Forward W&Z production probes small/large x and is complementary to the DIS → good quark disentangling*

- fully differential kinematics; existing NNLO codes, DYNNLO and FEWZ requre huge computing resources to achieve the promille accuracy required

- DYNNLO-FEWZ difference not fully resolved

Salam ATLAS SM workshop 2014

Yannick Ulrich, Barchelor thesis, Univ. of Hamburg 2015

12

Forward DY kinematics at Tevatron and the LHC

In the forward region $x_2 >> x_1$

$\sigma(W^+) \sim u(x_2)\, dbar\,(x_1)$

$\sigma(W^-) \sim d(x_2)\, ubar(x_1)$

$\sigma(Z) \sim Q_U^2 u(x_2)\, ubar\,(x_1) + Q_D^2 d(x_2)\, dbar(x_1)$

$\sigma(DIS) \sim q_u^2 u(x_2) + q_d^2 d(x_2)$

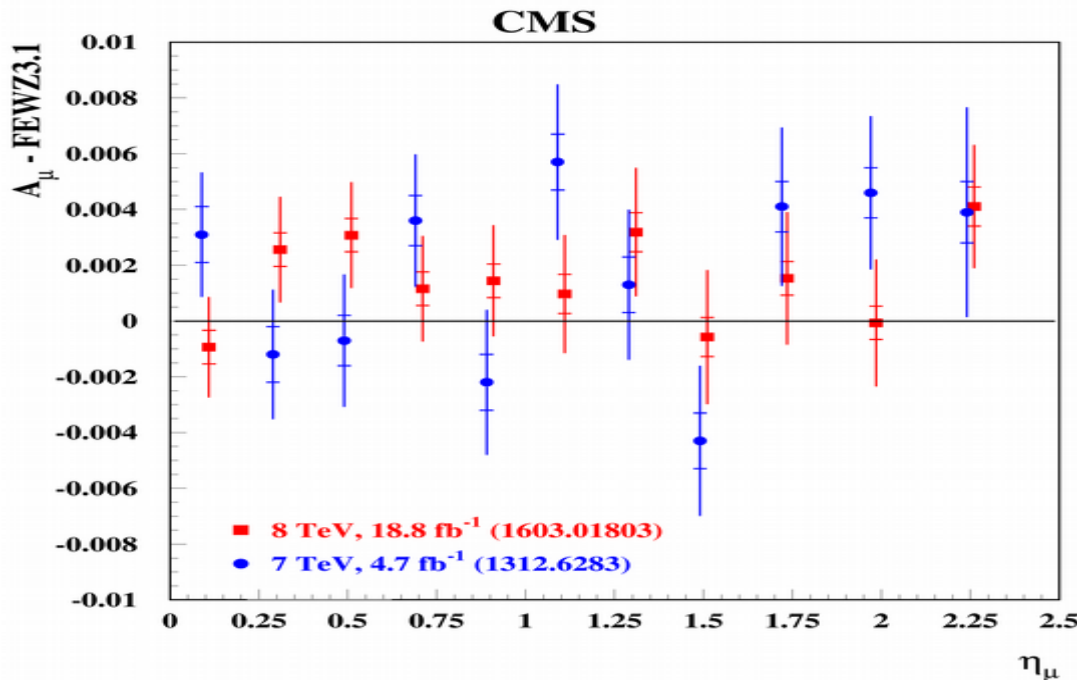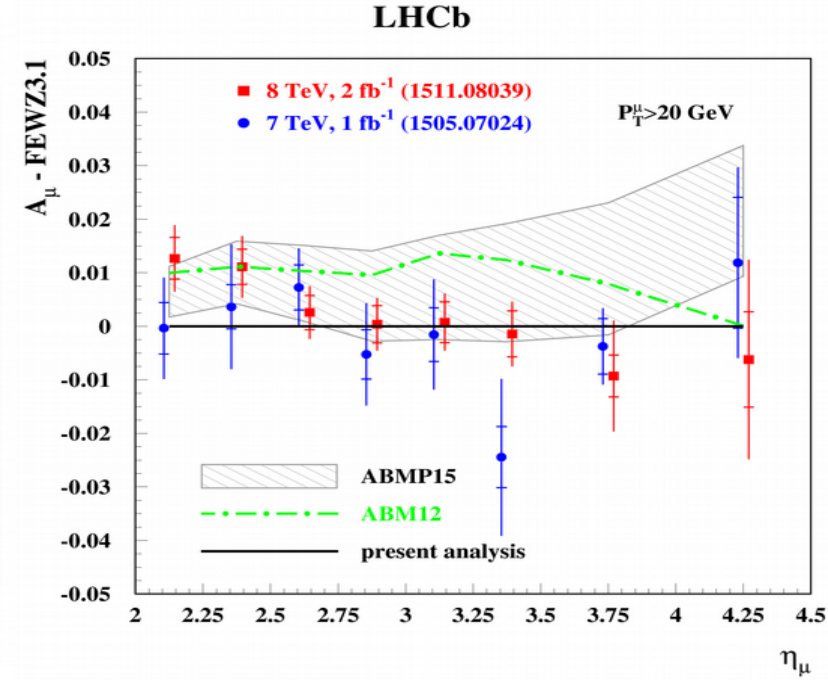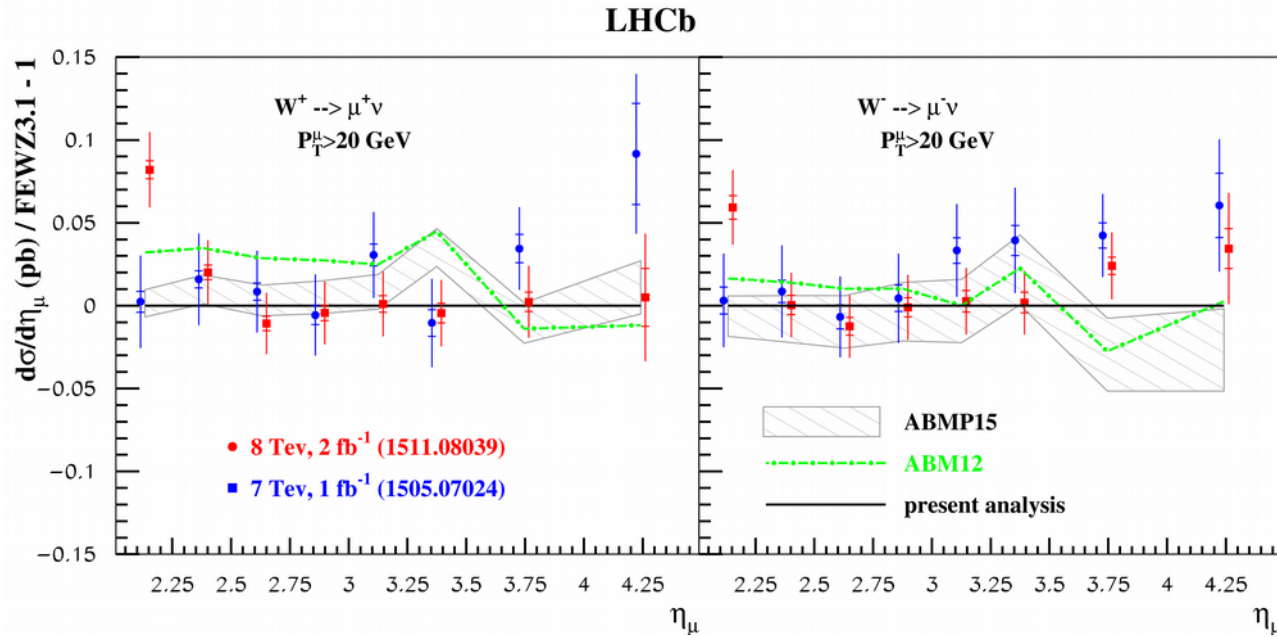*Forward W&Z production probes small/large x and is complementary to the DIS → good quark disentangling*

- fully differential kinematics; existing NNLO codes, DYNNLO and FEWZ requre huge computing resources to achieve the promille accuracy required

- DYNNLO-FEWZ difference not fully resolved

Salam ATLAS SM workshop 2014

Yannick Ulrich, Barchelor thesis, Univ. of Hamburg 2015

13

Most recent DY inputs

Filtering of the LHCb data has been performed:
  – a bump at 7 Tev and Y=3.275
(not confirmed by the LHCb data at 8 TeV)
  – and excess at 8 TeV and Y=2.125
(not confirmed by the CMS data at 8 TeV)

The CMS data at 8 TeV are much smoother than the ones at 7 TeV:
    χ²=17/22 versus 22/11

sa, Blümlein, Moch, Plačakytė PRD 96, 014011 (2017)

DY data selection in the ABMP16 fit

Experiment	ATLAS		CMS		DØ		LHCb		
$\sqrt{s}$ (TeV)	7	13	7	8	1.96		7		8
Final states	$W^+ \to l^+\nu$ $W^- \to l^-\nu$ $Z \to l^+l^-$	$W^+ \to l^+\nu$ $W^- \to l^-\nu$ $Z \to l^+l^-$	$W^+ \to \mu^+\nu$ $W^- \to \mu^-\nu$ (asym)	$W^+ \to \mu^+\nu$ $W^- \to \mu^-\nu$	$W^+ \to \mu^+\nu$ $W^- \to \mu^-\nu$ (asym)	$W^+ \to e^+\nu$ $W^- \to e^-\nu$ (asym)	$W^+ \to \mu^+\nu$ $W^- \to \mu^-\nu$ $Z \to \mu^+\mu^-$	$Z \to e^+e^-$	$W^+ \to \mu^+\nu$ $W^- \to \mu^-\nu$ $Z \to \mu^+\mu^-$
Cut on the lepton P_T	$P_T^l > 20$ GeV	$P_T^e > 25$ GeV	$P_T^\mu > 25$ GeV	$P_T^\mu > 25$ GeV	$P_T^\mu > 25$ GeV	$P_T^e > 25$ GeV	$P_T^\mu > 20$ GeV	$P_T^e > 20$ GeV	$P_T^\mu > 20$ GeV
Luminosity (1/fb)	0.035	0.081	4.7	18.8	7.3	9.7	1	2	2.9
NDP	30	6	11	22	10	13	31(33) [a]	17	32(34)
ABMP16	31.0	9.2	22.4	16.5	17.6	19.0	45.1(54.4)	21.7	40.0(59.2)
CJ15	–	–	–	–	20	29	–	–	–
CT14	42	–	–[b]	–	–	34.7	–	–	–
HERAFitter	–	–	–	–	13	19	–	–	–
MMHT16	39[c]	–	–	21	21[c]	26	(43)	29	(59)
NNPDF3.1	29	–	19	–	16	35	(59)	19	(47)

[a] The values of NDP and χ^2 correspond to the unfiltered samples.
[b] For the statistically less significant data with the cut of $P_T^\mu > 35$ GeV the value of $\chi^2 = 12.1$ was obtained.
[c] The value obtained in MMHT14 fit.

- Many early low-statistical Tevatron and LHC data are not included into the fit

- The D0 sample for the charge-lepton asymmetry is preferred as compared to the W-asymmetry: smaller sensitivity to the modeling details; might even introduce a bias due to data sets' discrepancy

D0 (1.96 TeV, 9.7 fb⁻¹)

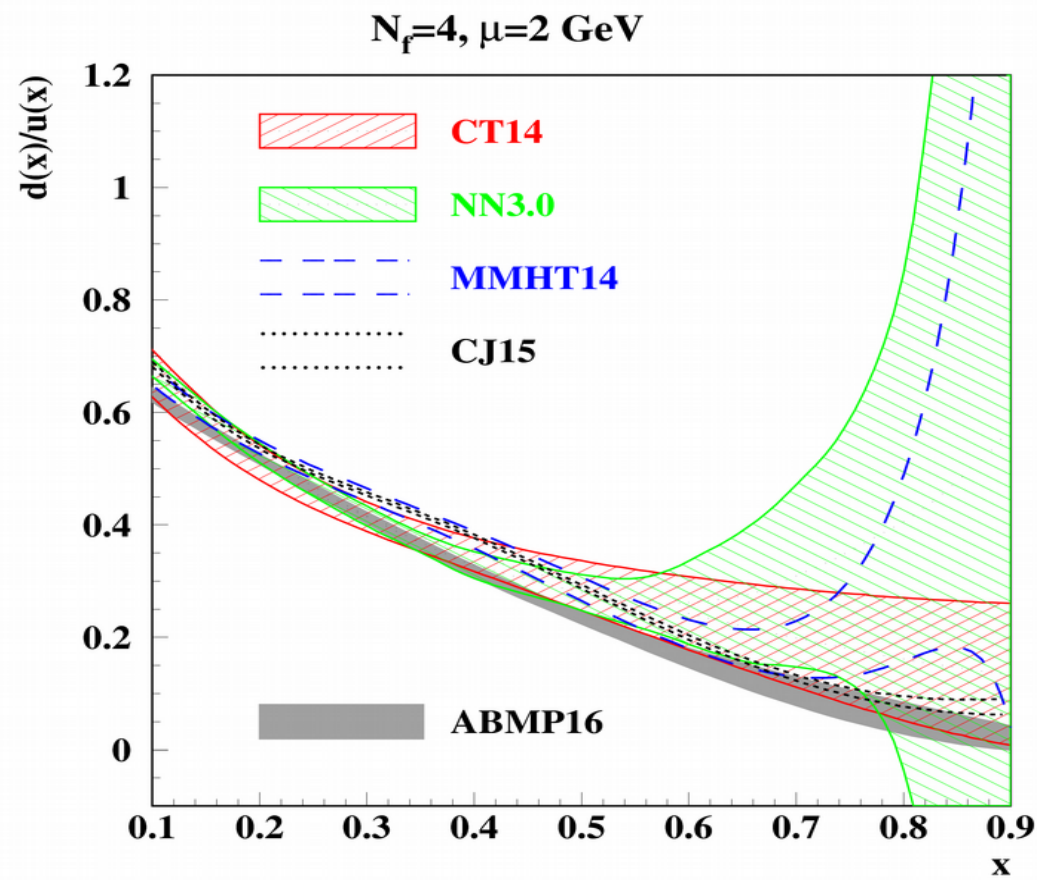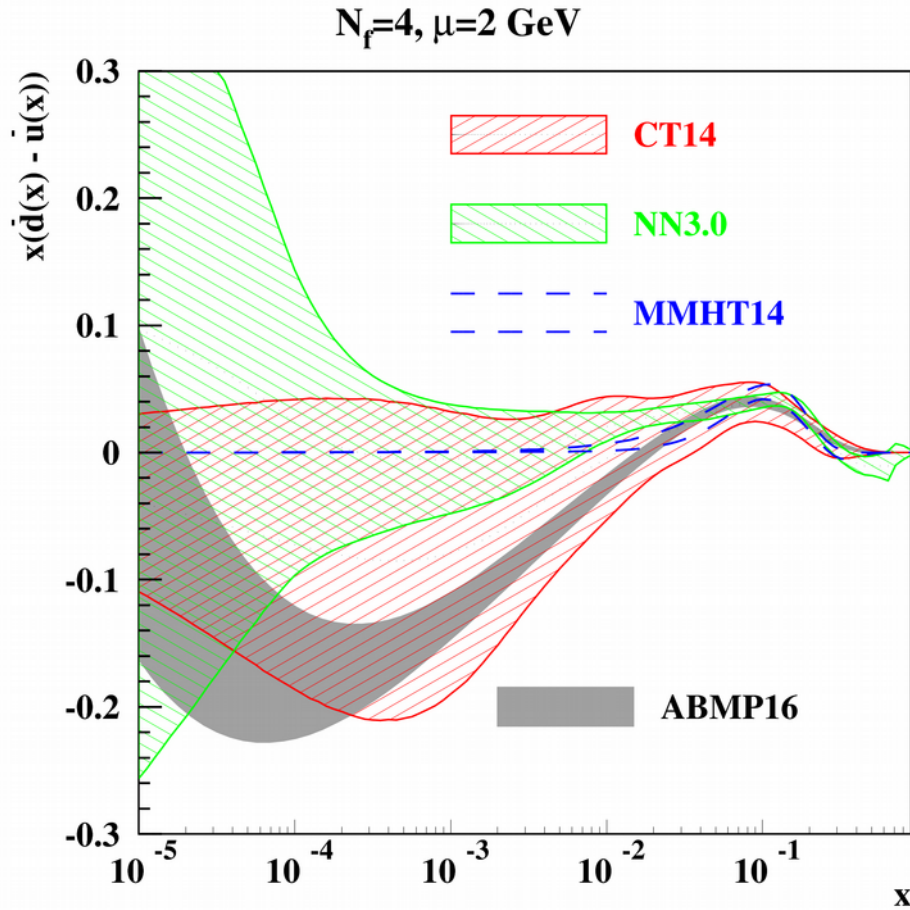sa, Blümlein, Moch, Plačakytė PRD 94, 114038 (2016)
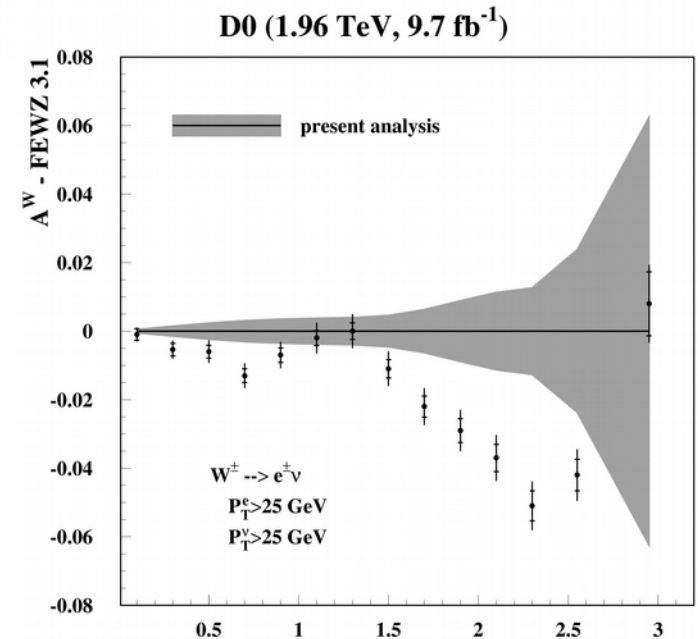
# Impact of the W-, Z-data in ABMP16 fit
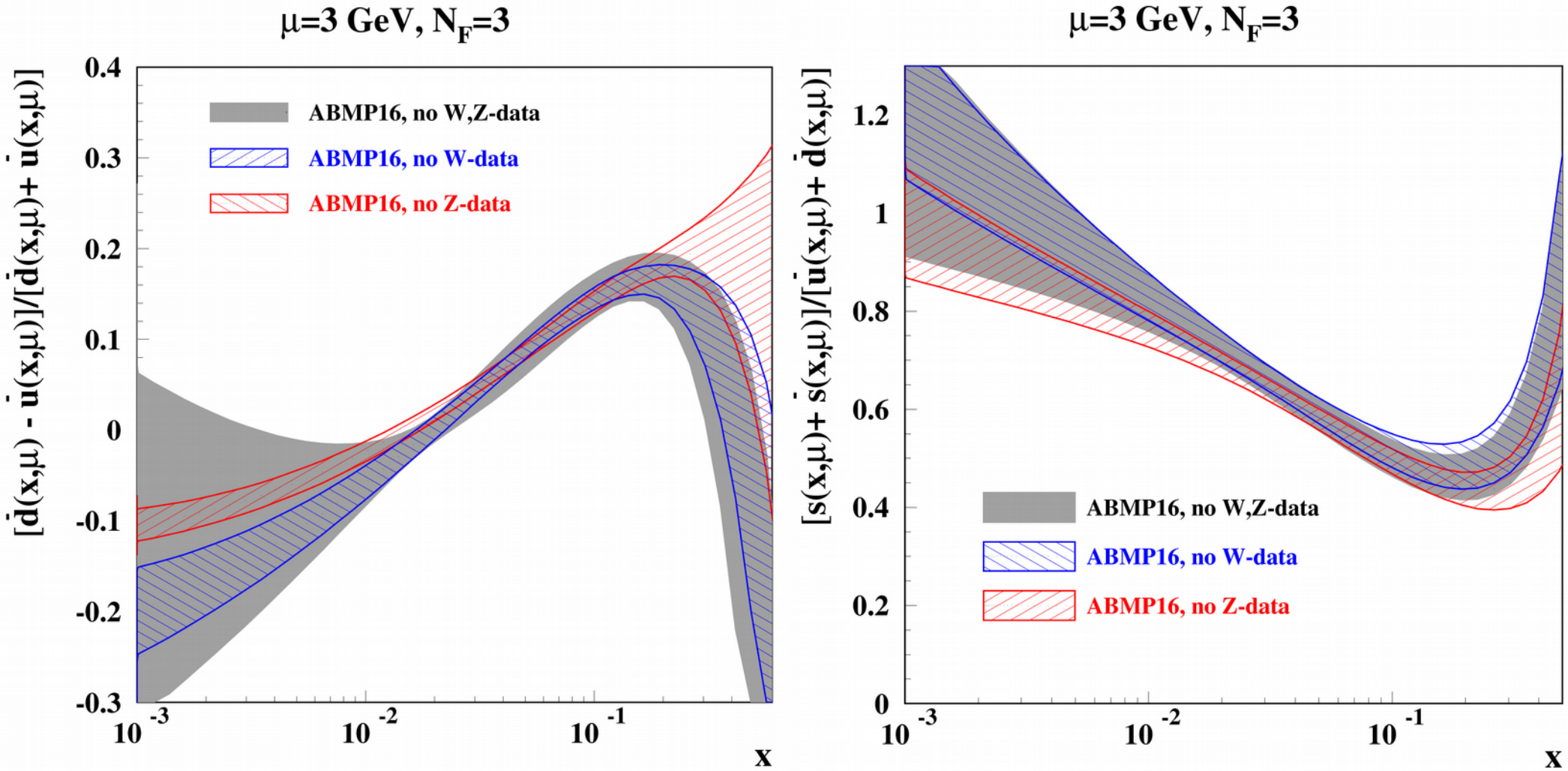

W-, Z-data really control quark disentangling at small x

Comparison of various PDF fits


- Relaxed form of the sea iso-spin asymmetry I(x) at small x; Regge-like behaviour is recovered only at x~10^{-6}; at large x it is still defined by the phase-space constraint

- Good constraint on the d/u ratio w/o deuteron data → independent extraction of the deuteron corrections   **Accardi, Brady, Melnitchouk, Owens, Sato hep-ph/1602.03154;**

- Big spread between different PDF sets, up to factor of 30 at large x → poor control of the BSM effects without constraints from the DY data
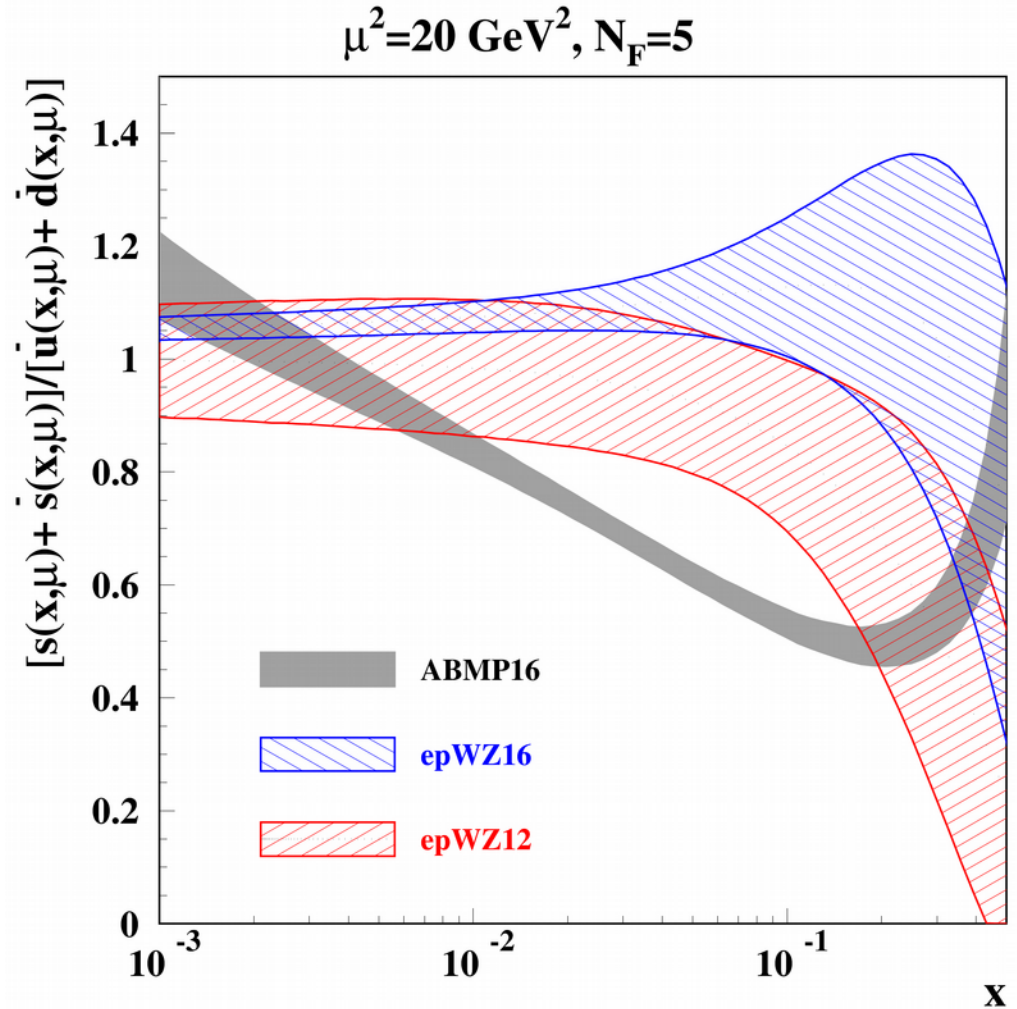
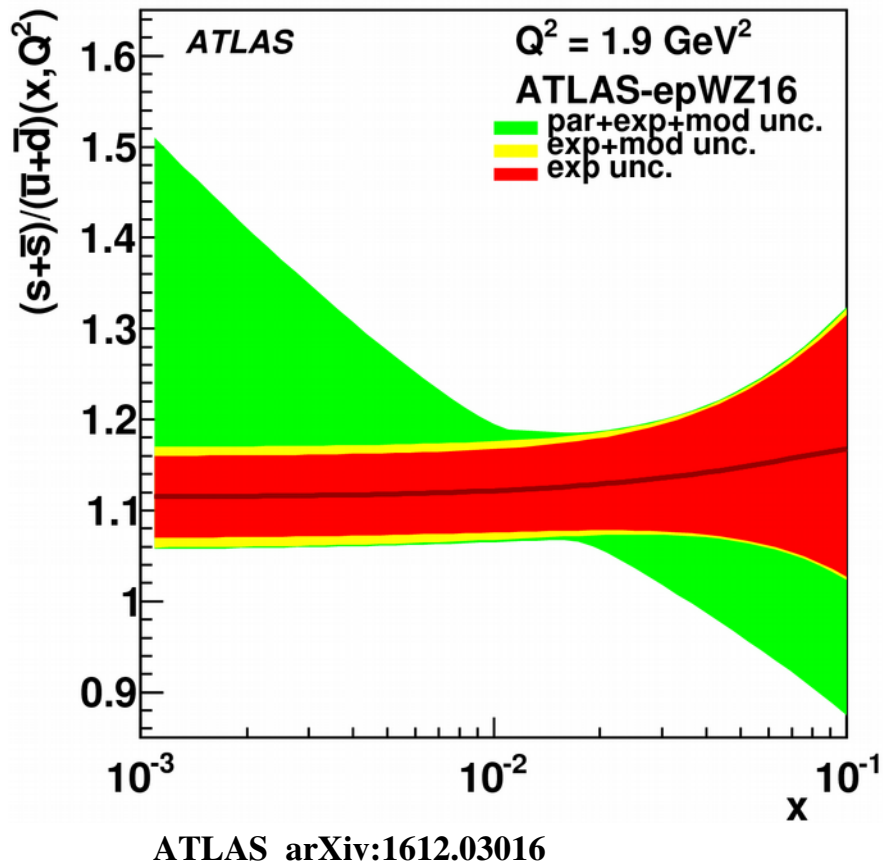# MMHT14 update with DY LHC data

Thorne, Harland-Lang, Martin hep-ph/1708.00047
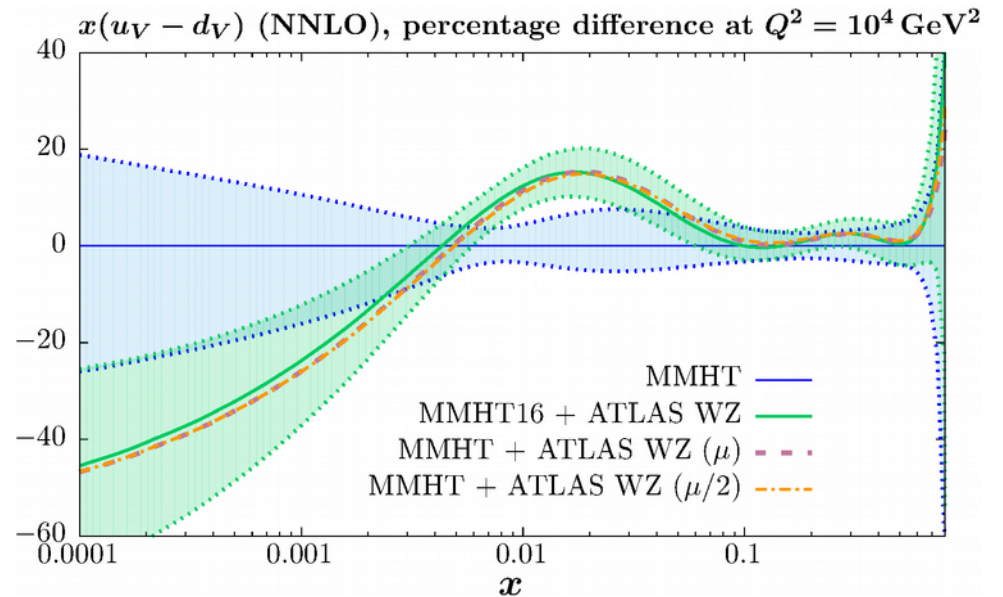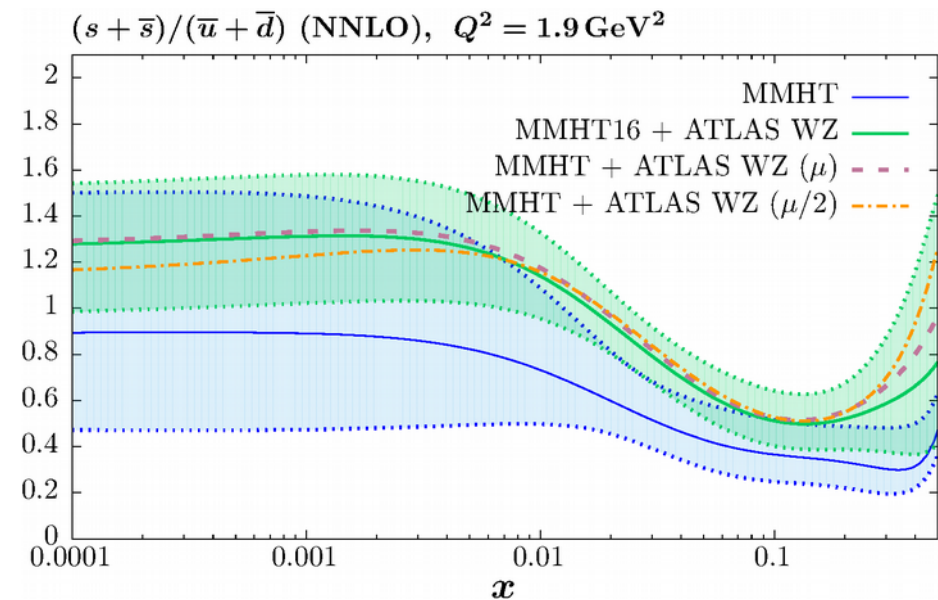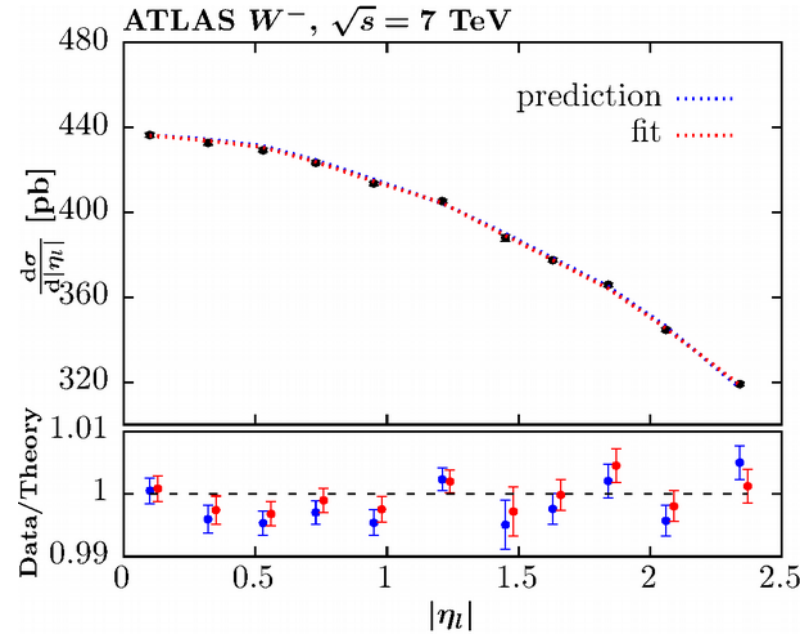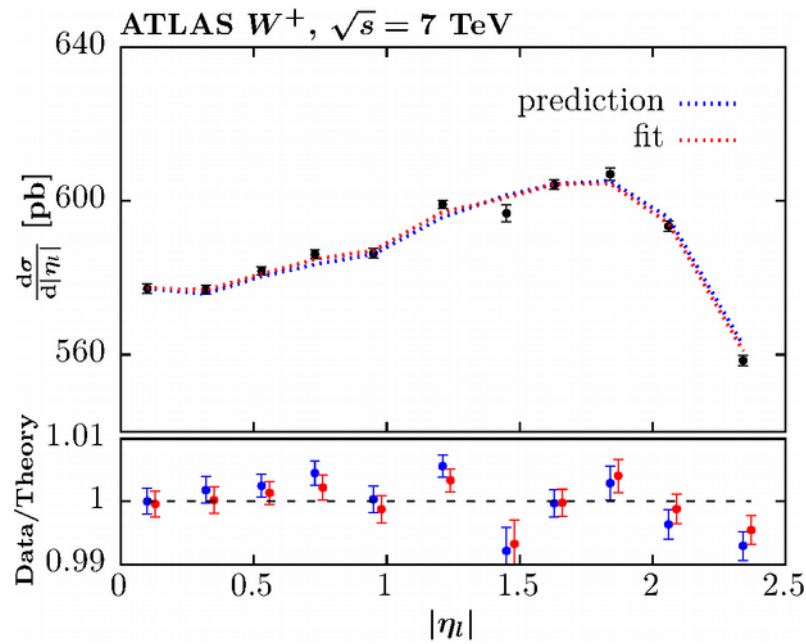
NNPDF update including DY LHC data
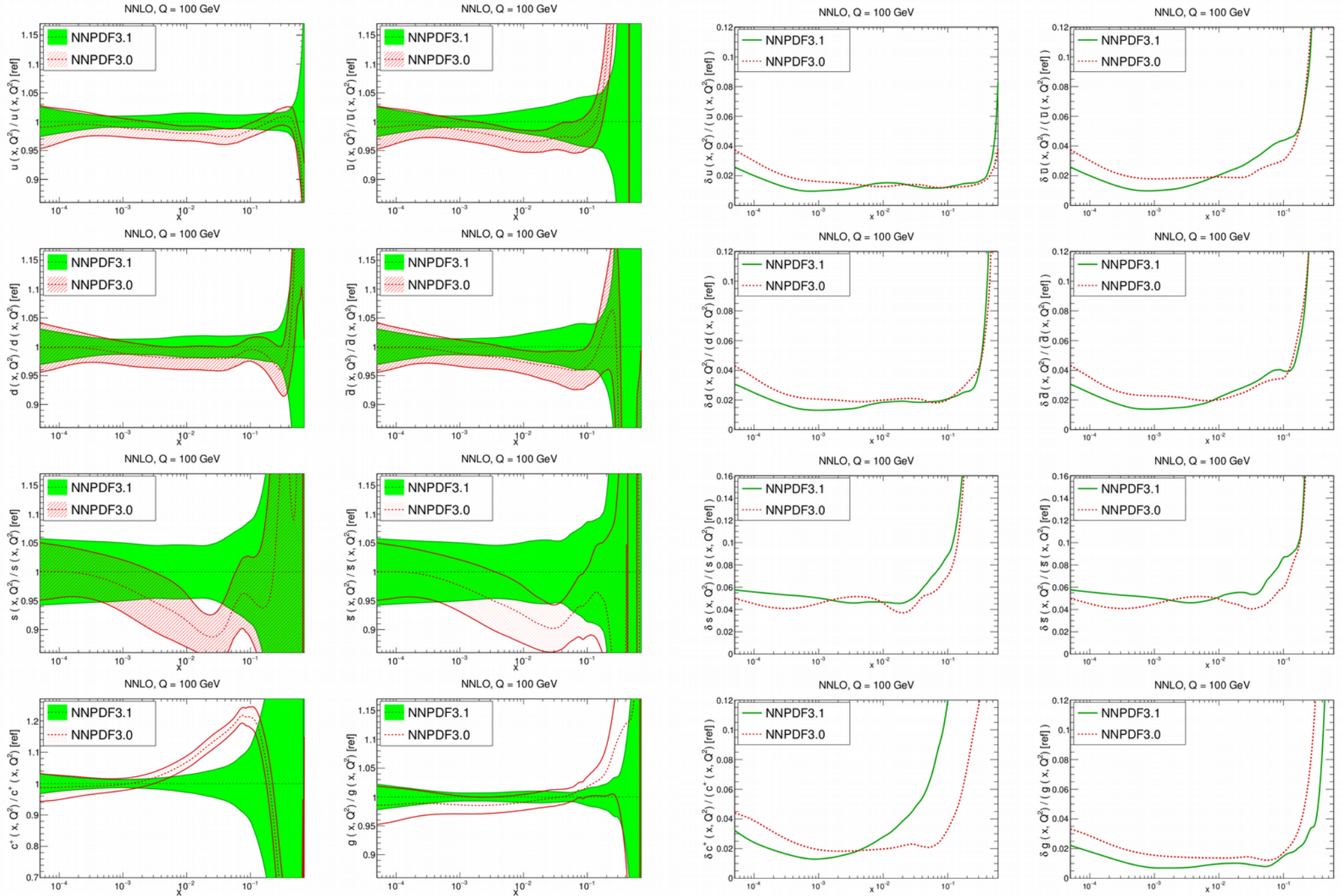
ATLAS strange enhancement

The epWZ16 strange-sea determined from analysis of the combined HERA-ATLAS data is enhanced as compared to other (earlier) determinations

ABM strange sea determination is in particular based on the dimuon neutrino-nucleon DIS production (NuTeV/CCFR and NOMAD) that gives a strange sea suppression ~0.5 at x~0.2

- *Disentangling d- and s- contribution?*
- *Impact of the nuclear corrections?*
- *.....?*

Test fit (the PDF shape comparison)
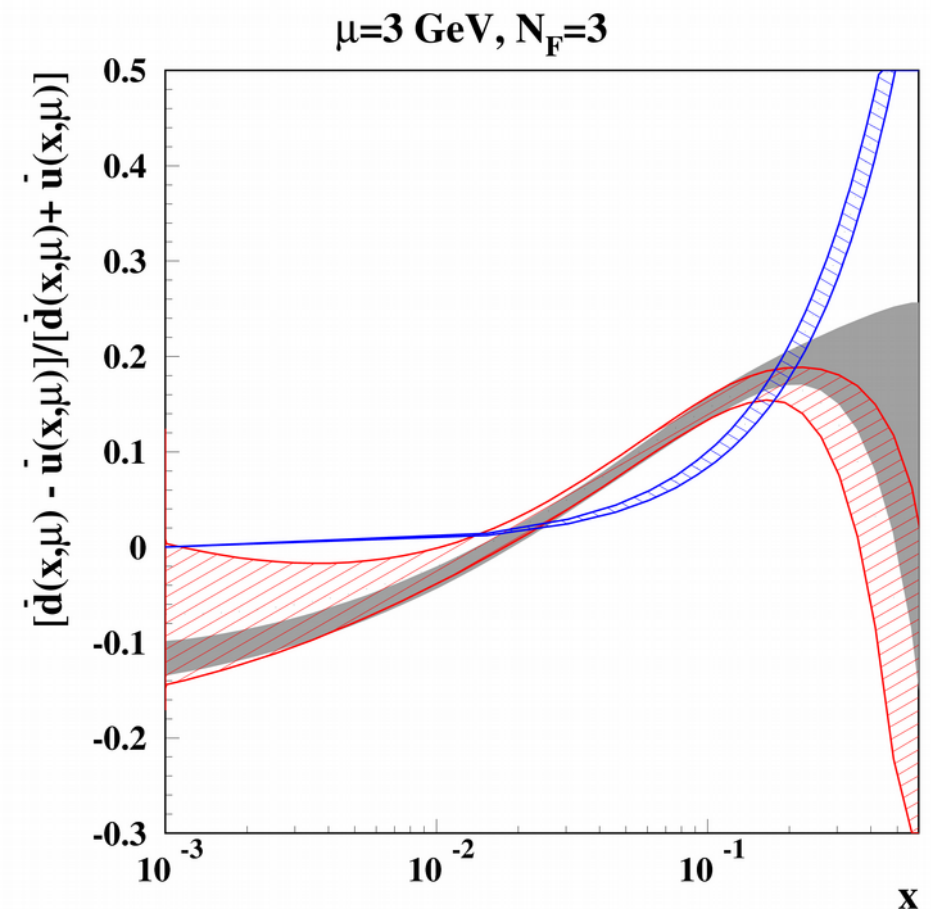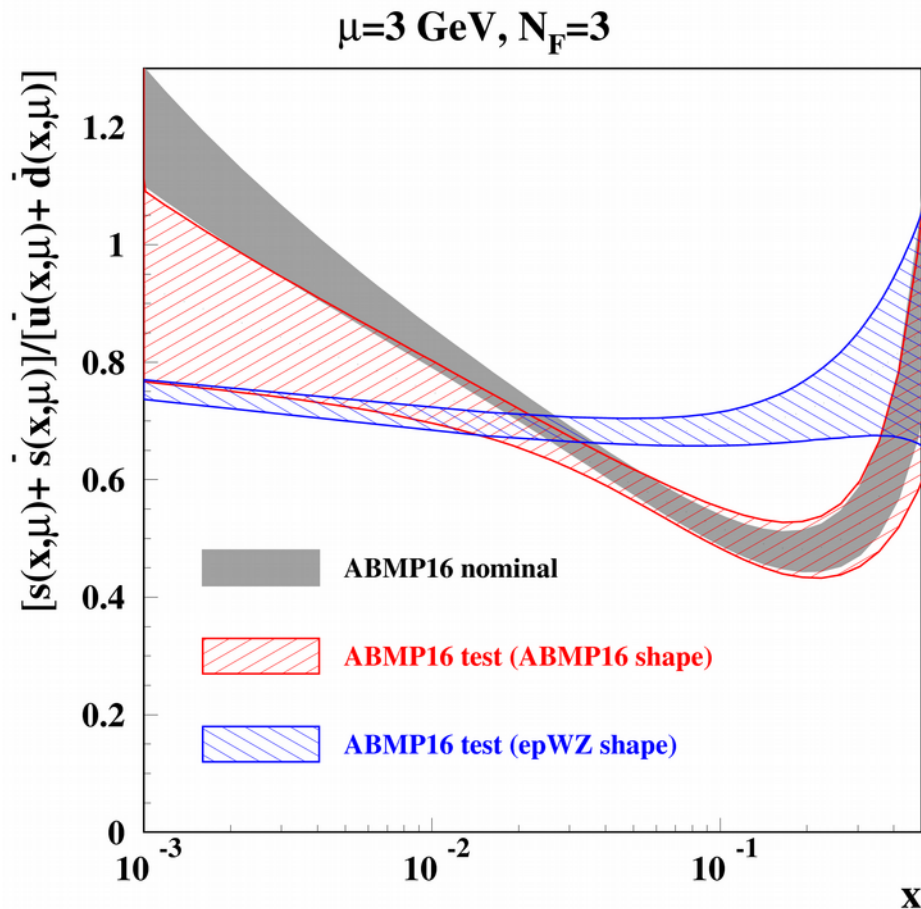
The data used in test fit: collider data discarded and replaced by the deuteron ones
(fit is consistent with the nominal ABMP16 at x>0.01)   sa, Kulagin, Petti hep-ph/1704.00204

The strange sea is enhanced for the epWZ shape despite the ATLAS data are not used.
However, the dimuon data description is not deteriorated: χ^2=167 versus 161 for
the ABMP shape ⇒ enhancement is achieved by the price of the d-quark sea suppression

sa, Blümlein, Caminada, Lipka, Lohwasser,
Moch, Petti, Plačakytė PRD 91, 094002 (2015)

E866 data in the test fit

FNAL-E866
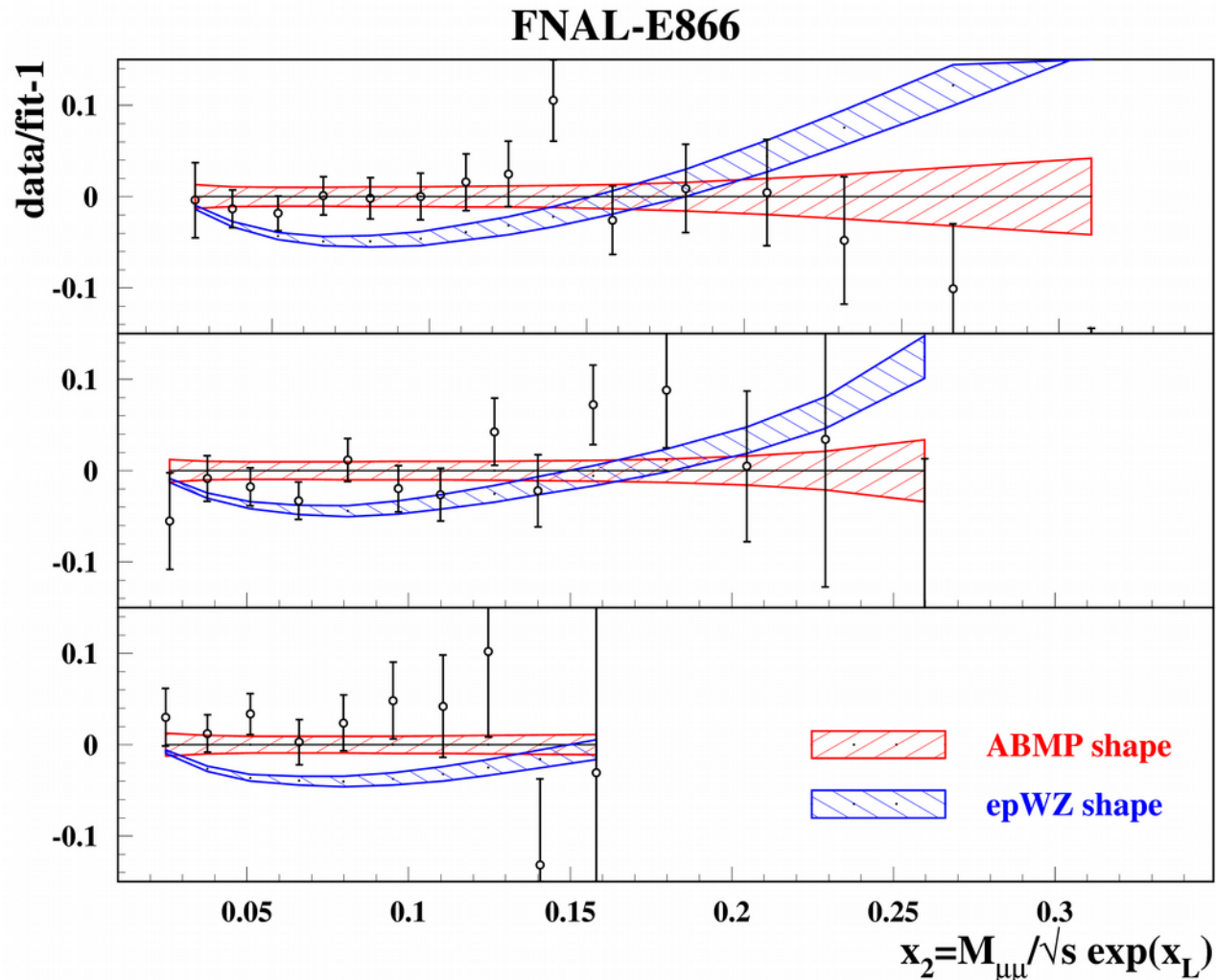
The E866 data on p/d DY cross sections are sensitive to the iso-spin sea asymmetry

The epWZ shape does not allow to accommodate E866 data: $\chi^2/NDP=96/39$ versus $49/39$ for the ABMP shape; the errors in epWZ predictions are suppressed at small x, evidently due to over-constrained PDF shape at small x

Impact of ATLAS data with flexible PDF shape

|	$\kappa_s(\mu^2=20 \text{ GeV}^2)$
HERA+ATLAS	0.81(18)
HERA+ATLAS+E866	0.72(8)
ABMP16(incl. NOMAD)	0.66(3)

κ_s is integral strange sea suppression factor:

$$\kappa_s(\mu^2) = \frac{\int\limits_0^1 x[s(x,\mu^2)+\bar{s}(x,\mu^2)]dx}{\int\limits_0^1 x[\bar{u}(x,\mu^2)+\bar{d}(x,\mu^2)]dx},$$
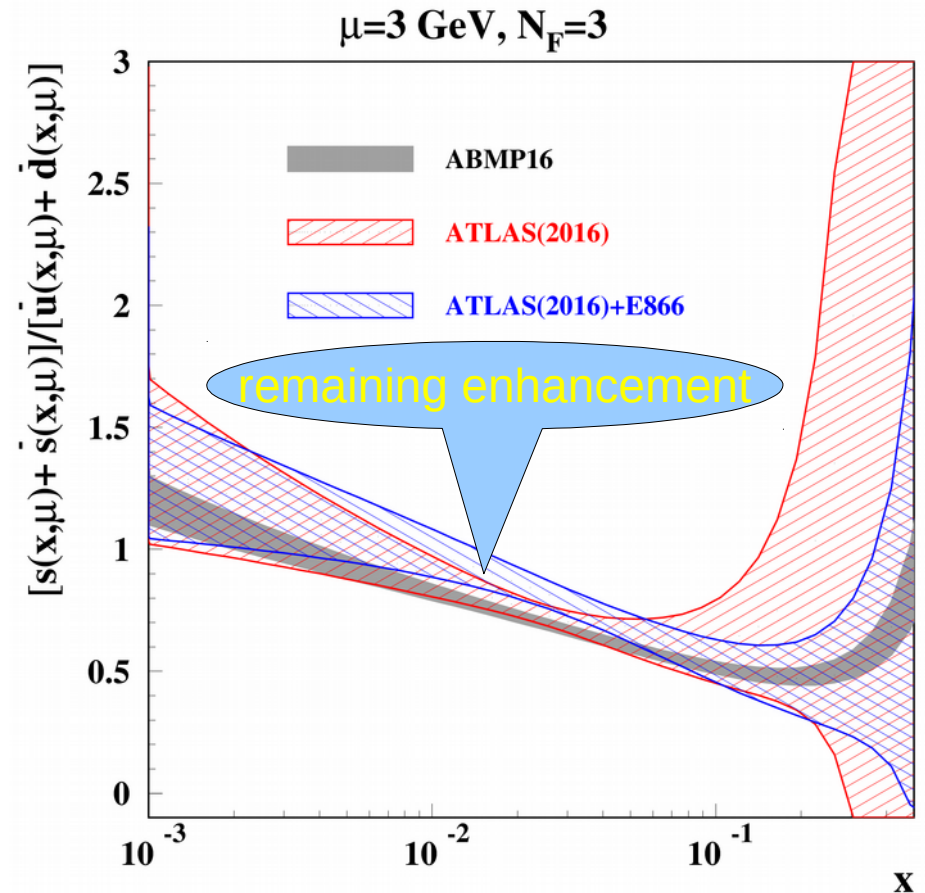
- For the flexible PDF shape the strangeness is in a broad agreement with the one extracted from the dimuon data

- The E866 data are consistent with the ATLAS(2016) set: χ^2/NDP=48/39 and 40/34, respectively.
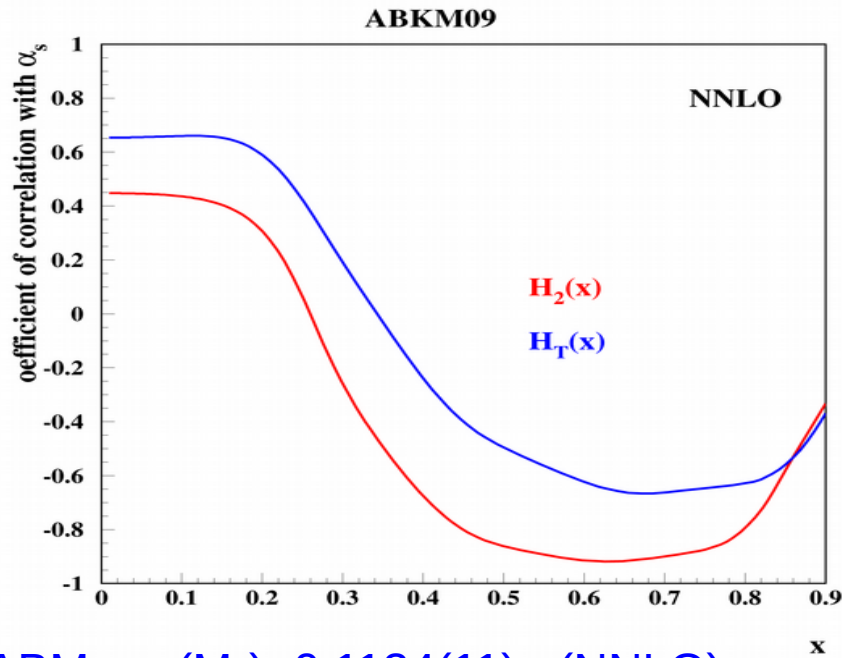
sa, Blümlein, Moch hep-ph/1708.01067

23

SeaQuest (FNAL-E906) prospects
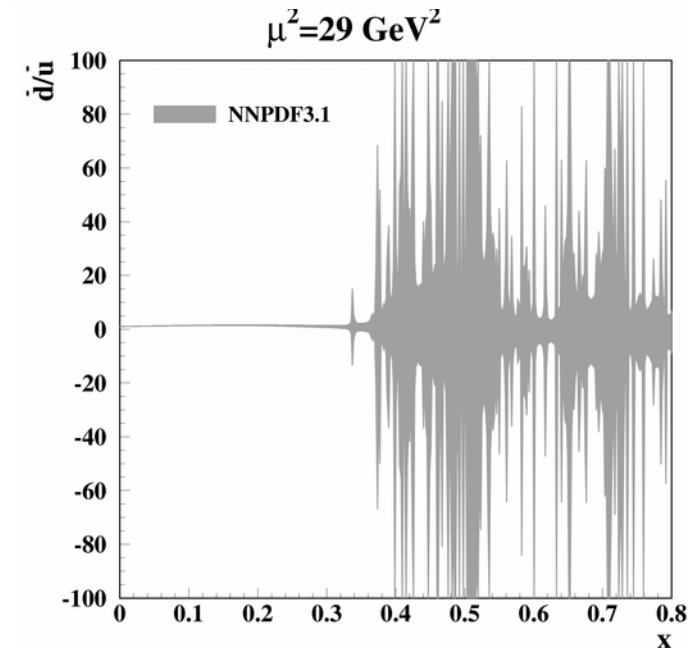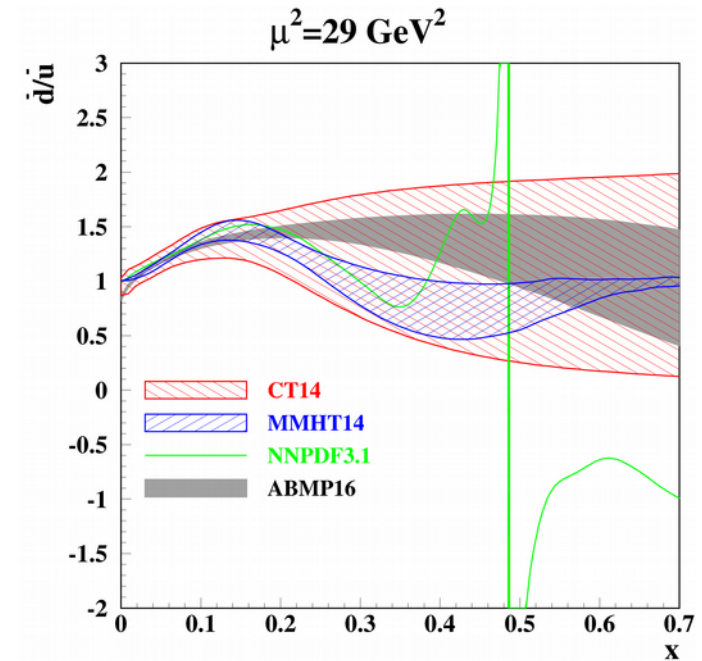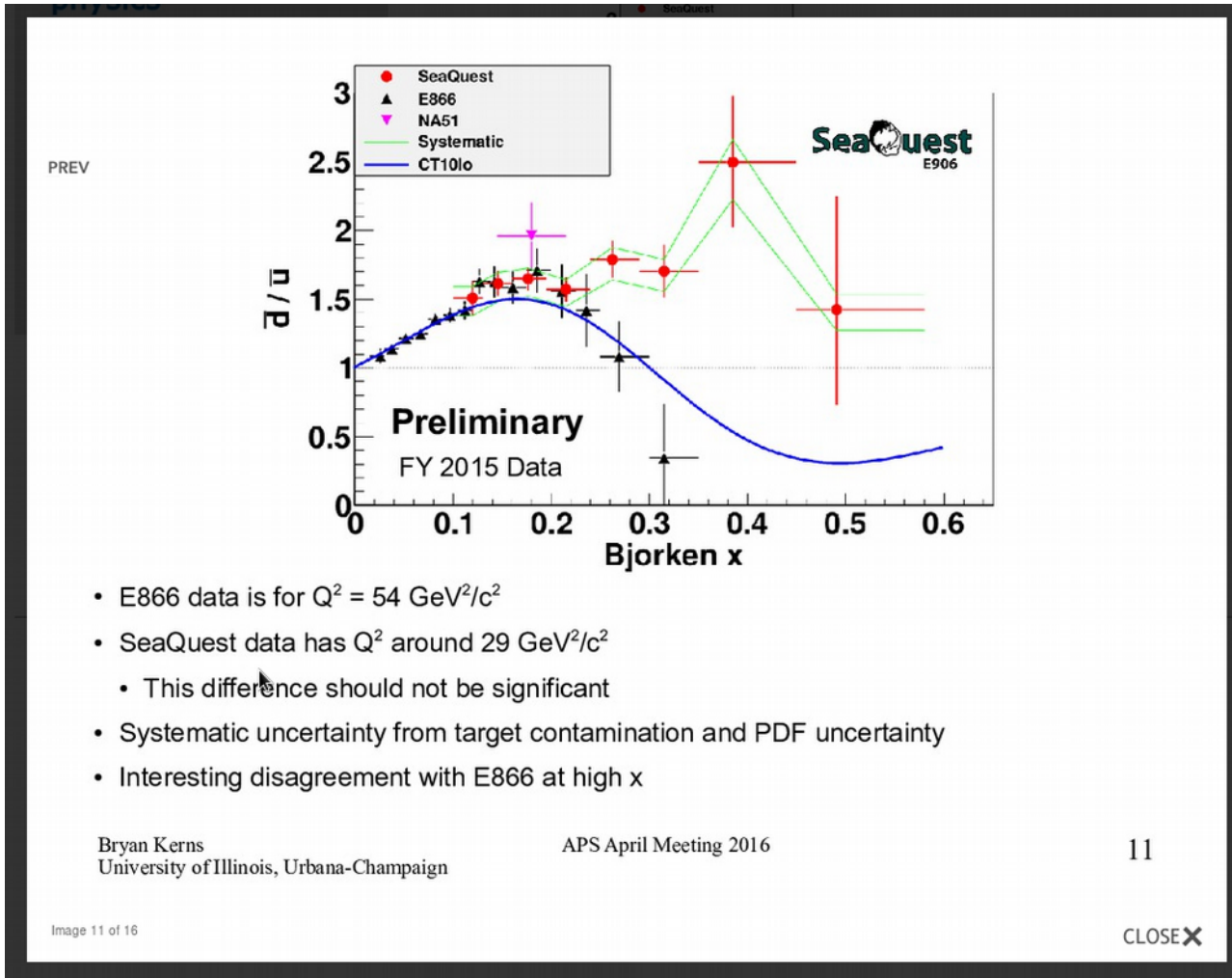
- E906 confirms the E866 results at x ~0.1 and continues the positive trend in the sea iso-spin asymmetry at bigger x

- The existing PDF sets can be consolidated with the E906 data

Correlation of α_s with twist-4 terms

ABKM09

NNLO

$H_2(x)$
$H_T(x)$

- The value of α_s and twist-4 terms are strongly correlated

- With HT=0 the errors are reduced → no uncertainty due to HTs

- With account of the HT terms the value of α_s is stable with respect to the cuts

- With the HT terms fitted the fit is sensitive to the ansatz details

ABM: $\alpha_s(M_z)$=0.1134(11)   (NNLO)
(W>1.8 GeV, Q^2> 2.5 GeV^2, fitted twist-4 terms in $F_{2,T}$)

MRST: $\alpha_s(M_z)$=0.1153(20)   (NNLO)
(W^2>15 GeV^2, Q^2> 10 GeV^2)
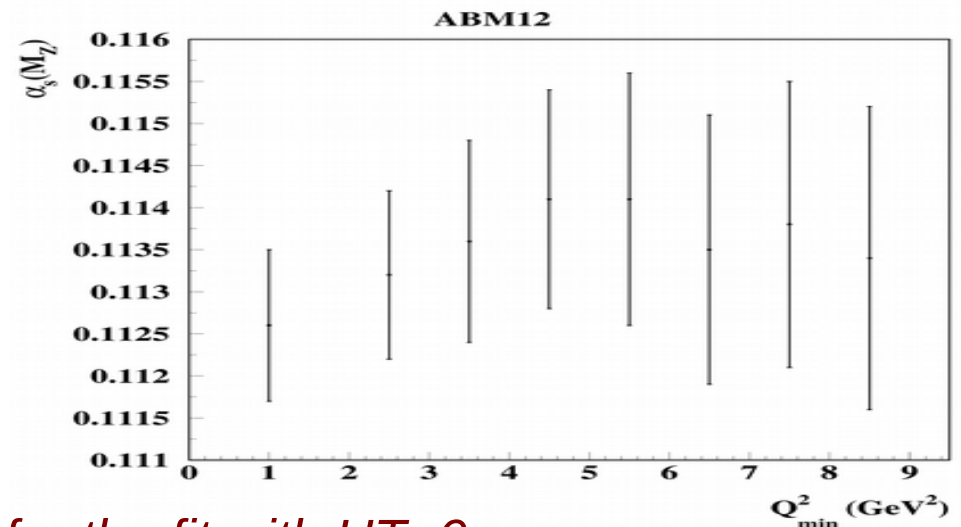
	W^2>12.5 GeV^2 Q^2>2.5 GeV^2	W^2>12.5 GeV^2 Q^2>10 GeV^2
HT fixed	0.1125(7)	0.1125(10)
HT=0	0.1168(7)	0.1143(10)

ABM12

Very stringent cut on Q at x~0.1 is necessary for the fit with HT=0

Moch et al. hep-ph/1405.4781   25

Strong coupling constant
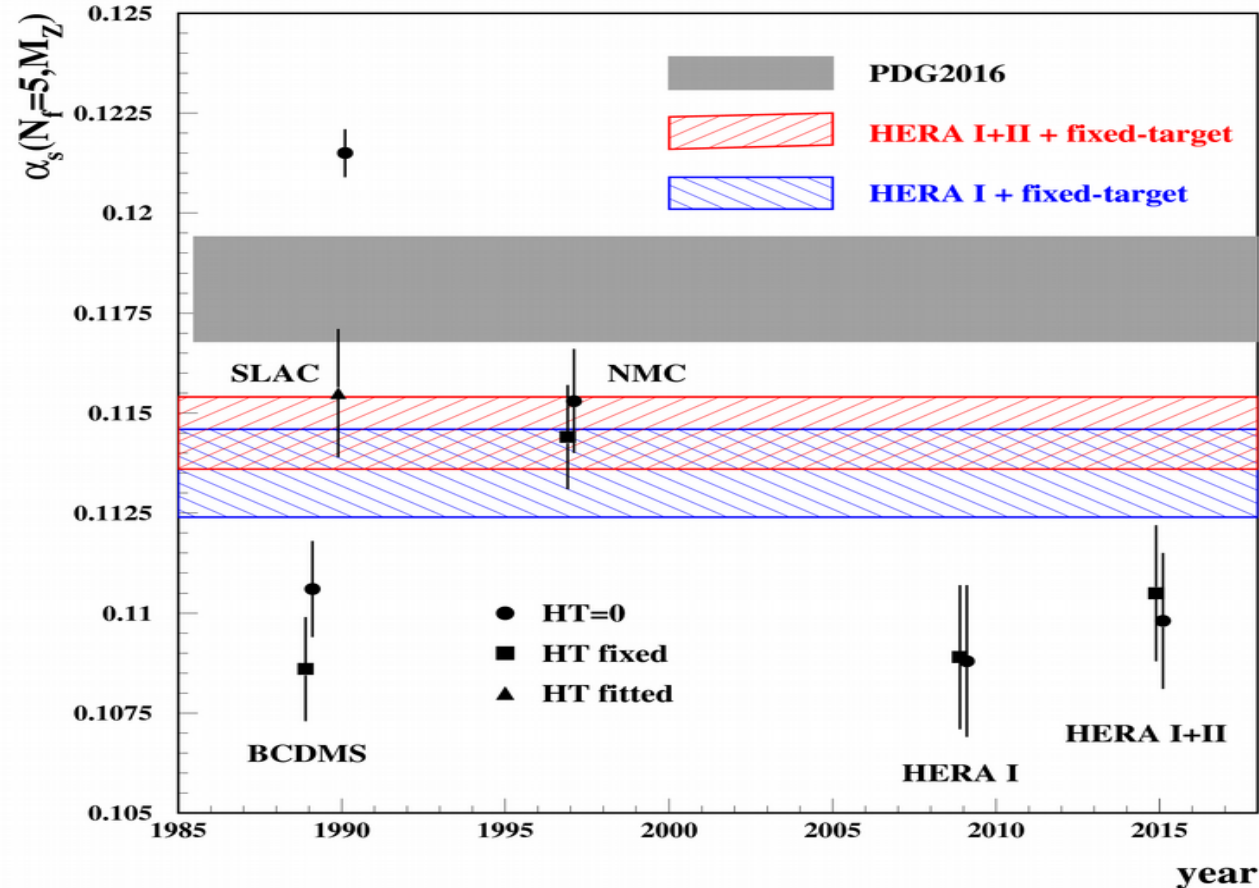
- combination of the DY data (disentangle PDFs) and the DIS ones (constrain α_s)
- Run-II HERA data pull α_s up by 0.001
- the value of α_s is still lower than the PDG one: pulled up by the SLAC and NMC data; pulled down by the BCDMS and HERA ones
- only SLAC determination overlap with the PDG band provided the high-twist terms are taken into account

High twists at small x
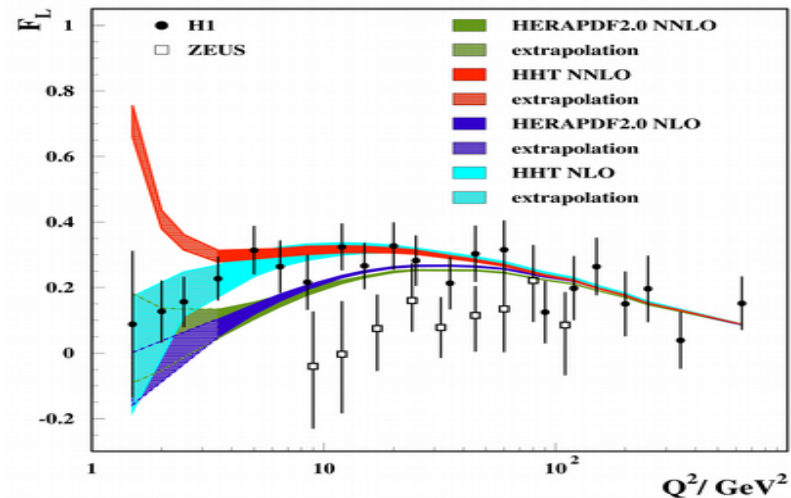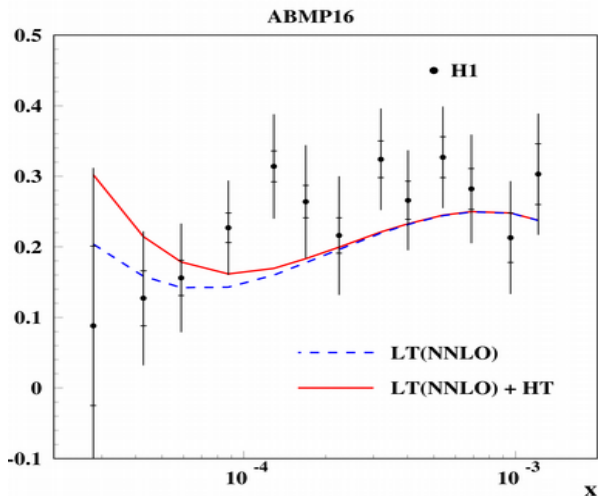
$$F_{2,L} = F_{2,L}(\text{leading twist}) + H_{2,L}(x)/Q^2 \qquad H(x) = x^h P(x)$$

sa, Blümlein, Moch
PRD 86, 054009 (2012)
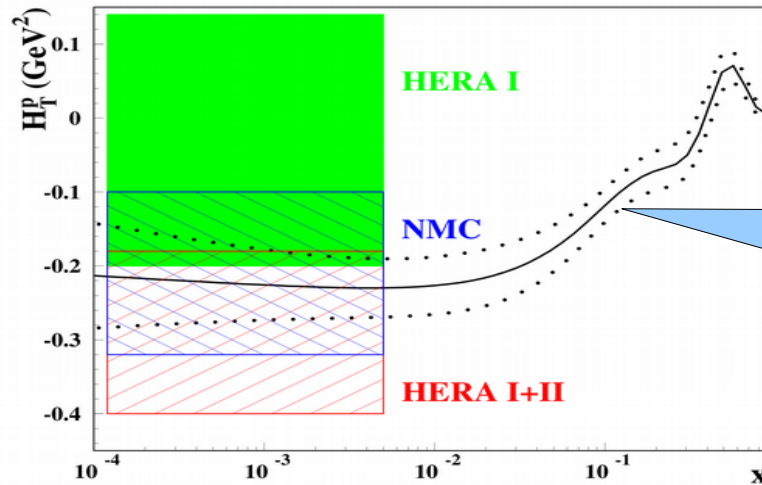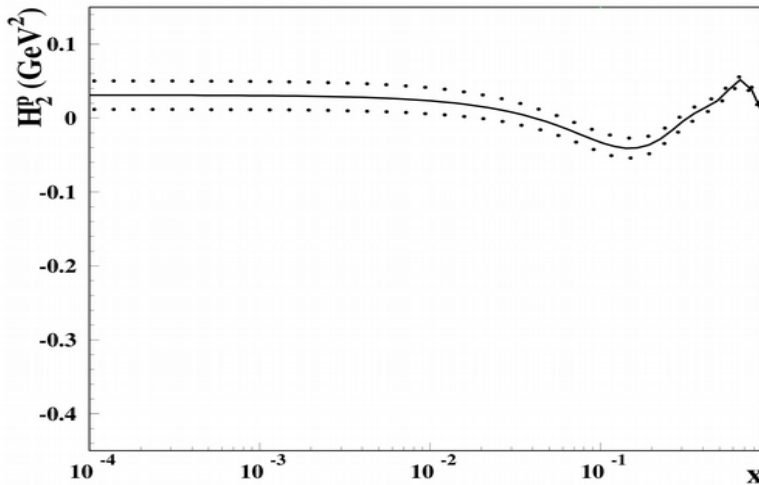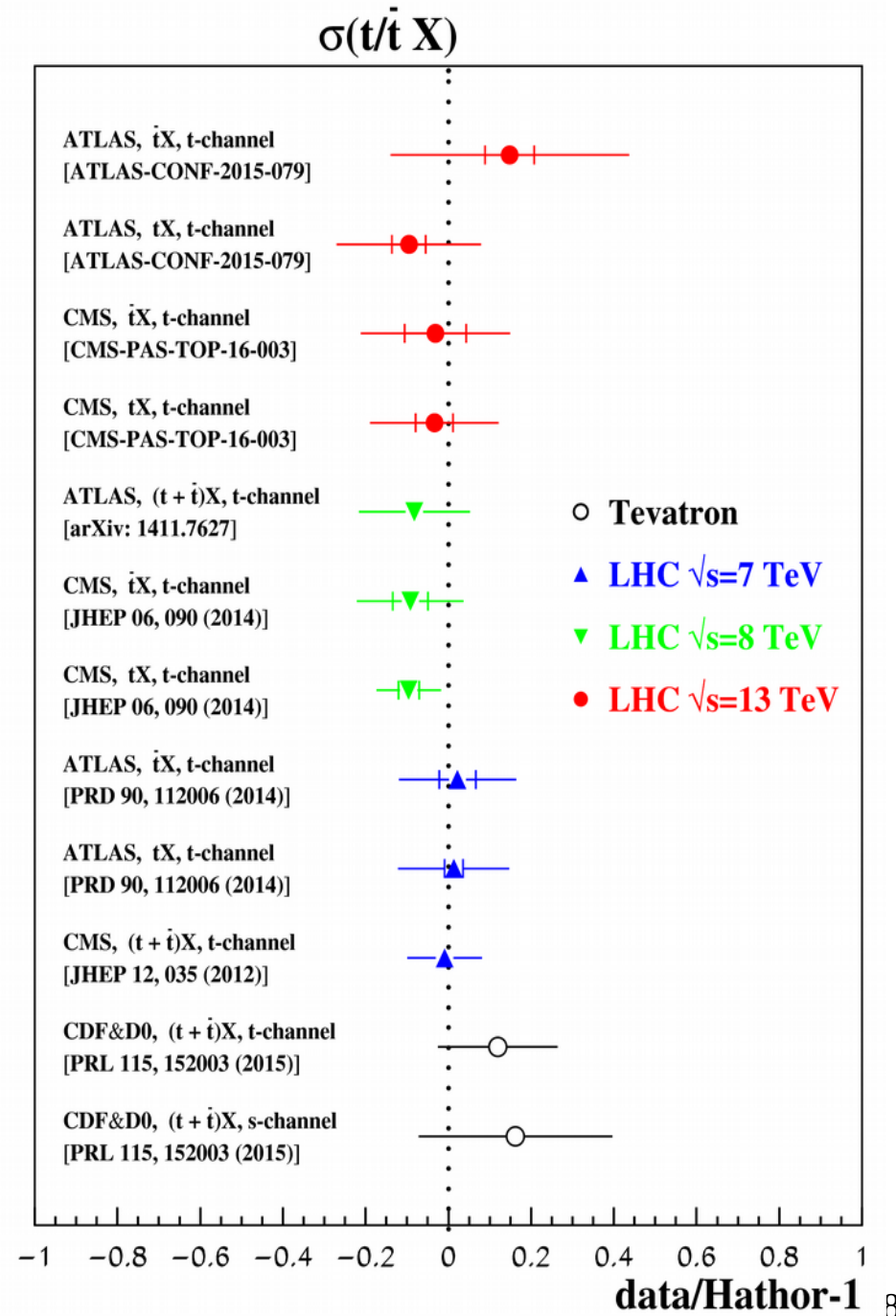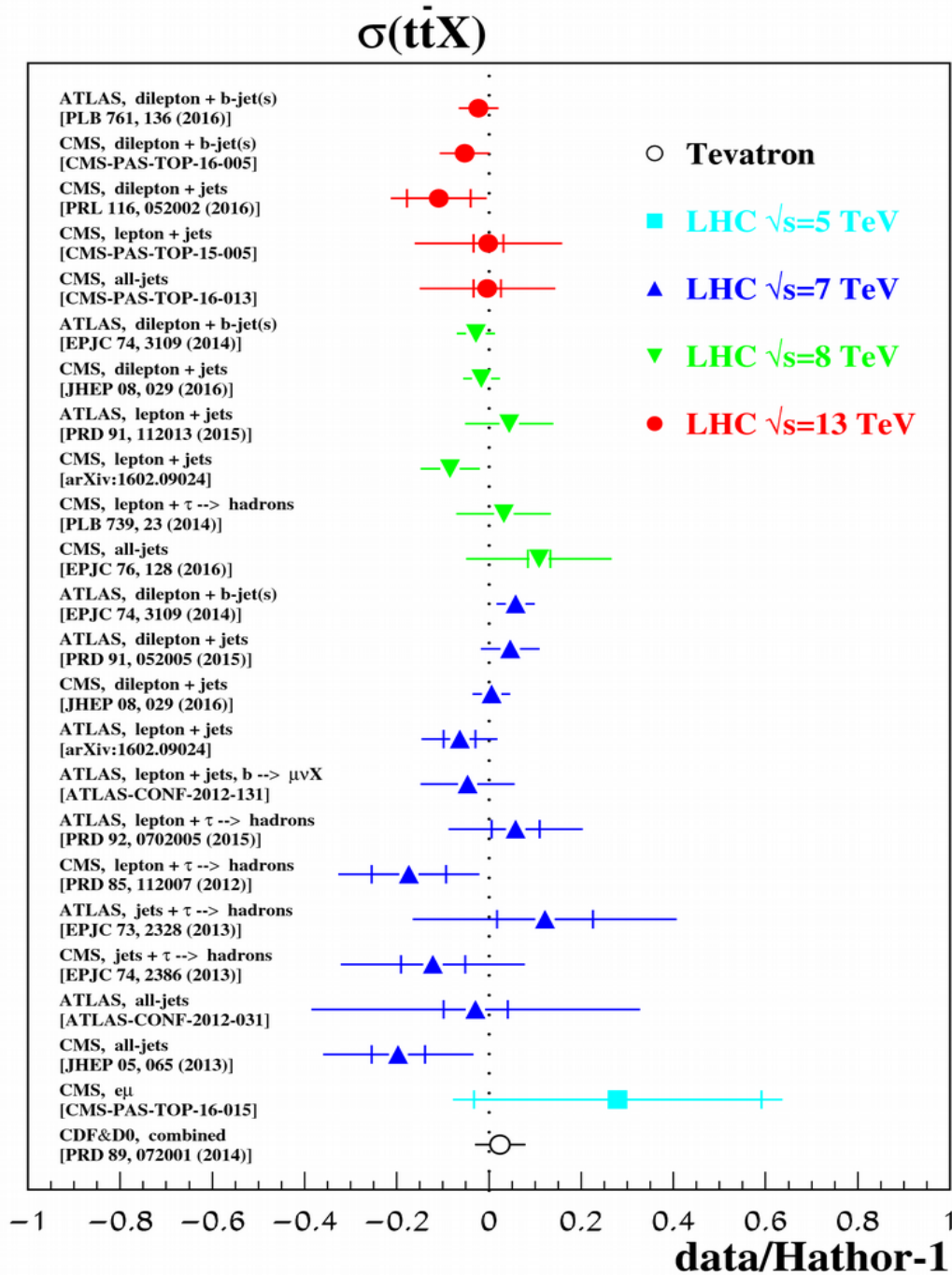
Controlled by SLAC and NMC data

- $H_T(x)$ continues a trend observed at larger x; $H_2(x)$ is comparable to 0 at small x
- $h_T = 0.05 \pm 0.07 \rightarrow$ slow vanishing at $x \rightarrow 0$
- $\Delta\chi^2 \sim -40$ Harland-Lang, Martin, Motylinski, Thorne hep-ph/1601.03413

No dramatic increase of F_L at small x

Abt, et al. PRD 94, 034032 (2016)

27

t-quark production

Impact of the t-quark data on the ABMP16 fit

MSbar
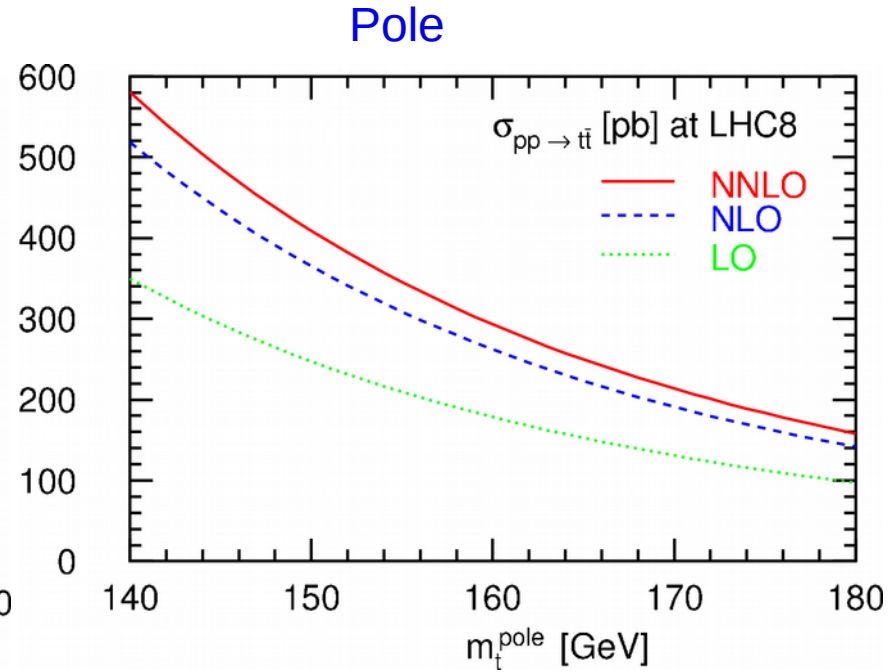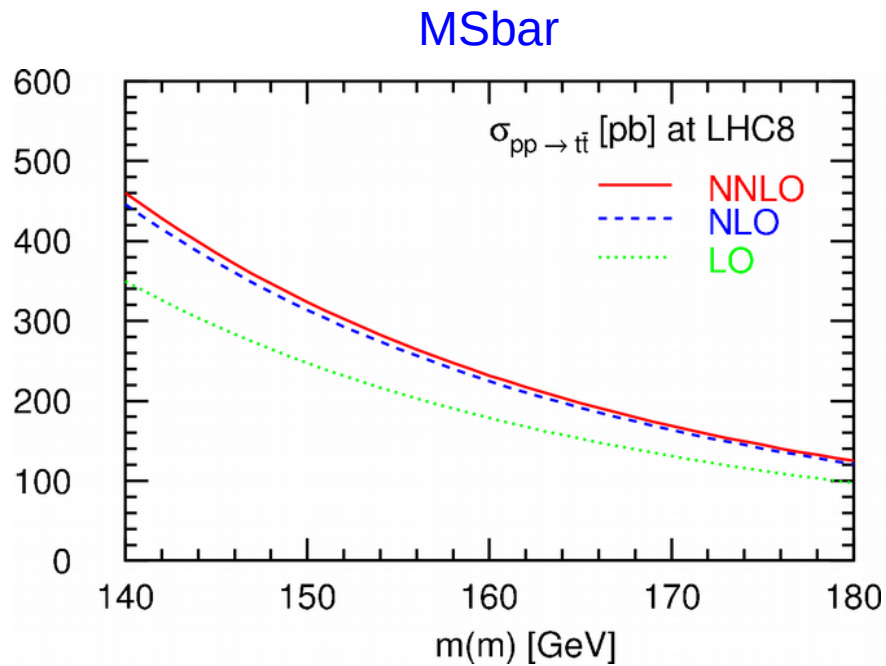
Pole

HATHOR (NNLO terms are checked with TOP++)   Langenfeld, Moch, Uwer PRD 80, 054009 (2009)

Running mass definition provides nice perturbative stability   Czakon, Fiedler, Mitov PRL 110, 252004 (2013)

- $m_t(m_t)$=160.9±1.1(exp.) GeV   NNLO
  m_t(pole)=170.4±1.2(exp.) GeV

- $\alpha_s(M_z)$=0.1145(9) → 0.1147(8)   NNLO

- moderate change in the large-x gluon distribution

Electroweak vacuum stability

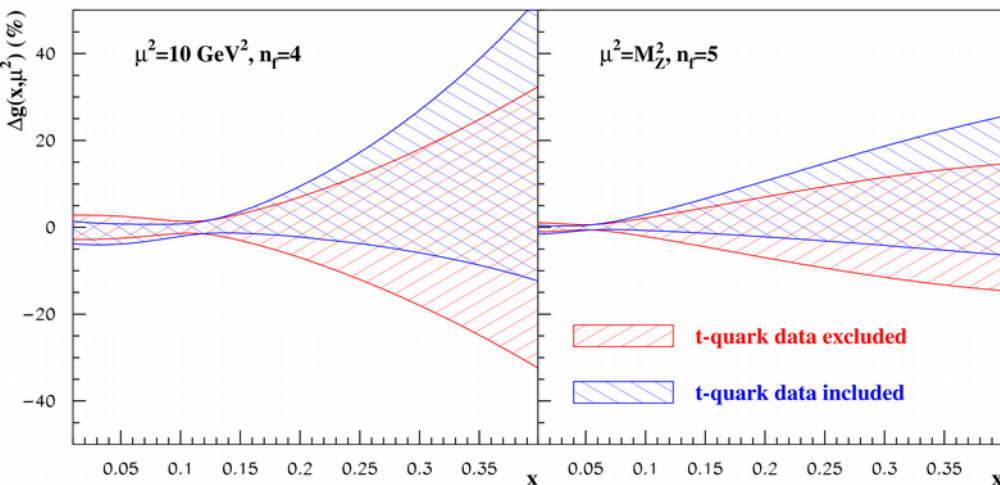$$m_H = 129.6\,\text{GeV} + 1.8 \times \left(\frac{m_t^{\text{pole}} - 173.34\ \text{GeV}}{0.9} \right) - 0.5 \times \left(\frac{\alpha_s^{(n_f=5)}(M_Z) - 0.1184}{0.0007} \right) \text{GeV} \pm 0.3\ \text{GeV},$$

Buttazzo et al., JHEP 12, 089 (2013)

Higgs self coupling $\lambda(\mu_r)$
$m_H = 125.09 \pm 0.24$ GeV
$m_t^{\text{pole}} = 170.4 \pm 1.2$ GeV
$\alpha_s(M_Z) = 0.1147 \pm 0.0008$
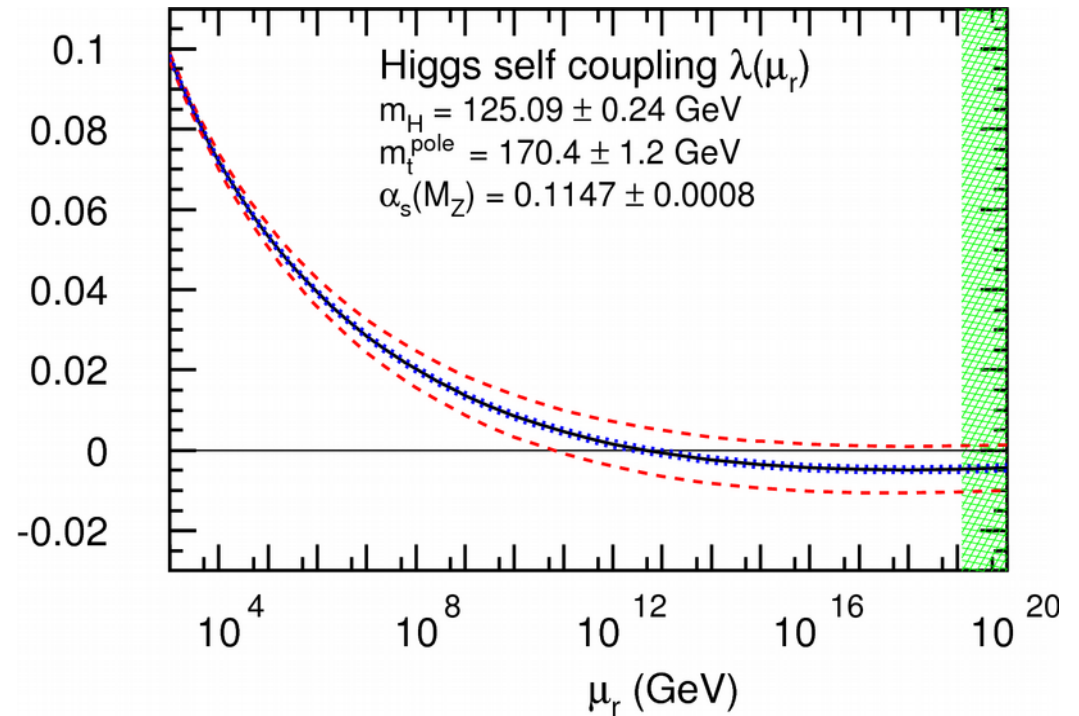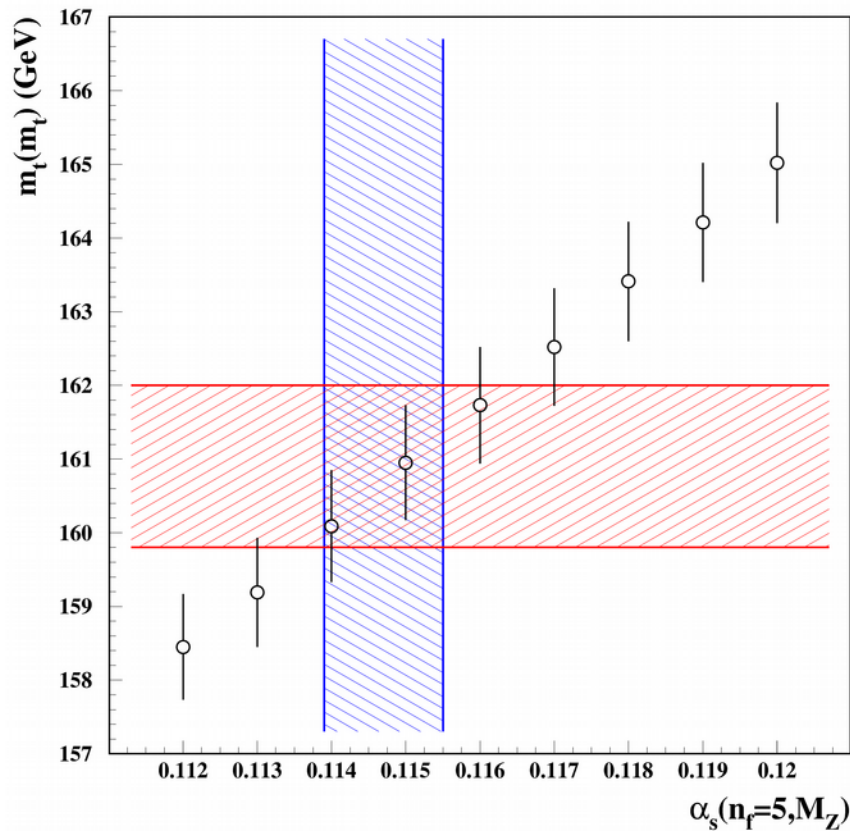
mr: **Kniehl, Pikelner, Veretin CPC 206, 84 (2016)**

Vacuum stability is quite sensitive to the t-quark mass; strong correlation m_t and α_s extracted from the ttbar data

30

NNLO t-quark mass from the single-top data
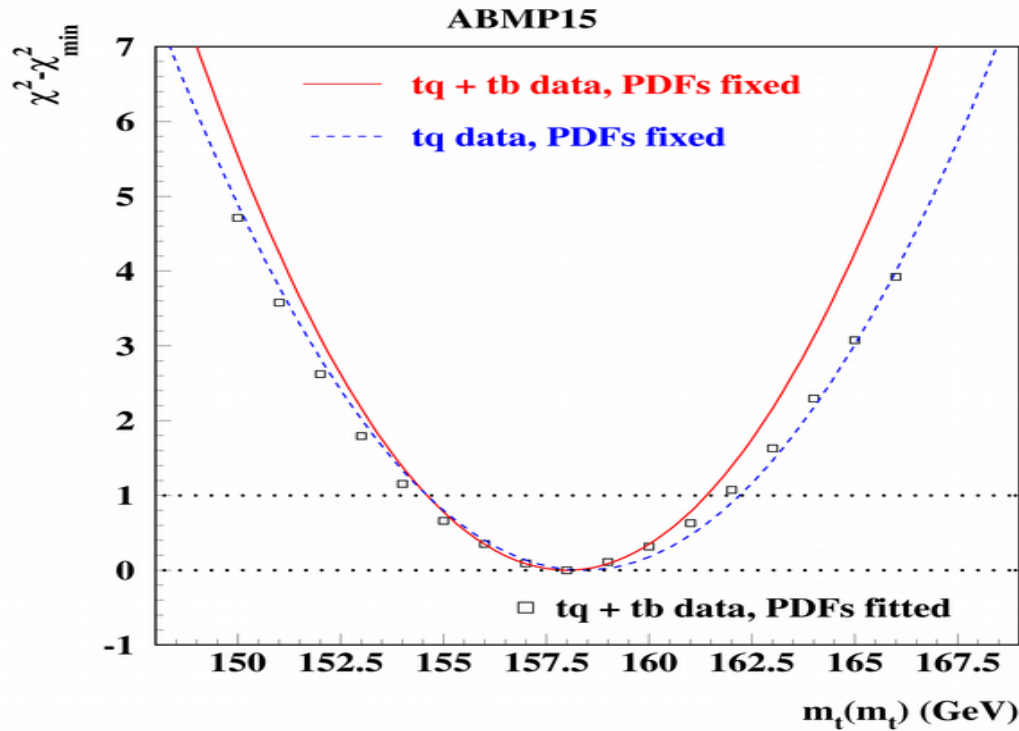
PDFs fixed:

- Different PDFs prefer value of

  $m_t(m_t) \sim 160 \pm 3.5$ GeV

  NNPDF goes higher by 3 GeV.

- The CT14 and MMHT14 go higher by 3 GeV with the ttbar channel

- Electroweak production → reduced impact of α_s and the PDF umcertainties

- HATHOR framework
  t-channel: NNLO
  Brucherseifer, Caola, Melnikov PLB 736, 58 (2014)

  s-channel: NNLO threshold. resum.
  sa, Moch, Thier PLB 763, 341 (2016)

Intrinsic charm: pitfalls

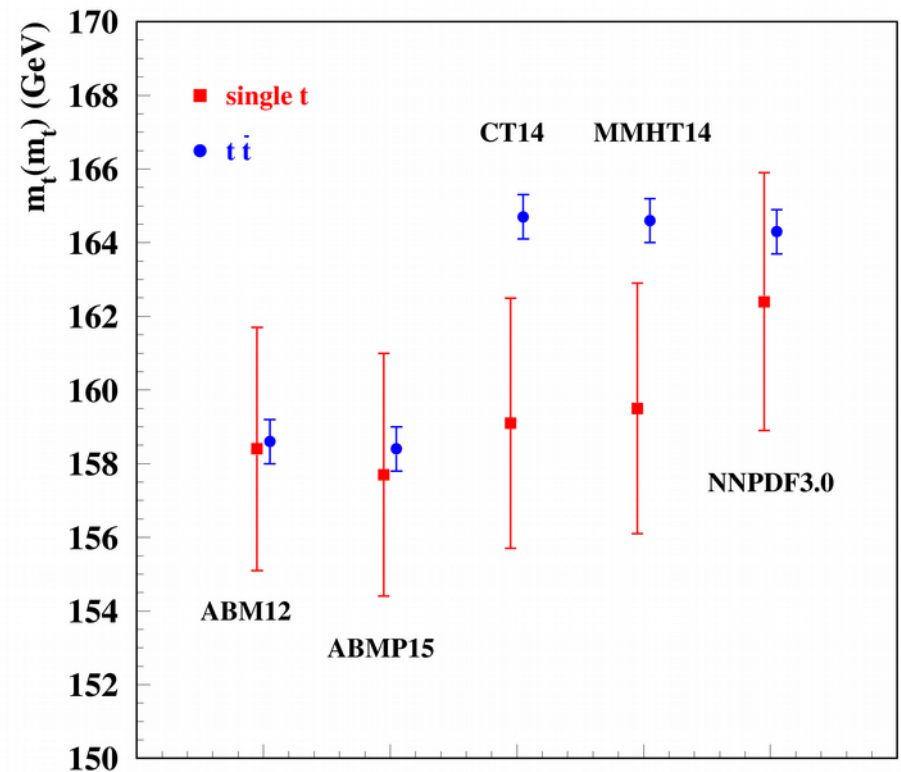- No mass singularities for massive partons ⇒ collinear QCD evolution does not work

- The mass singularities $\sim \ln(\mu/m_h)$ appear at $\mu \gg m_h$ and the evolution restores. New charm(bottom) quark distribution may be introduced, however, extrapolation to smaller scales is still problematic

- Intrinsic charm is often introduced within the VFN framework ⇒ interplay with the "standard" VFN modeling of power-like terms

- Original formulation of the intrinsic charm implies its power-like behavior;
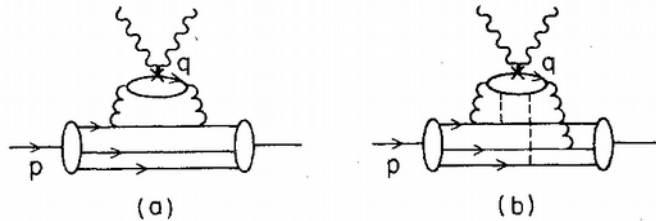
Brodsky, Peterson, Sakai PRD 23, 2745 (1981)

FIG. 7. (a) Example with contribution to the deep-inelastic structure functions from an extrinsic quark q; (b) from an intrinsic quark q.

strong constraint on such terms was obtained from analysis of the EMC data on charm prduction   **Jimenez-Delgado, Hobbs, Londergan, Melnitchouk PRL 114, 082002 (2015)**

Intrinsic charm in the CT and NNPDF fits

Hou et al. hep-ph/1707.00657
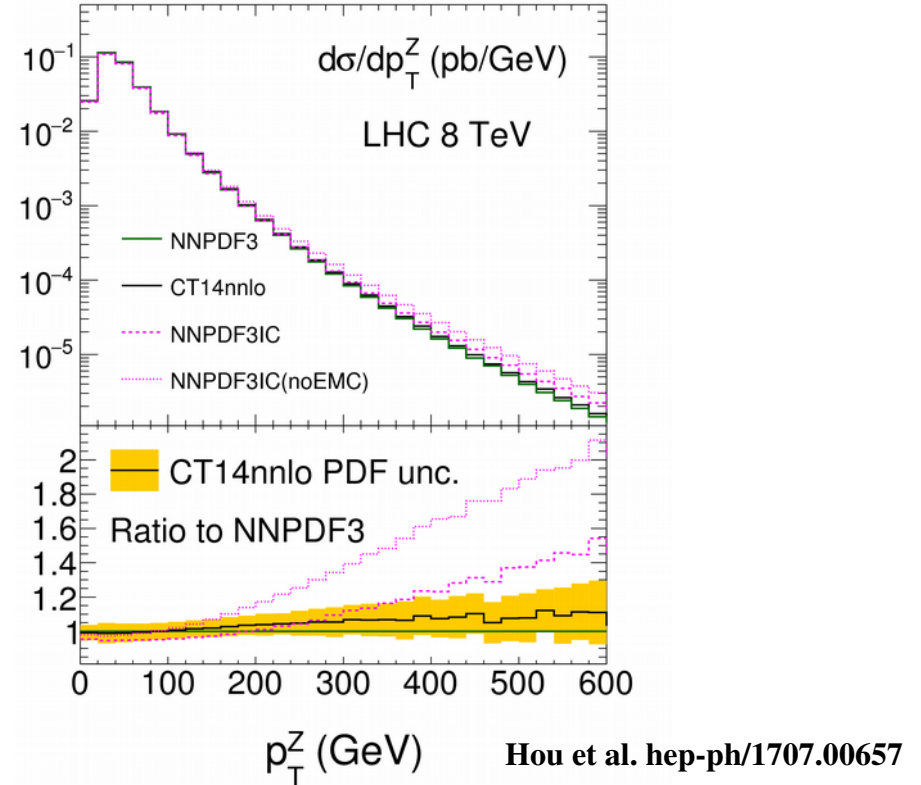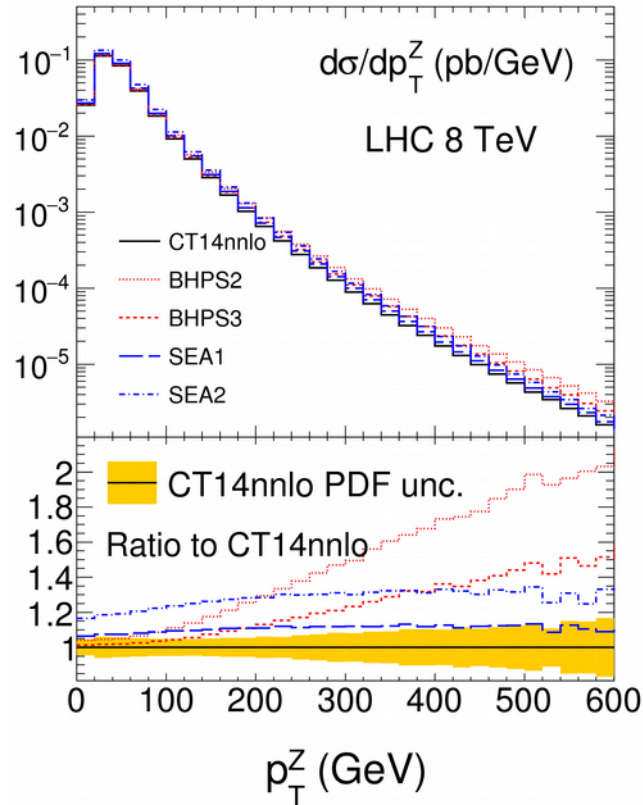
- The intrinsic-charm (IC) component is evolved starting from the small scale with the collinear DGLAP

- The value of m_c(pole)=1.31 (CT) and 1.51(NNPDF) GeV is used

- Several IC shapes are considered by CT: BHPS, SEA,…; free form by NNPDF

- An agreement with the Z+charm LHC data might be improved

33

Summary

We have steady improvement due to new experimental input from LHC:

– disentangling quark distributions at small x

– deuteron data can be replaced by the DY ones: no impact of the nuclear model uncertainties with a comparable d-quark distribution accuracy at large x

– somewhat enhanced strange distribution at small x, however, the large-x enhancement reported by ATLAS seems to be an artefact of the PDF shape used

The HERA inclusive and semi-inclusive data allow to distinguish between the FFN and VFN factoriazation schemes. The FFN scheme provides nice agreement with existing data and

$$m_c(m_c) = 1.252 \pm 0.018(\text{exp.}) - 0.01(\text{th.}) \text{ GeV},$$

which is in agreement with other precision determinations. The values

$$\alpha_s(M_z) = 0.1147(8) \qquad \text{DIS+t-quark}$$
$$\alpha_s(M_z) = 0.1145(9) \qquad \text{DIS}$$

are obtained with and without t-quark data included, respectively.

EXTRAS

The ABMP16 fit ingredients

QCD:

NNLO evolution

NNLO massless DIS and DY coefficient functions

NLO+ massive DIS coefficient functions (**FFN scheme**)

– NLO + NNLO(approx.) corrections for NC

– NNLO CC at $Q >> m_c$

– running mass

NNLO exclusive DY (FEWZ 3.1)

NNLO inclusive ttbar production (pole / running mass)

Relaxed form of (dbar-ubar) at small x

DATA:

DIS NC/CC inclusive (HERA I+II added, no deuteron data included)

DIS NC charm production (HERA)

DIS CC charm production (HERA, NOMAD, CHORUS, NuTeV/CCFR)

fixed-target DY

LHC DY distributions (ATLAS, CMS, LHCb)
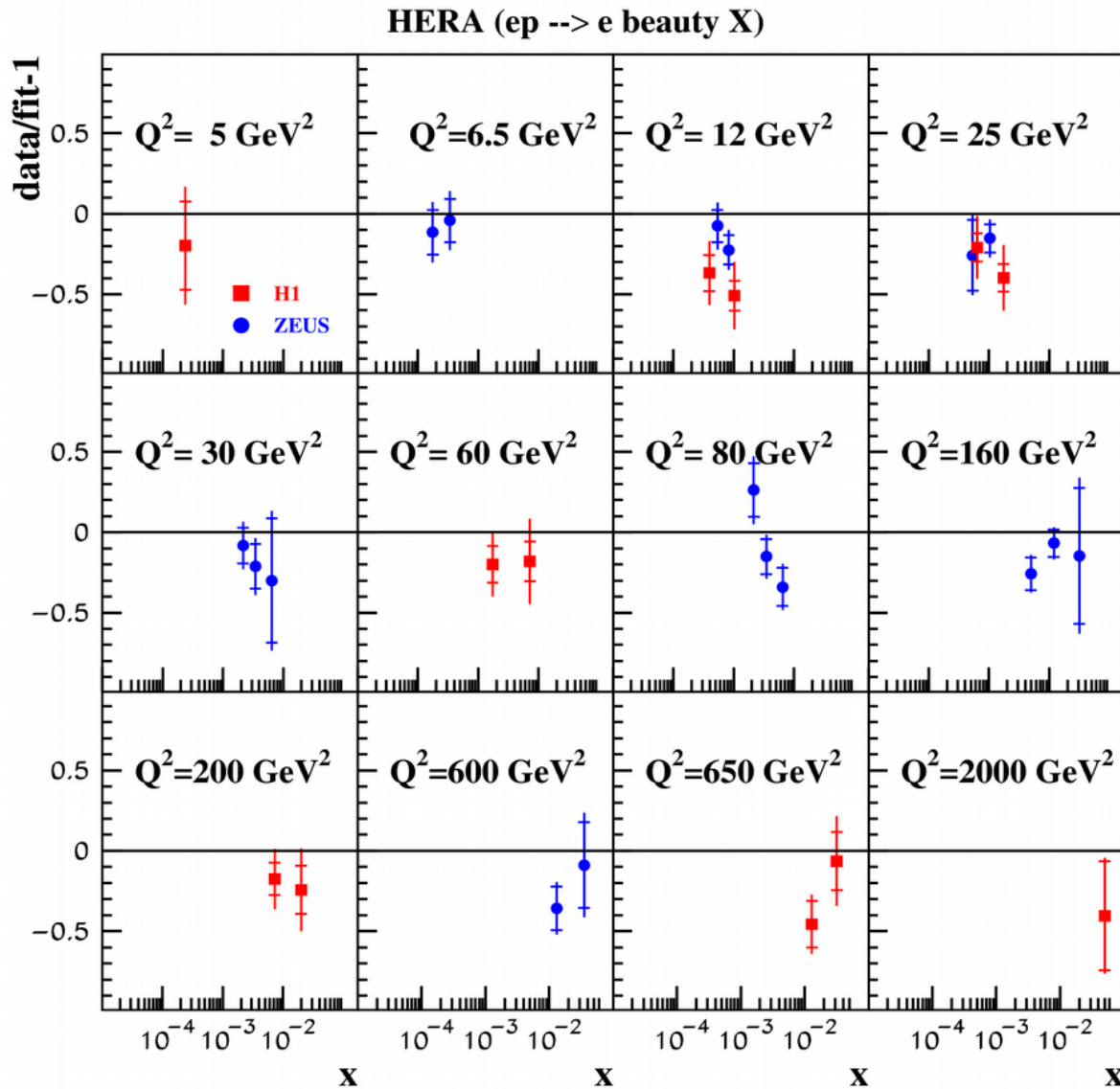
t-quark data from the LHC and Tevatron

deuteron data are excluded

Power corrections:

target mass effects

dynamical twist-4 terms

HERA bottom data and $m_b(m_b)$

HERA (ep --> e beauty X)

ZEUS JHEP 1409, 127 (2014)

χ^2/NDP=16/17

H1 EPJC 65, 89 (2010)

χ^2/NDP=5/12

$m_b(m_b)$=3.83±0.12(exp.)-0.1(th.) GeV

NNLO DY corrections in the fit

The existing NNLO codes (DYNNLO, FEWZ) are quite time-consuming →
fast tools are employed (FASTNLO, Applgrid,......)

- the corrections for certain basis of PDFs are stored in the grid
- the fitted PDFs are expanded over the basis
- the NNLO c.s. in the PDF fit is calculated as a combination of
  expansion coefficients with the pre-prepared grids

The general PDF basis is not necessary since the PDFs are already constrained
by the data, which do not require involved computations → *use as a PDF basis
the eigenvalue PDF sets obtained in the earlier version of the fit*

$P_0 \pm \Delta P_0$ – vector of PDF parameters with errors obtained in the earlier fit
E – error matrix
P – current value of the PDF parameters in the fit

- store the DY NNLO c.s. for all PDF sets defined by the eigenvectors of E
- the variation of the fitted PDF parameters ($P - P_0$) is transformed into this
  eigenvector basis
- the NNLO c.s. in the PDF fit is calculated as a combination of transformed ($P - P_0$)
  with the stored eigenvector values

DY at large rapidity

D0 (1.96 TeV)

LHCb (7 TeV, 1 fb⁻¹)

sa, Blümlein, Moch, Plačakytė, hep-ph/1508.07923
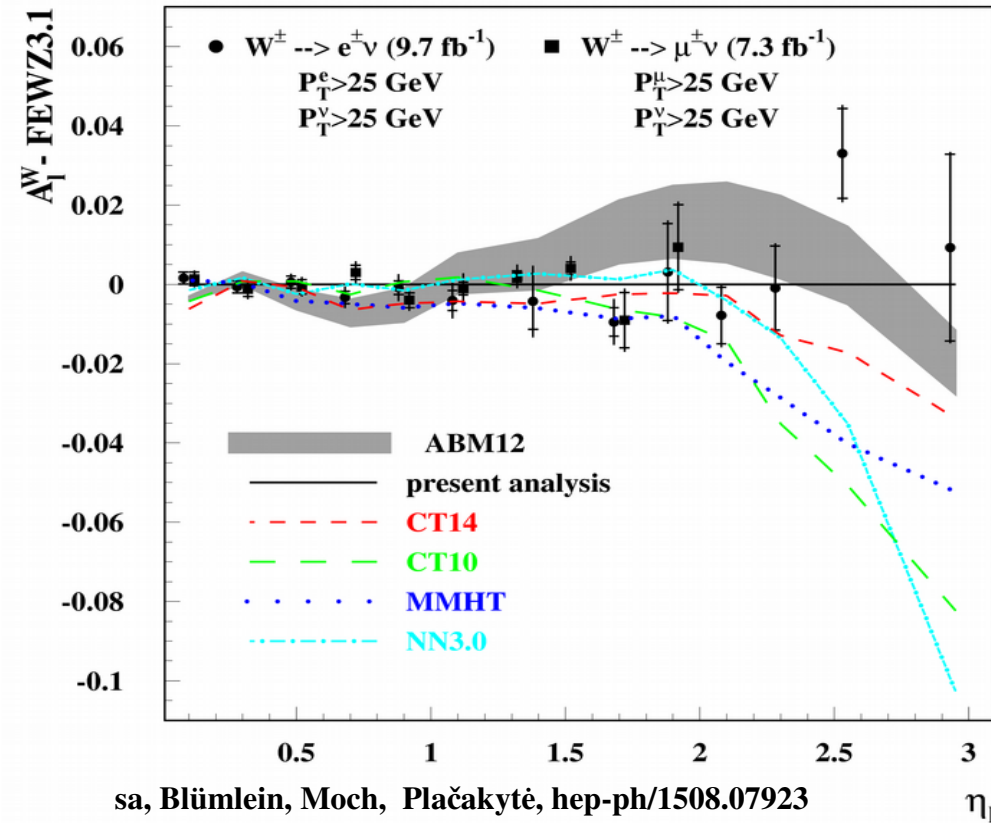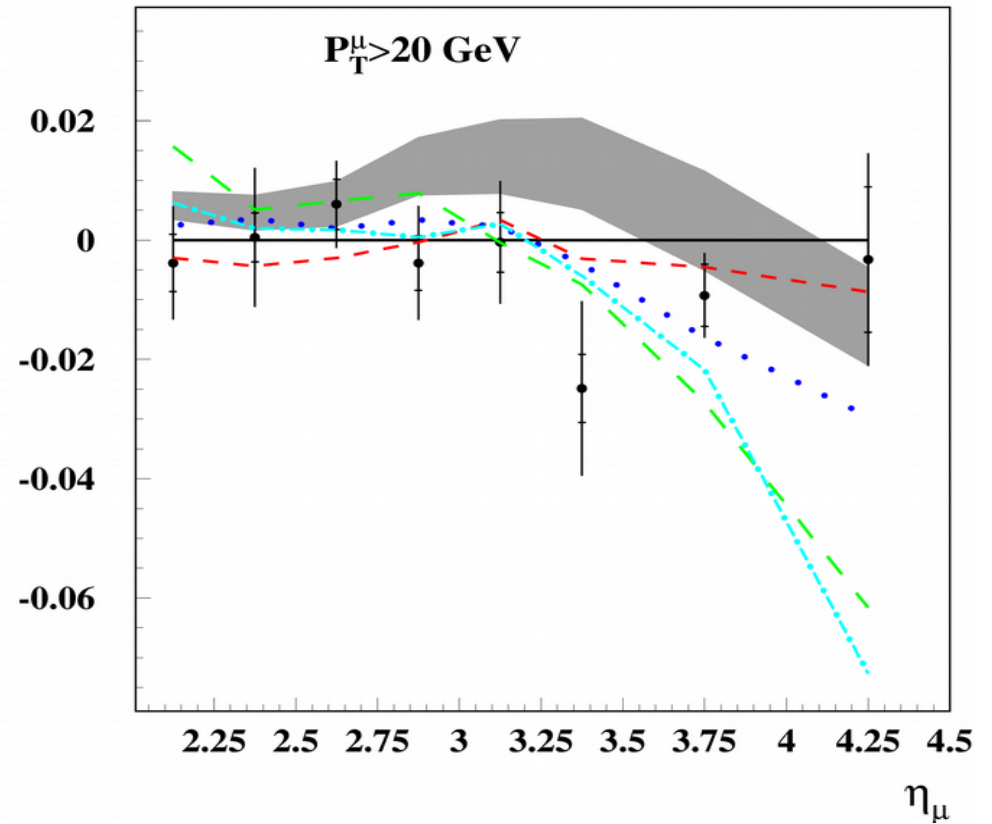
- The data can be evidently used for consolidation of the PDFs, however, unification of the theoretical accuracy is also needed

ABM	CT	MMHT	NNPDF
Interpolation of accurate NNLO grid (a la FASTNLO)	NNLL (ResBos)	NLO + NNLO K-factor	NLO + NNLO C-factors (y-dependent K-factors)

PDF sets	m_c [GeV]	m_c renorm. scheme	theory method (F_2^c scheme)	theory accuracy for heavy quark DIS Wilson coeff.	χ^2/NDP for HERA data [127] with xFitter [128, 129]	
ABM12 [2] [a]	$1.24^{+0.05}_{-0.03}$	$\overline{MS}$ $m_c(m_c)$	FFNS ($n_f = 3$)	NNLO$_{approx}$	65/52	66/52
CJ15 [1]	1.3	m_c^{pole}	SACOT [122]	NLO	117/52	117/52
CT14 [3] [b]						
(NLO)	1.3	m_c^{pole}	SACOT(χ) [123]	NLO	51/47	70/47
(NNLO)	1.3	m_c^{pole}	SACOT(χ) [123]	NLO	64/47	130/47
HERAPDF2.0 [4]						
(NLO)	1.47	m_c^{pole}	RT optimal [125]	NLO	67/52	67/52
(NNLO)	1.43	m_c^{pole}	RT optimal [125]	NLO	62/52	62/52
JR14 [5] [c]	1.3	$\overline{MS}$ $m_c(m_c)$	FFNS ($n_f = 3$)	NNLO$_{approx}$	62/52	62/52
MMHT14 [6]						
(NLO)	1.4	m_c^{pole}	RT optimal [125]	NLO	72/52	78/52
(NNLO)	1.4	m_c^{pole}	RT optimal [125]	NLO	71/52	83/52
NNPDF3.0 [7]						
(NLO)	1.275	m_c^{pole}	FONLL-B [124]	NLO	58/52	60/52
(NNLO)	1.275	m_c^{pole}	FONLL-C [124]	NLO	67/52	69/52
PDF4LHC15 [8] [d]	–	–	FONLL-B [124]	–	58/52	64/52
	–	–	RT optimal [125]	–	71/52	75/52
	–	–	SACOT(χ) [123]	–	51/47	76/47

No advantage of the GMVFN schemes: the VFN χ^2 values are systematically bigger than the FFN ones

Accardi, et al. hep-ph/1603.08906

Charm quark mass and the Higgs cross section

MMHT

- "Tuning" Charm mass m_c parameter effects the Higgs cross section
  - linear rise in $\sigma(H) = 40.5 \ldots 42.6$ pb for $m_c = 1.15 \ldots 1.55$ GeV with MMHT14 PDFs Martin, Motylinski, Harland-Lang, Thorne '15

m_c^{pole} [GeV]	$\alpha_s(M_Z)$ (best fit)	χ^2/NDP (HERA data on $\sigma^{c\bar{c}}$)	$\sigma(H)^{\text{NNLO}}$ [pb] best fit $\alpha_s(M_Z)$	$\sigma(H)^{\text{NNLO}}$ [pb] $\alpha_s(M_Z) = 0.118$
1.15	0.1164	78/52	40.48	(42.05)
1.2	0.1166	76/52	40.74	(42.11)
1.25	0.1167	**75/52**	**40.89**	(42.17)
1.3	0.1169	76/52	41.16	(42.25)
1.35	0.1171	78/52	41.41	(42.30)
1.4	0.1172	**82/52**	41.56	**(42.36)**
1.45	0.1173	88/52	41.75	(42.45)
1.5	0.1173	96/52	41.81	(42.51)
1.55	0.1175	105/52	42.08	(42.58)

Deuteron corrections in the PDF fits
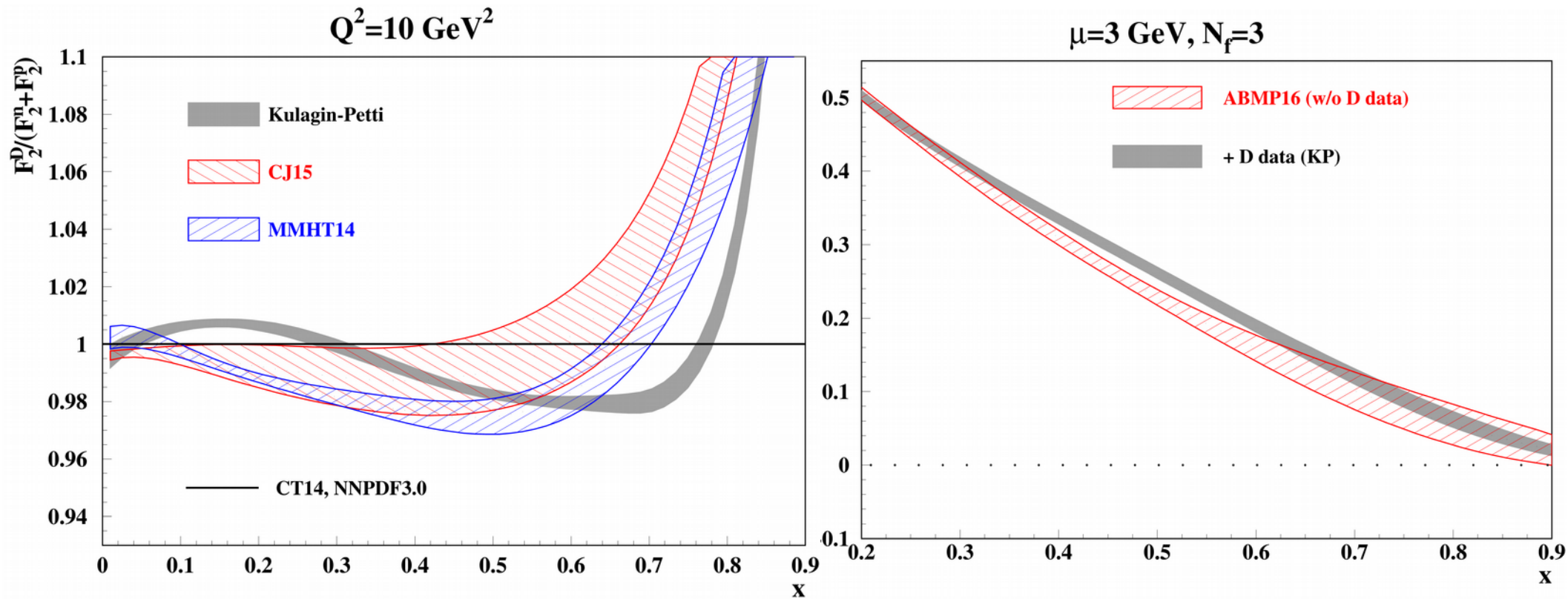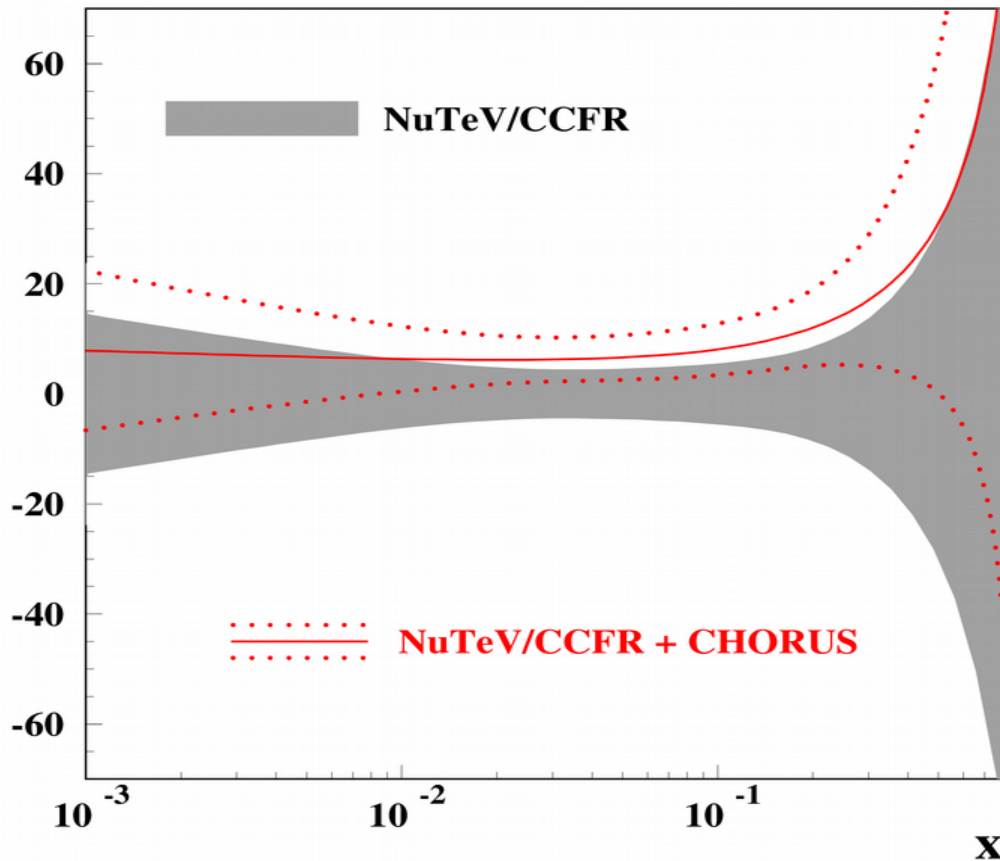

Spread between different deuteron models O(%); quite big for the purposes of precision measurements

DY data help to keep accuracy of the PDF determination avoiding uncertainty due to the modeling of nuclear effects

43
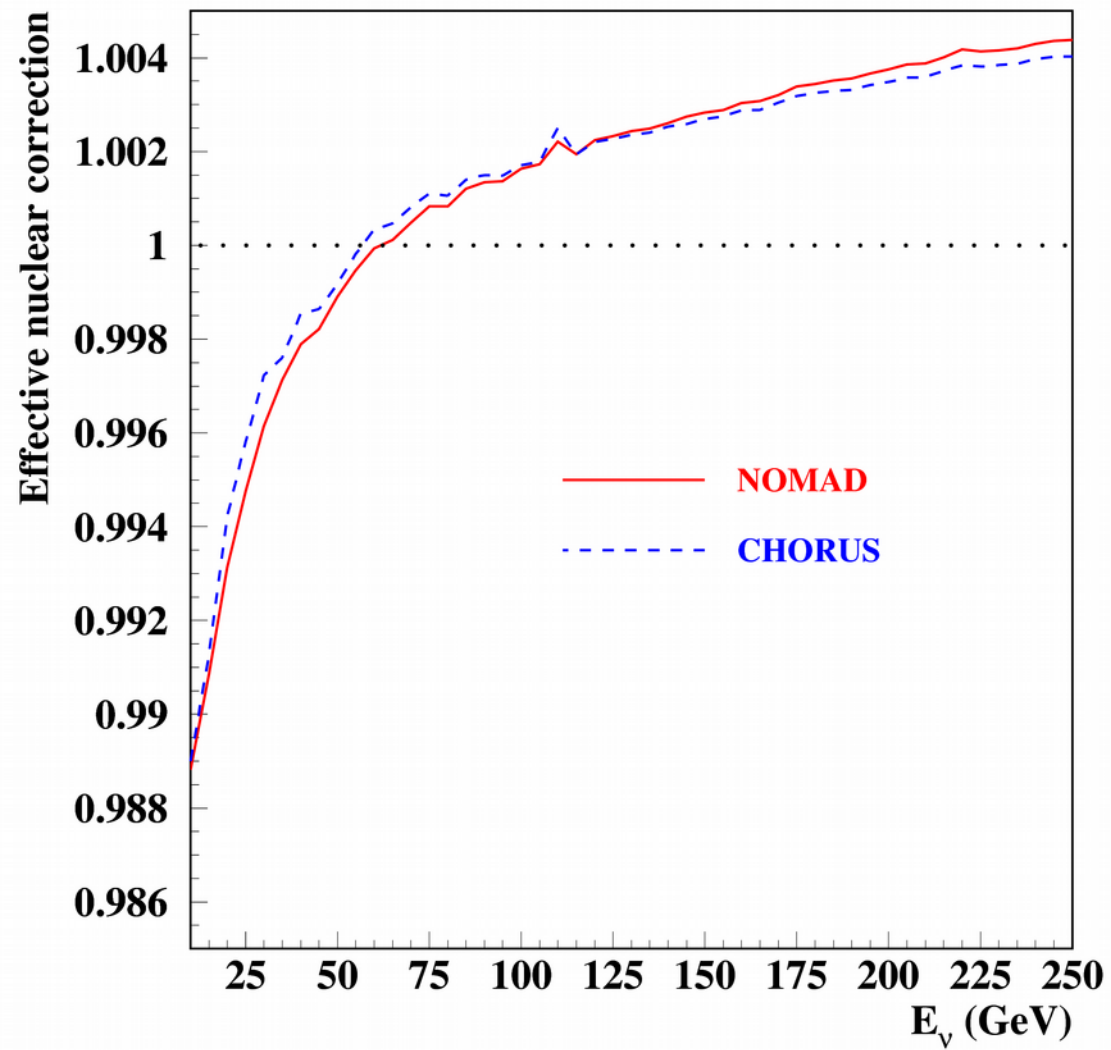
CHORUS charm data

$\mu = 3$ GeV, $n_f = 3$

Emulsion data on charm/CC ratio with the charmed hadron vertex measured

CHORUS NJP 13, 093002 (2011)

– full phase space measurements

– no sensitivity to B_μ

– low statistics (2013 events)

CHORUS data pull strangeness up, however the statistical significance of the effect is poor

sa, Blümlein, Caminada, Lipka, Lohwasser, Moch, Petti, Placakyte hep-ph/1404.6469

44
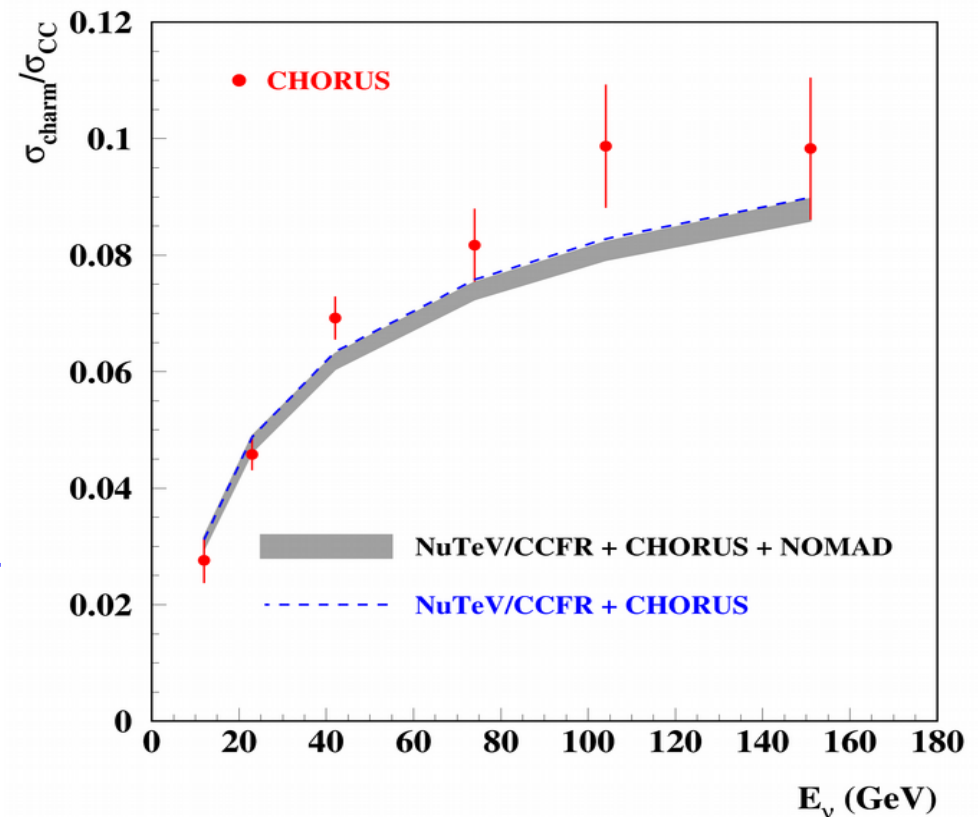
CMS W+charm data

CMS Collaboration JHEP 02, 013 (2014)
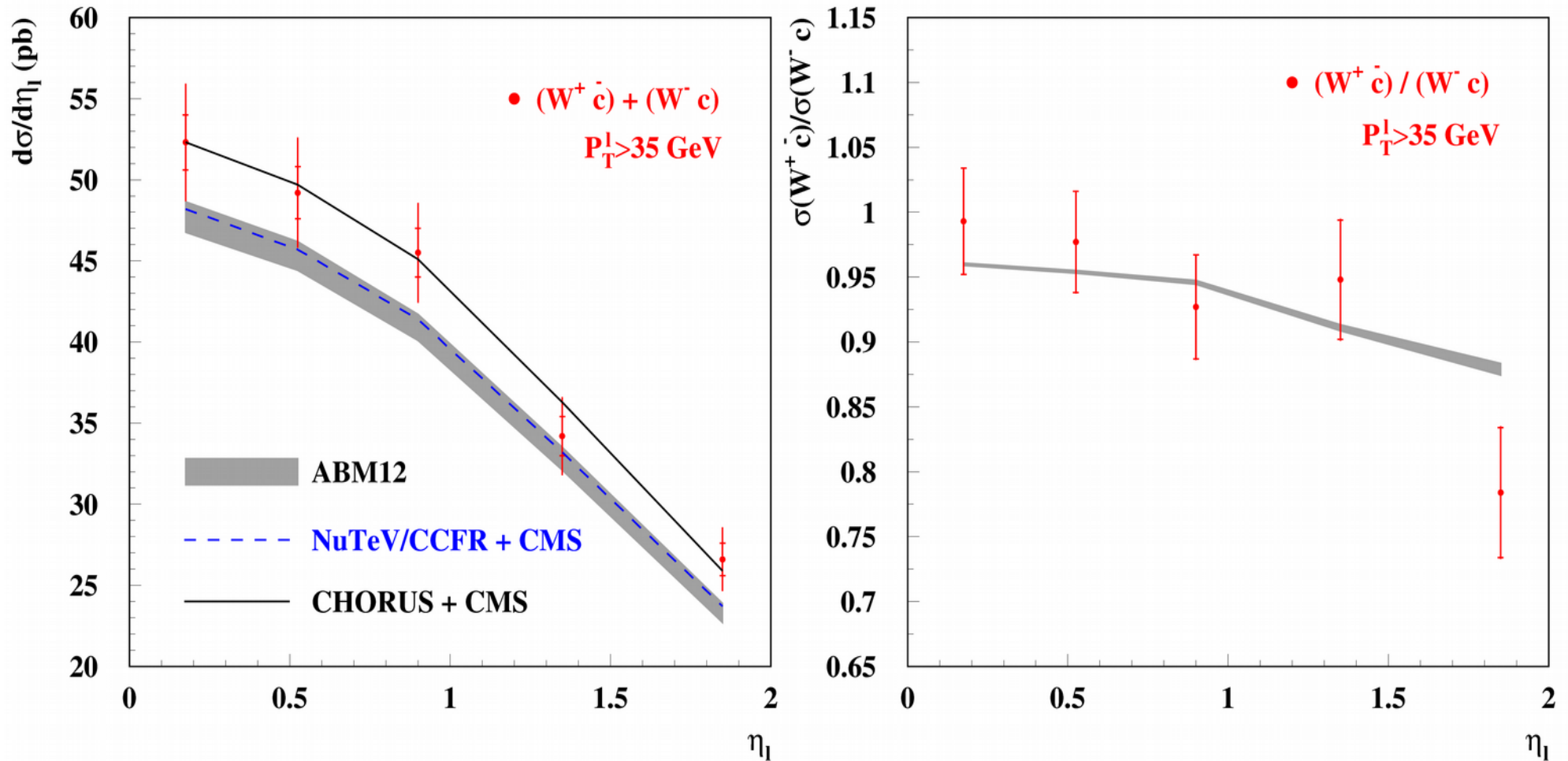
- CMS data go above the NuTeV/CCFR by 1σ; little impact on the strange sea

- The charge asymmetry is in a good agreement with the charge-symmetric strange sea
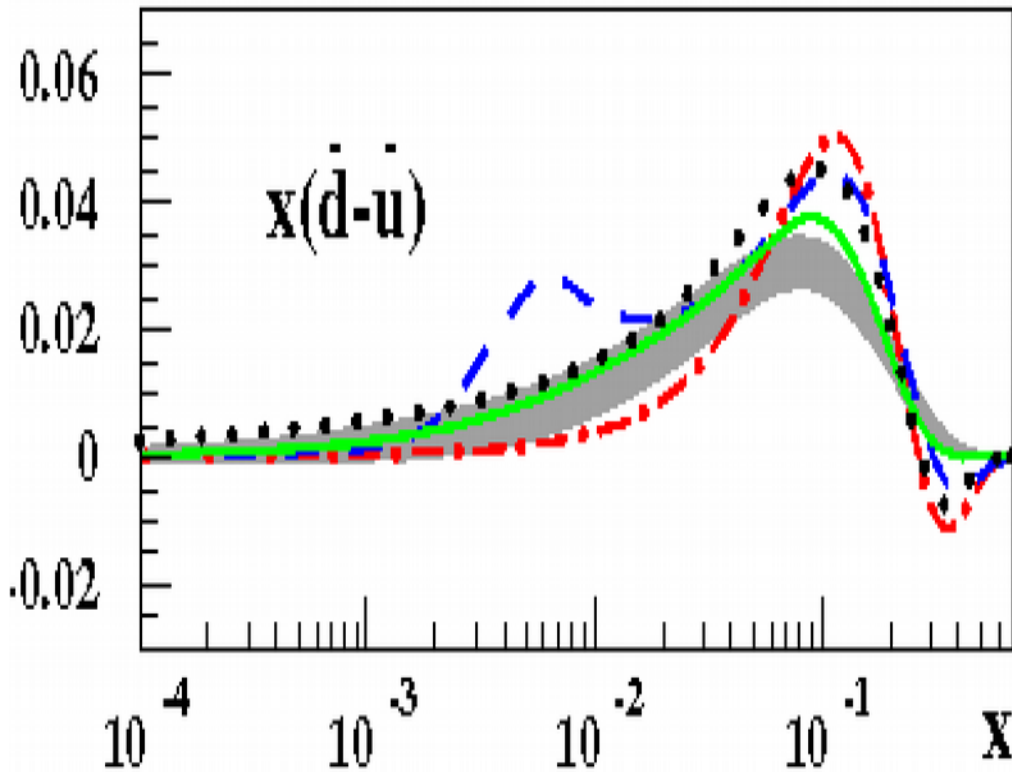
- Good agreement with the CHORUS data

ATLAS W+charm data

ATLAS (7 TeV, 4.6 1/fb)
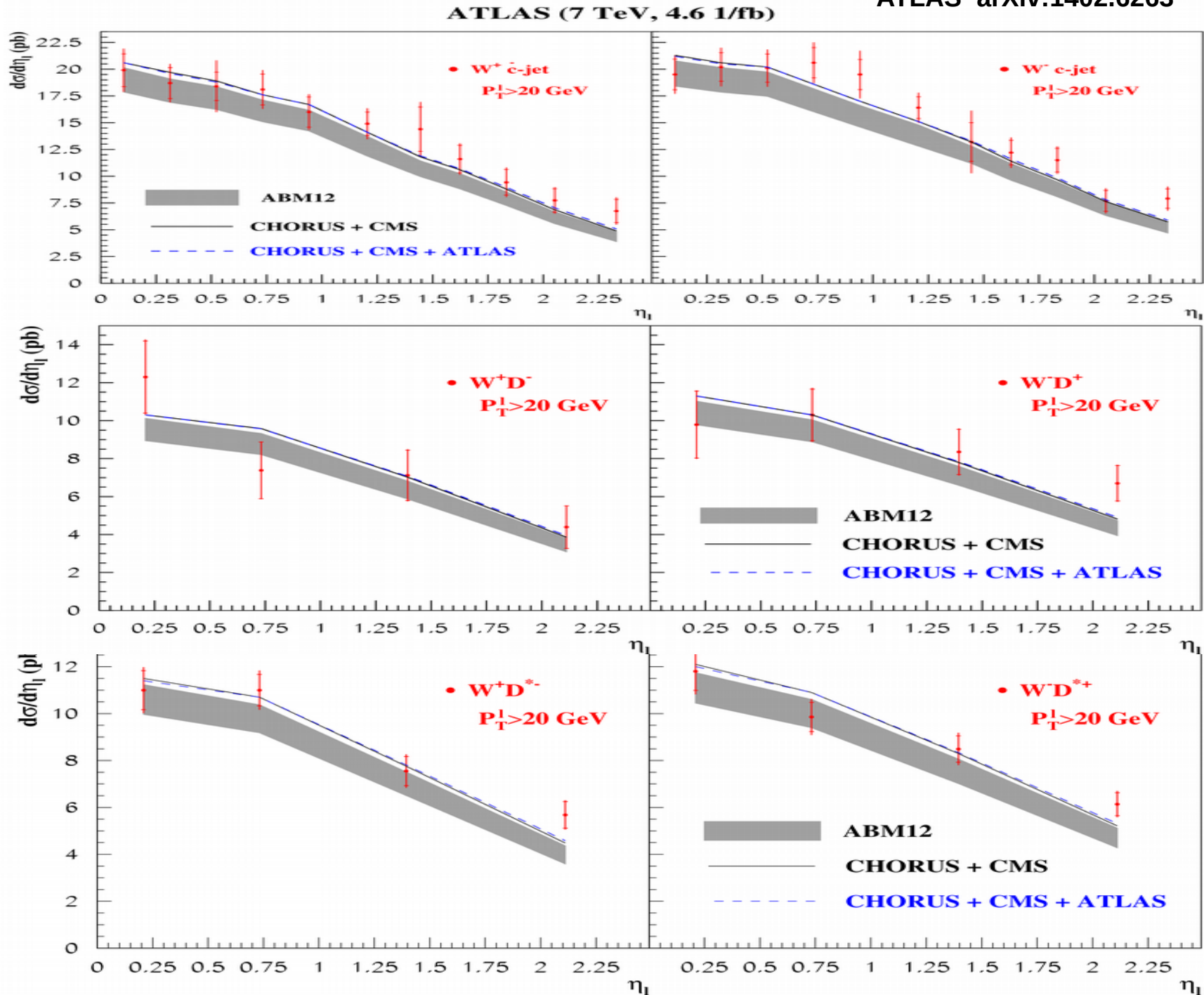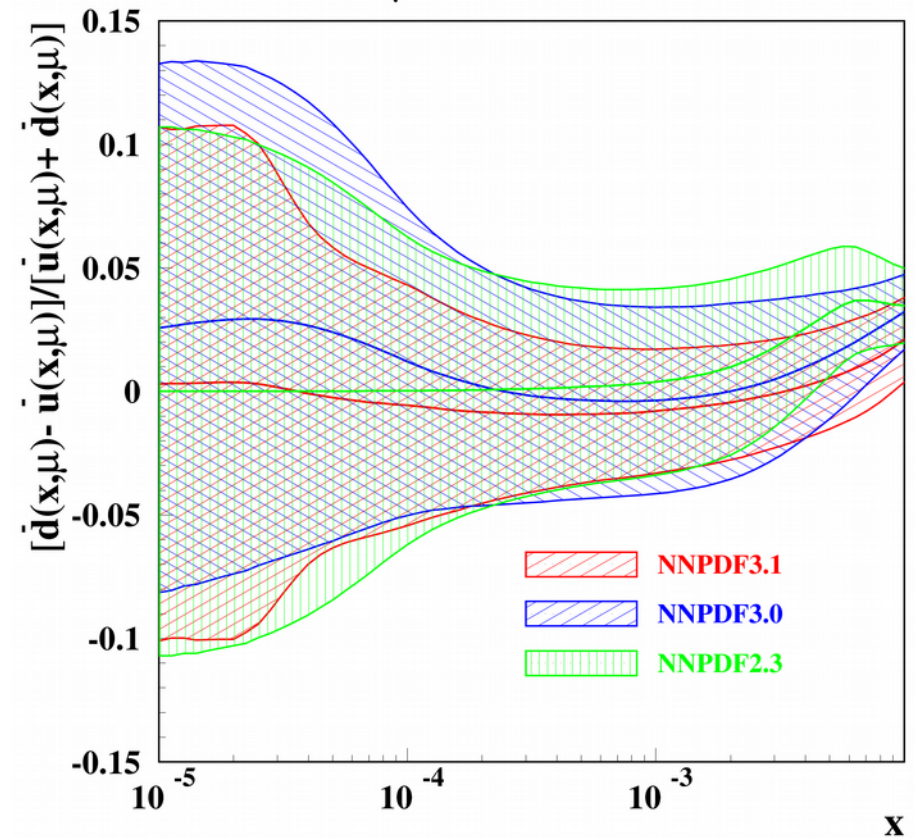
Sea quark iso-spin asymmetry

ABM12 CT10 JR09 MSTW08 NNPDF2.3

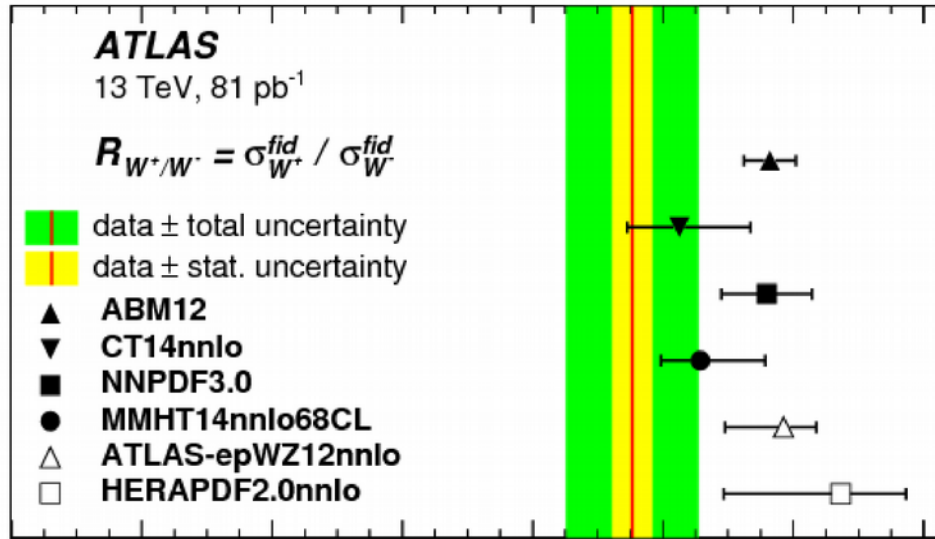sa, Blümlein, Moch PRD 89, 054028 (2014)

- At x~0.1 the sea quark iso-spin asymmetry is controlled by the fixed-target DY data (E-866), weak constraint from the DIS (NMC)

- At x<0.01 Regge-like constraint like $x^{(a-1)}$, with a close to the meson trajectory intercept; the "unbiased" NNPDF fit follows the same trend
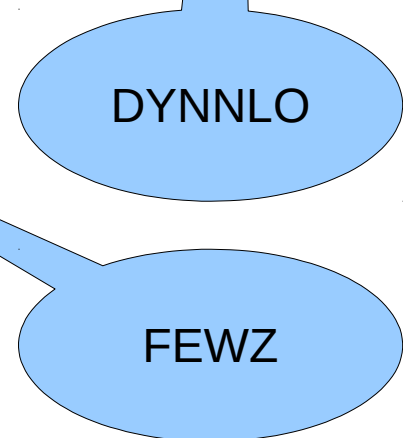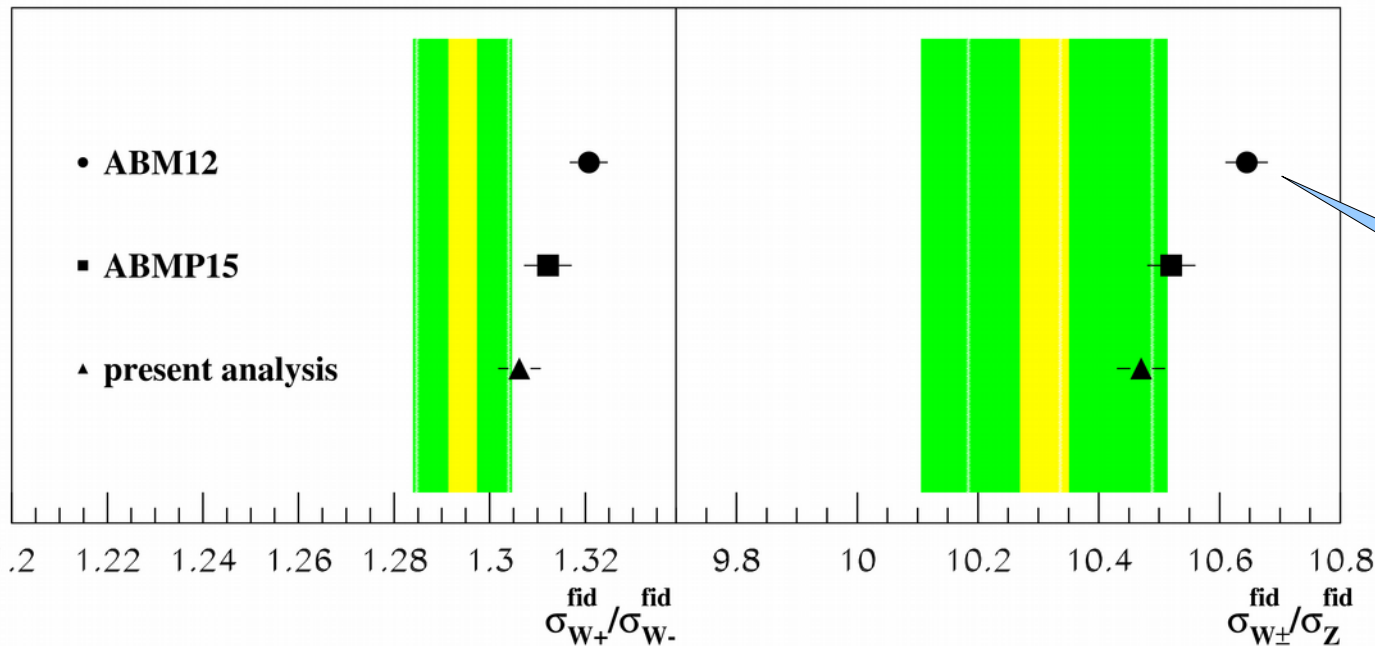
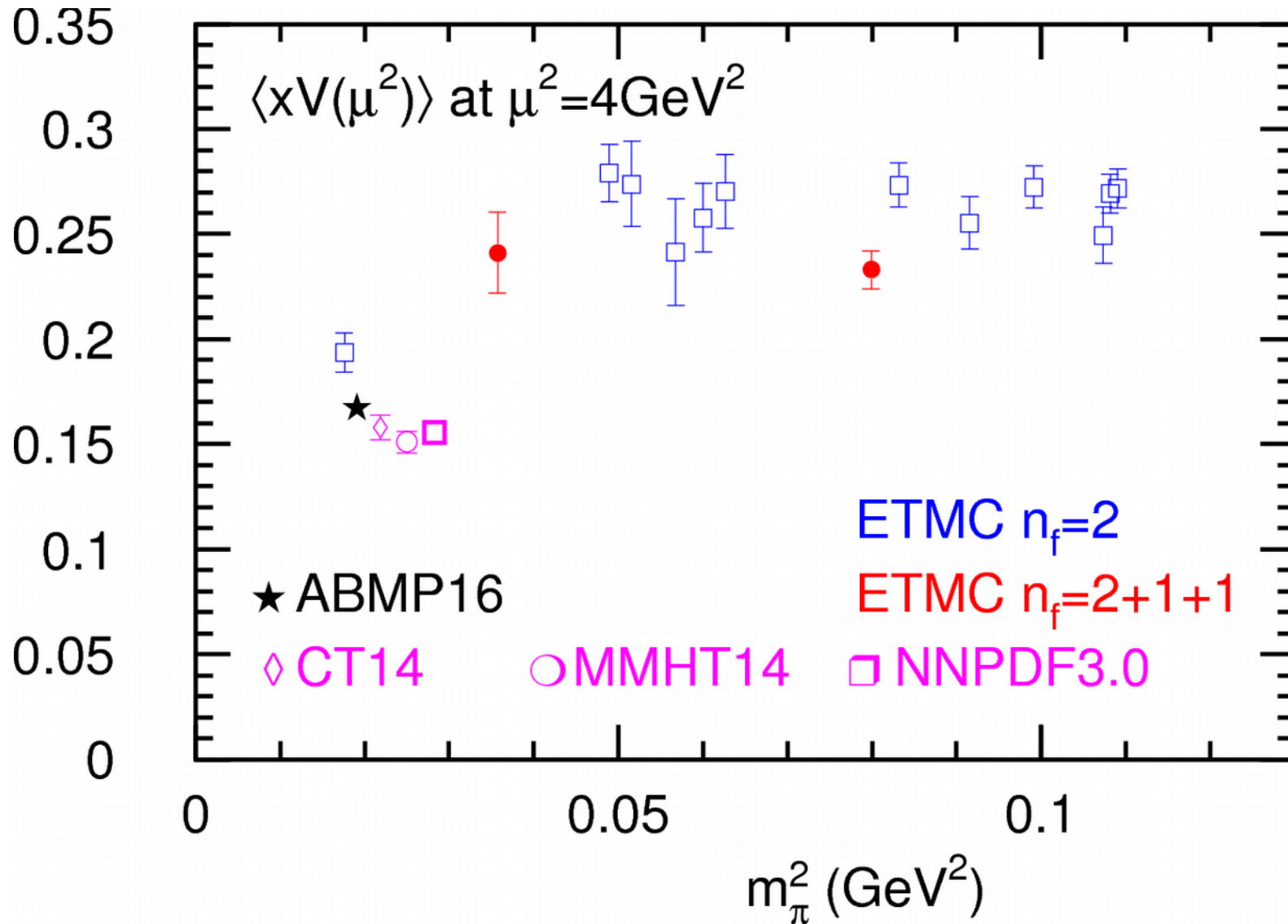*Onset of the Regge asymptotics is out of control*

ATLAS W&Z at 13 TeV
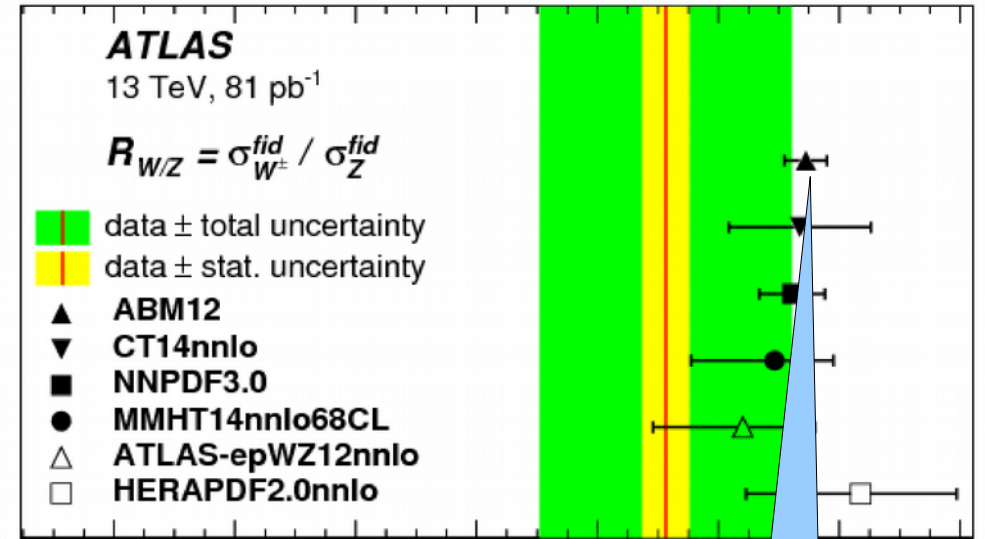
Data are well accommodated into the fit χ²/NDP=9/6

Comparison with lattice results

NOMAD charm data

μ=3 GeV, n_f=3

ΔS (%)

NuTeV/CCFR

NuTeV/CCFR + NOMAD

X
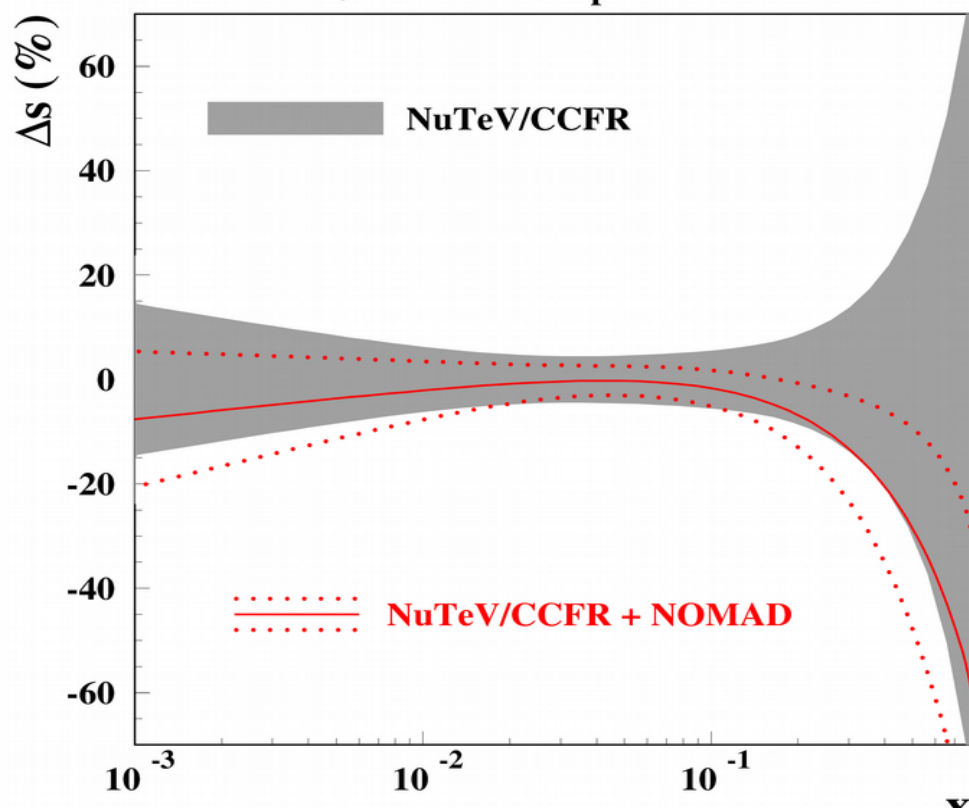
The data on ratio 2μ/incl. CC ratio with the 2μ statistics of 15000 events (much bigger than in earlier CCFR and NuTeV samples).

NOMAD NPB 876, 339 (2013)

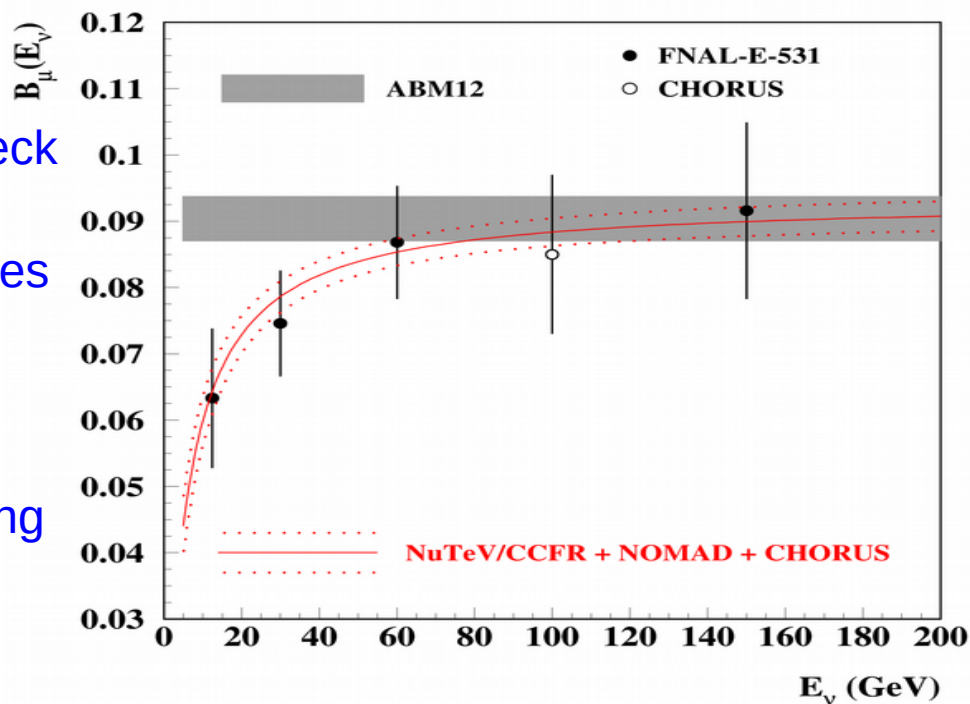Systematics, nuclear corrections, etc. cancel in the ratio

- pull down strange quarks at x>0.1 with a sizable uncertainty reduction

- $m_c(m_c)$=1.23±0.03(exp.) GeV is comparable to the ABM12 value

The semi-leptonic branching ratio $B_μ$ is a bottleneck

- weighted average of the charmed-hadron rates

$$B_μ(E_ν)=\sum_h r^h(E_ν)B^h_μ = a/(1+b/E_ν)$$

- fitted simultaneously with the PDFs, etc. using the constraint from the emulsion data

$B_μ(E_ν)$

- FNAL-E-531
- CHORUS
- ABM12

NuTeV/CCFR + NOMAD + CHORUS

$E_ν$ (GeV)

50

Details of the epWZ and ABMP16 fits

	epWZ16	ABMP16
Data	HERA, ATLAS W&Z	HERA, LHC and Tevatron W&Z, fixed-target DIS and charm production, fixed-target DY, ….
PDF shape	$$xu_v(x,\mu_0^2) = A_{u_v} x^{B_{uv}} (1-x)^{C_{uv}} (1+E_{u_v} x^2),$$ $$xd_v(x,\mu_0^2) = A_{d_v} x^{B_{d_v}} (1-x)^{C_{d_v}},$$ $$x\bar{u}(x,\mu_0^2) = A_{\bar{u}} x^{B_{\bar{u}}} (1-x)^{C_{\bar{u}}},$$ $$x\bar{d}(x,\mu_0^2) = A_{\bar{d}} x^{B_{\bar{d}}} (1-x)^{C_{\bar{d}}},$$ $$xg(x,\mu_0^2) = A_g x^{B_g} (1-x)^{C_g} - A'_g x^{B'_g} (1-x)^{C'_g},$$ $$x\bar{s}(x,\mu_0^2) = A_{\bar{s}} x^{B_{\bar{s}}} (1-x)^{C_{\bar{s}}},$$ 15 free parameters	$$xq_v(x,\mu_0^2) = \frac{2\delta_{qu}+\delta_{qd}}{N_q^v} (1-x)^{b_{qv}} x^{a_{qv}} P_{qv}(x),$$ $$xq_s(x,\mu_0^2) = A_{qs} (1-x)^{b_{qs}} x^{a_{qs}} P_{qs}(x),$$ $$xg(x,\mu_0^2) = A_g (1-x)^{b_g} x^{a_g} P_g(x),$$ $$P_p(x) = (1+\gamma_{-1,p}\ln x)\left(1+\gamma_{1,p}x+\gamma_{2,p}x^2+\gamma_{3,p}x^3\right),$$ 25 free parameters

ABMP16 PDFs are selected more flexible in order to accommodate more data as compared to the EpWZ16 fit, which was evolved form the HERA data analysis
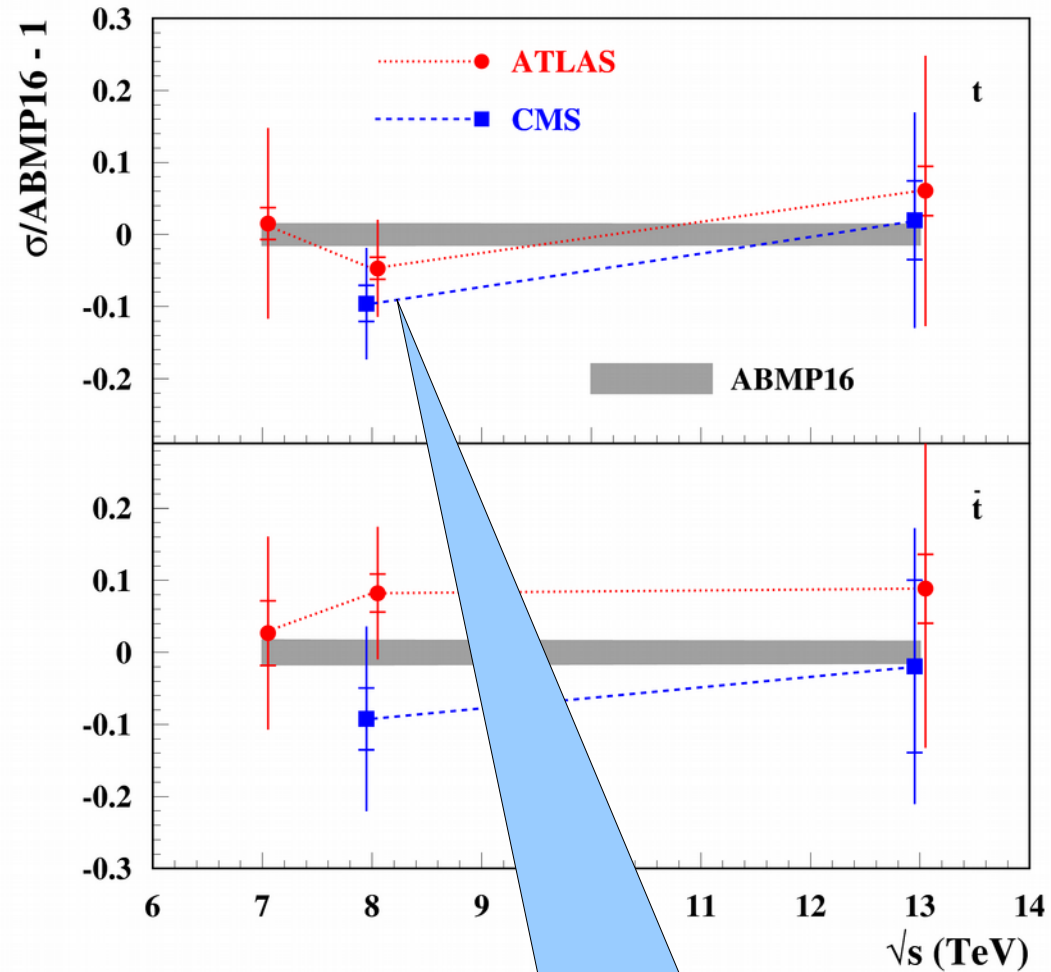
Implication for(of) the single-top production

sa, Blümlein, Moch, Plačakytė hep-ph/1508.07923
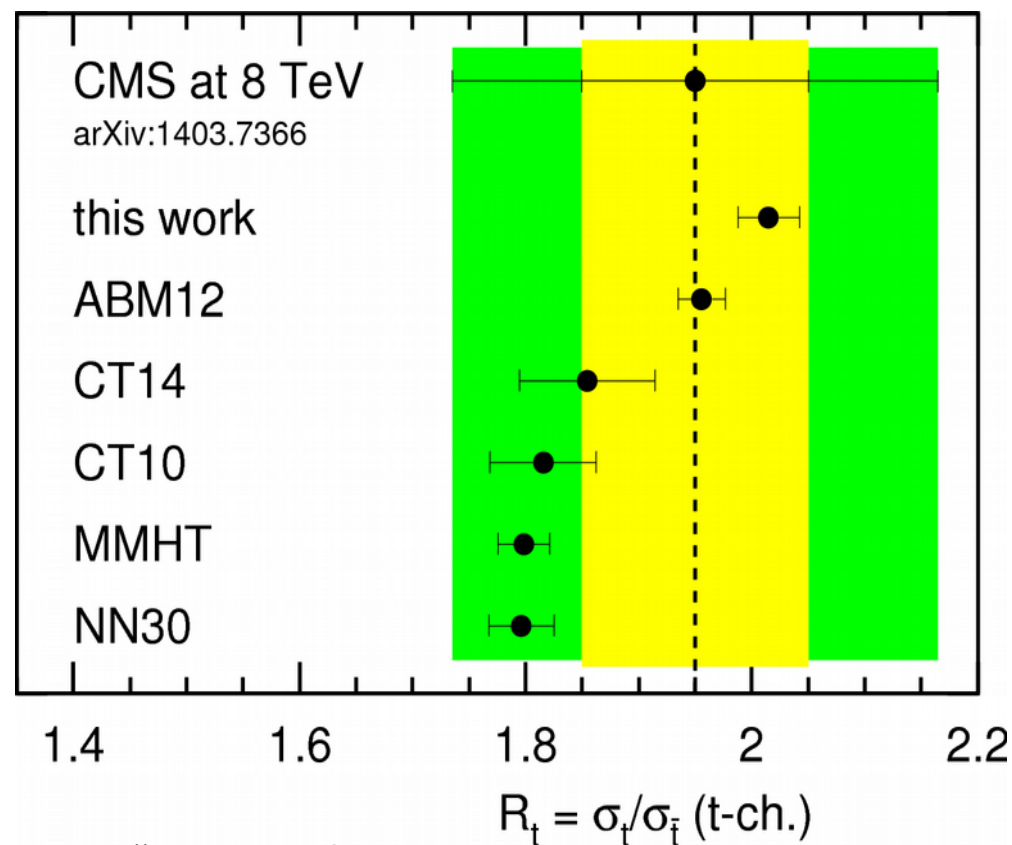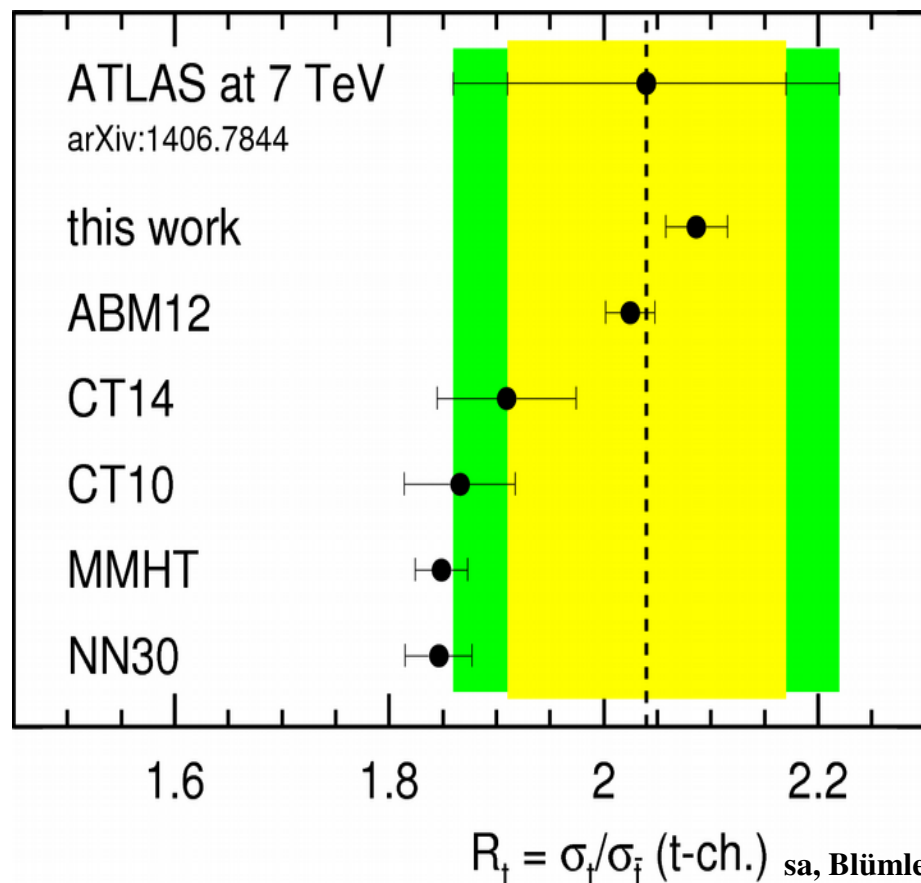
- ATLAS and CMS data on the ratio t/tbar are in a good agreement

- The predictions driven by the froward DY data are in a good agreement with the single-top data (N.B.: ABM12 is based on the deuteron data → consistent deuteron correction was used)   talks by Petti at DIS2016

Single-top production discriminate available PDF sets and can serve as a standard candle process
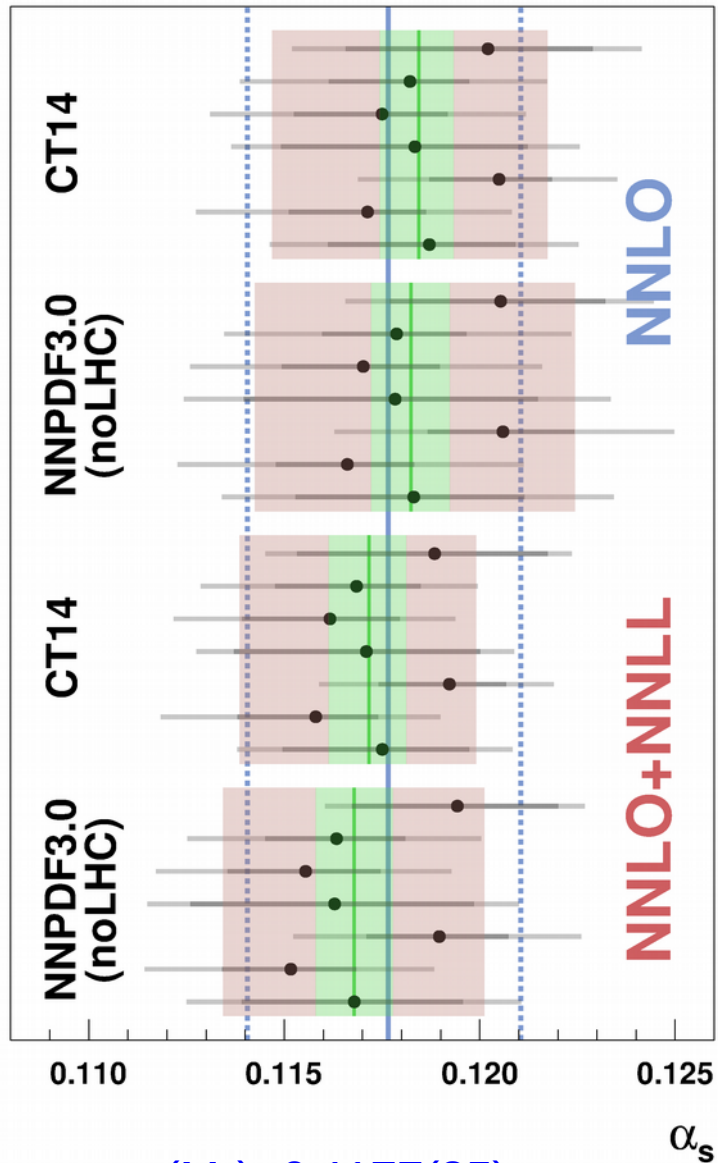
Single-top production: ATLAS and CMS
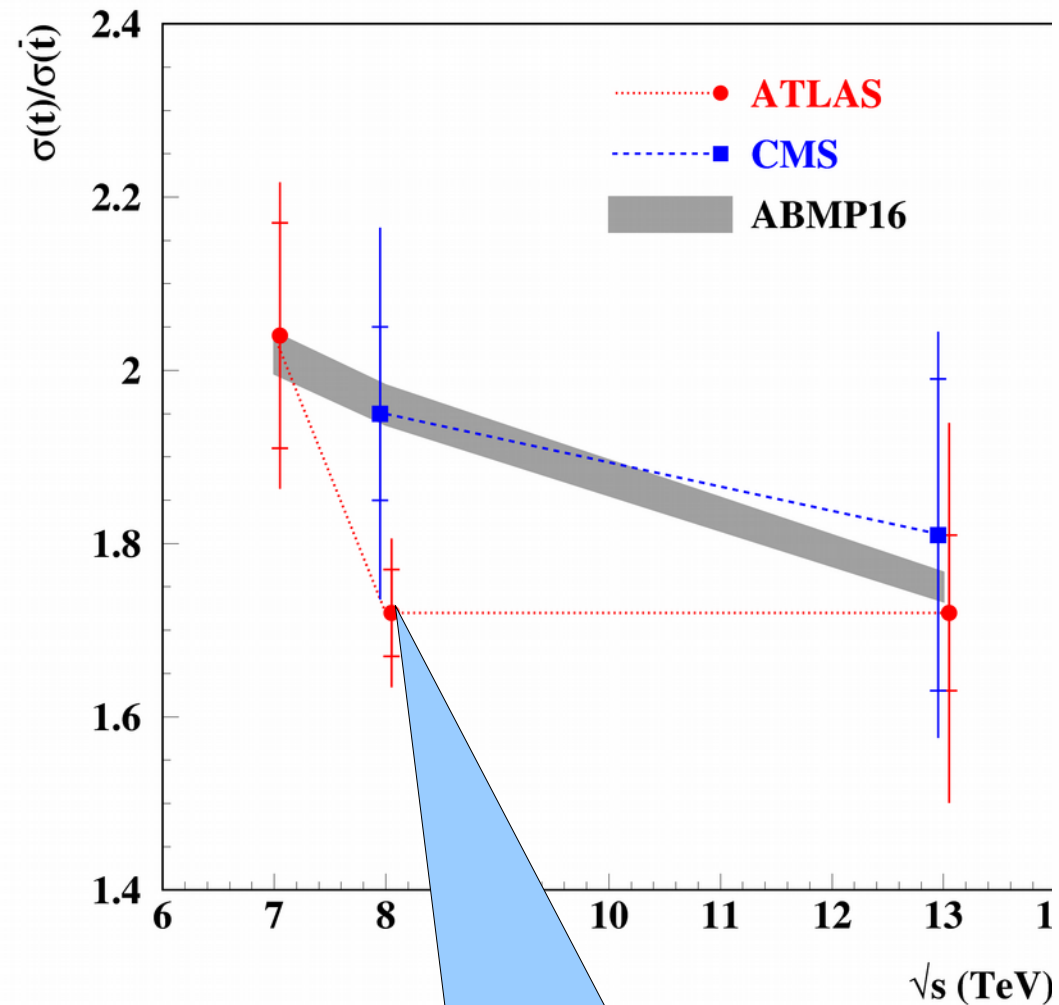
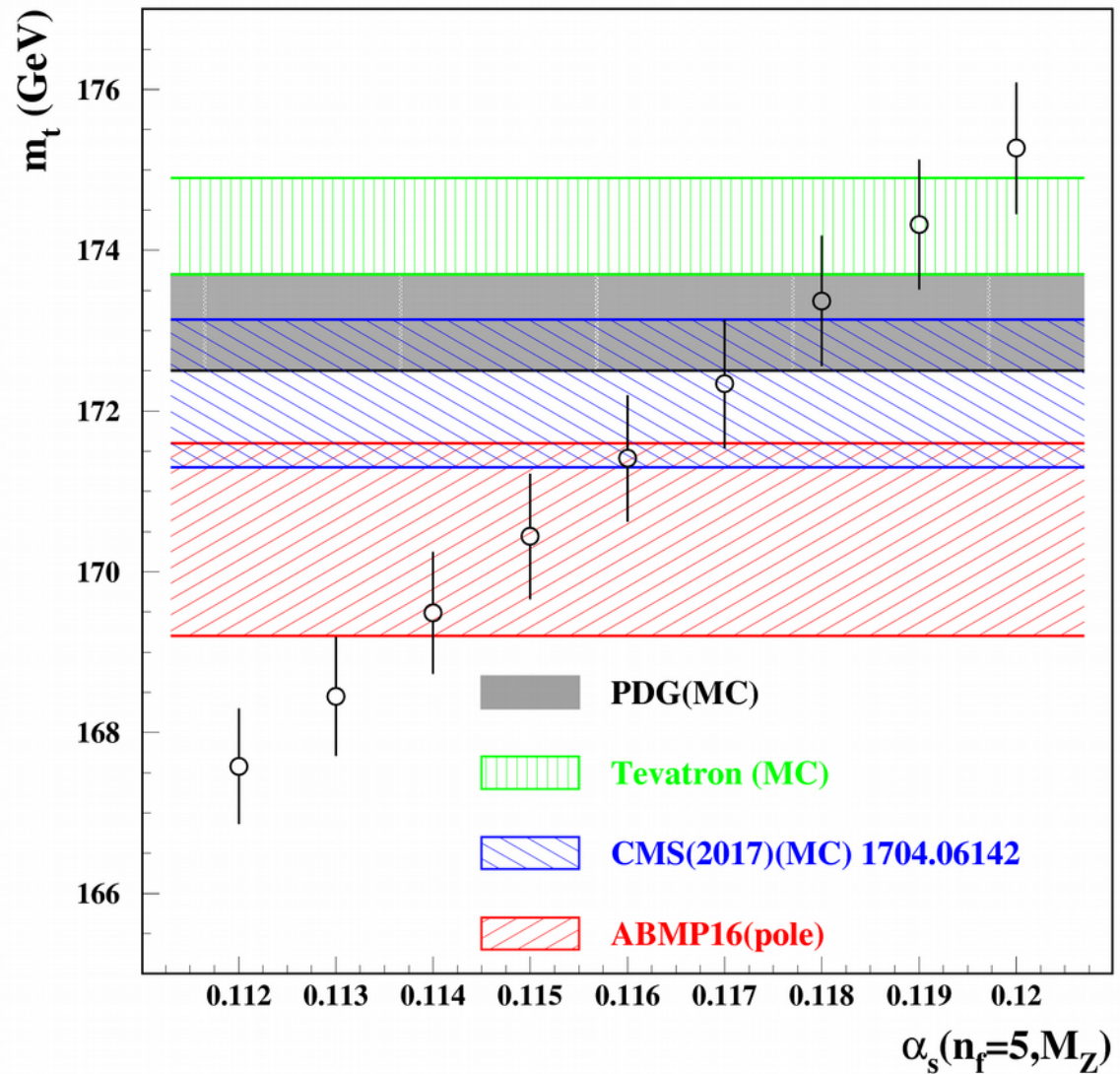The errors in ATLAS data are much smaller: prefect cancellation of the errors in ratio

The trend in ATLAS data is different for t and tbar samples

α_s from ttbar data (m_t fixed)

$\alpha_s(M_z)=0.1177(35)$
$m_t(pole)=173.2$ GeV

Klijnsma, Bethke, Dissertori, Salam hep-ph/1708.07495

- The value of α_s extracted strongly depends on m_t
- m_t is different for Tevetraon and LHC
- m_t is (pole) is smaller than m_t(MC) by O(1 GeV)